# PROCESSING OF EXPANDABLE THERMOPLASTIC/THERMOSET SYNTACTIC FOAM

A Dissertation
Presented to
The Academic Faculty

By

Yifeng Hong

In Partial Fulfillment
Of the Requirements for the Degree
Doctor of Philosophy in the
School of Materials Science and Engineering

Georgia Institute of Technology

August 2015

**PROCESSING OF EXPANDABLE THERMOPLASTIC/THERMOSET**

**SYNTACTIC FOAM**

Approved by:


Dr. Donggang Yao, Advisor
School of Materials Science and Engineering
*Georgia Institute of Technology*

Dr. Karl I. Jacob
School of Materials Science and Engineering
*Georgia Institute of Technology*

Dr. Meisha L. Shofner
School of Materials Science and Engineering
*Georgia Institute of Technology*

Dr. Yulin Deng
School of Chemical & Biomolecular Engineering
*Georgia Institute of Technology*

Dr. Youjiang Wang
School of Materials Science and Engineering
*Georgia Institute of Technology*


Date Approved: 05/06/2015

*To my dearest mother, Rui Yu, for her love and support*

## ACKNOWLEDGEMENTS

I would like to thank my academic committee members, labmates, family members, and friends. Without your sincere support in the past four years, I would not be able to finish my Ph.D. work and complete this dissertation.

First of all, I would like to greatly appreciate my Ph.D. Advisor, Prof. Yao. He is a very wise and knowledge advisor who not only teaches me the knowledge but also shares his philosophy. He is a very patient and warm-hearted educator who is always ready to learn about my troubles and figure out ways to help me out. He is a serious and intelligent researcher who helps me to develop critical thinking and encourages me to overcome the challenges one after another. Without him, I cannot imagine how many detours I would have gone through in my Ph.D. years.

I would also like to thank Prof. Shofner, Prof. Wang, Prof. Jacob, and Prof. Deng for their helpful comments and suggestions toward my research and generosity to share their experimental instruments. Without their knowledgeable opinions, the significance of this dissertation would be considerably reduced. I would like to show my gratefulness to the National Science Foundation, Golden Eagle Enterprise, and Georgia Tech for the financial support to my research, and the School of Materials Science and Engineering for the excellent Ph.D. program.

I would like to appreciate my labmates, Xudong Fang, Tom Wyatt and Sarang Deodhar for their support in my research. My special thanks should be given to Xudong. For the past four years, we collaborated closely and effectively. He has contributed significantly to many of my research projects. Xudong also helped me to deal with a lot

of trivial or non-trivial problems that happened randomly in my life. To me, he just seems to be a big brother. I have always been feeling so lucky to have him around since the very beginning of my life in Georgia Tech.

I would like to thank some of my friends who offered their generous helps to me when I needed. Among them, Dr. Zhuo Li, Liyi Li, Dr. Cait Meree, and Prateek Verma should receive my special appreciation. Many aspects of my research haven been greatly benefited from their help and suggestions.

At last, my sincere gratefulness should be given to my family members, especially my dearest mother, Rui Yu, and my dearest grandmother, Suqin Yun. Their selfless love and support in the past so many years is one of the irreplaceable impetuses for me to continuously advance and survive from the hard times. For so many endless nights and days, they worried about me in the other side of the Pacific Ocean just because of some tiny weakness that I expressed to them inadvertently. They give me life but require simply nothing from me. I am wondering whether there would be others that love me more than they do.

## TABLE OF CONTENTS

# LIST OF TABLES

Table 4.4 Summary of constants in the exponential fitting of dimensionless bubble radius and dimensionless bubble pressure as functions of dimensionless expansion time in numerical solution.

## LIST OF FIGURES

## LIST OF SYMBOLS

(In the order of appearance)

| | |
|---|---|
| $\varphi_{EPS}$ | Weight fraction of expandable polystyrene |
| $E_{EPS\ Expasion}$ | Specific energy needed to fully expand expandable polystyrene |
| $C_{p\ EPS}$ | Heat capacity of expandable polystyrene |
| $C_{p\ Epoxy}$ | Heat capacity of epoxy |
| $\Delta T$ | Temperature difference |
| $F_t$ | Compensation factor for heat transfer efficiency |
| $E_{Decomp}$ | Epoxy decomposition activation energy |
| $\eta_{EPS}$ | Expandable polystyrene volume fraction |
| $\rho_{Epoxy}$ | Neat epoxy density |
| $\rho_{Foam}$ | Expandable polystyrene/epoxy syntactic foam density |
| $\rho_{expanded\ EPS}$ | Density of expandable polystyrene microsphere expanded in epoxy |
| $\sigma_M$ | Flexural strength in 3-point bending test |
| $E$ | Flexural modulus in 3-point bending test |
| $P_M$ | Maximum load in 3-point bending test |
| $L$ | Support span length in 3-point bending test |

| | |
|---|---|
| $b$ | Width of the beam in 3-point bending test |
| $d$ | Depth of the beam in 3-point bending test |
| $m$ | Slope of the initial linear portion of the load-deflection curve in 3-point bending test |
| $\rho_{FRMixture}$ | Density of fire-retardant compound after curing |
| $\rho_{FRFoam}$ | Density of the composite expandable polystyrene foam |
| $\rho_{NeatFoam}$ | Density of the neat expandable polystyrene foam |
| $\varepsilon$ | Flexural strain in 3-point bending test |
| $D_f$ | Deflection of the center of the sample in 3-point bending test |
| $R(t,t')$ | Bubble radius at time $t$ of the bubble nucleated at time $t'$ |
| $P_b(t,t')$ | Bubble pressure at time $t$ of the bubble nucleated at time $t'$ |
| $P_a$ | Ambient pressure |
| $\bar{c}(t')$ | Average pentane concentration in expandable polystyrene matrix |
| $c_0$ | Initial pentane concentration in expandable polystyrene matrix |
| $R_0$ | Initial bubble radius |
| $P_{b0}$ | Initial bubble pressure |
| $r$ | Radial distance in the spherical coordinate system in single bubble |

| | |
|---|---|
| $\theta$ | Polar angle in the spherical coordinate system in single bubble |
| $\varphi$ | Azimuthal angle in the spherical coordinate system in single bubble |
| $v_r$ | Bubble expanding velocity in $rr$ direction |
| $\tau_{rr}$ | Principle stress in $rr$ direction |
| $\tau_{\theta\theta}$ | Principle stress in $\theta\theta$ direction |
| $D$ | Diffusion coefficient of pentane in polystyrene |
| $c$ | Pentane concentration in expandable polystyrene matrix |
| $n_g$ | Mole number of pentane molecules in the bubble |
| $\Re$ | Universal gas constant |
| $R^*$ | Dimensionless bubble radius |
| $P_b^*$ | Dimensionless bubble pressure |
| $t^*$ | Dimensionless expansion time |
| $t_c$ | Characteristic bubble expansion time |
| $R_c$ | Characteristic bubble radius |
| $J(t')$ | Bubble nucleation rate as a function of bubble nucleation time $t'$ |
| $N_1$ | Pre-exponential nucleation constant in semi-analytical solution |
| $N_2$ | Nucleation time constant in semi-analytical solution |

| | |
|---|---|
| $\hat{R}(t)$ | Radius of expandable polystyrene |
| $\hat{R}_0$ | Initial radius of expandable polystyrene microsphere |
| $V_0$ | Initial volume of expandable polystyrene microsphere |
| $f_0$ | Zeldovich correction factor |
| $N_A$ | Avogardro's number |
| $M_W$ | Molecular weight of pentane |
| $F$ | Correction factor of free energy barrier |
| $\Delta E$ | Heterogeneous nucleation free energy barrier |
| $k_B$ | Boltzmann's constant. |
| $c_i$ | Constant of Generalized Wagner model |
| $P_{b0}^c$ | Critical saturated pressure of pentane of Generalized Wagner model |
| $T^c$ | Critical temperature of Generalized Wagner model |
| $\tau$ | Reduced temperature of Generalized Wagner model |
| $\underline{\underline{\tau}}$ | Stress tensor |
| $\underline{\underline{\dot{\gamma}}}$ | Shear rate tensor |
| $n$ | Index of power-law model |

| | |
|---|---|
| $\eta_0$ | Pre-exponent coefficient of power-law model |
| $K$ | Pre-exponent constant of Andrade-Eyring model |
| $E_\eta$ | Activation energy of Andrade-Eyring model |
| $k_H$ | Henry's solubility constant |
| $\beta$ | Diffusion radius correlation constant |
| $D_0$ | Pre-exponential diffusion coefficient |
| $E_D$ | Activation energy of diffusion |
| $\hat{r}$ | Radial distance in the spherical coordinate system in expandable polystyrene microsphere |
| $\hat{\theta}$ | Polar angle in the spherical coordinate system in expandable polystyrene microsphere |
| $\hat{\varphi}$ | Azimuthal angle in the spherical coordinate system in expandable polystyrene microsphere |
| $\eta_E$ | Viscosity of uncured epoxy liquid |
| $A_{Ai}$ | Fitting parameters of dimensionless bubble radius as a function of dimensionless bubble expansion time in semi-analytical solution |
| $B_{Ai}$ | Fitting parameters of dimensionless bubble pressure as a function of dimensionless bubble expansion time in semi-analytical solution |

$A_{Ni}$ Fitting parameters of dimensionless bubble radius as a function of dimensionless bubble expansion time in numerical solution

$B_{Ni}$ Fitting parameters of dimensionless bubble pressure as a function of dimensionless bubble expansion time in numerical solution

# SUMMARY

While hollow glass microspheres are commonly used in syntactic foam production, their abrasive and brittle properties usually result in poor processability and have adverse effects on the foam performance. Therefore, a number of attempts have been made in the industry to replace hollow glass microspheres with polymeric foamed microspheres. Among many choices, syntactic foam filled with expandable thermoplastic microspheres has shown high potential to become a novel class of engineering materials, especially for lightweight structural applications. However, conventional processing techniques for syntactic foam usually experience difficulties such as high processing viscosity, low loading of foam fillers, and ineffective microsphere expansion.

To address the issues mentioned above, a microwave expansion process to produce thermoset-matrix syntactic foam containing thermoplastic foam beads was designed and developed in this thesis work. Expandable polystyrene (EPS) microspheres and epoxy resin were chosen as a model material system. This process is featured with a capability to effectively expand EPS microspheres in syntactic foam with high EPS loading. The resin viscosity and the specific microwave energy are found to be the two primary control parameters determining the process window. Mechanical characterization showed that the specific flexural strength and modulus of the syntactic foam are similar to those of the neat epoxy. By comparison, the flexural moduli over density squared or cubed of the foam are much higher, especially at high EPS loadings, than those of the neat resin. The foamed EPS microspheres can also effectively toughen the syntactic foam, preventing propagation of cracks. Furthermore, the microwave expansion process was found to be capable of molding syntactic foamed parts of relatively sophisticated geometry with smooth surfaces.

In order to broaden the impact of the research, the microwave expansion process was extended to produce composite EPS foam with improved fire-retardant performance. This process converts an expandable suspension containing a fire-retardant compound, unexpanded EPS microspheres and a diluent, into a composite foam with a honeycomb-like barrier structure. The expandable suspension process is featured with incorporation of high loadings of environmentally friendly and low-cost inorganic fire-retardant agents without undermining the foamability of EPS microspheres. Optical observations confirmed the formation of such a unique structure that encapsulates each expanded polystyrene microsphere in the resulting foam. The suspension viscosity was found to highly influence the foam morphology. Results from mechanical tests showed that the existence of the barrier structure can considerably improve the mechanical performance of the composite foam. Fire-retardation tests demonstrated that the barrier structure can effectively stop the fire path into the foam, suppress toxic smoke generation, and maintain foam structure integrity, enabling the composite foam to have improved fire-resistance in comparison with neat foam.

A further understanding on the fundamental aspect of this process is highly desired to optimize the microwave expansion process. It requests to establish a model that can simulate the core part of the process, the expansion of EPS microsphere, since kinetic parameters related to bubble nucleation and growth cannot be measured easily by experimental methods. A general formulation was thus developed to model the EPS expansion. A semi-analytical solution was first obtained based on the case of a single bubble expansion in an infinite matrix. The dimensionless bubble radius and pressure are defined and found to be as exponential functions of dimensionless expansion time. The characteristic bubble expansion time is able to characterize the time scale of expansion process. The semi-analytical solution can qualitatively predict the radial

expansion of EPS microsphere observed in a real-time experiment. To have an accurate prediction, a numerical solution was obtained to the model that couples the nucleation and expansion of multiple bubbles in a finite matrix at various temperatures. The results showed that the numerical solution is able to quantitatively predict the radial expansion of EPS. A parameter sensitivity study was performed to examine the effect of each parameter over the expansion process.

In summary, in this thesis work, a microwave expansion process was designed to solve some emerging issues existing in the syntactic foam industry. The application of this process was then extended to produce a composite EPS foam in order to address the fire retardation problems of polyolefin foams. At last, a process model was developed to improve the fundamental understanding of expansion kinetics of EPS microsphere and provide important reference to optimize the microwave expansion process.

# CHAPTER 1

# INTRODUCTION

## 1.1 Syntactic Foam

### *1.1.1 Overview*

Syntactic foam is a special kind of gas-filled polymeric materials in which hollow or foamed microspheres, named as fillers, are embedded in a polymer matrix designated as binder [1]. Since the fillers are directly introduced into the binder materials, the processing technique to produce syntactic foams can also be termed as the micro-capsulation.

Syntactic foam can be categorized into the class of foamed plastics because their heterophase gas-solid structure is similar to those of gas-blown cellular plastics [2]. However, the cellular structure in syntactic foam is not formed by blowing agents but via introducing gas-filled particles into polymer binders. Moreover, since the microspheres usually have continuous shells, the syntactic foam made from such fillers thus has a completely closed-cell structure along with the absence of microstructural anisotropy [3]. Also, different from the ordinary foamed plastics, syntactic foam is usually a ternary system rather than the binary one, since the material to make the shells of fillers is not the same one to make the binder. Sometimes, during the manufacturing process, air pockets will also be introduced into the binder purposely to further reduce the part density [2]. A scheme is drawn in Figure 1.1 to illustrate the structure and composition of syntactic foams.

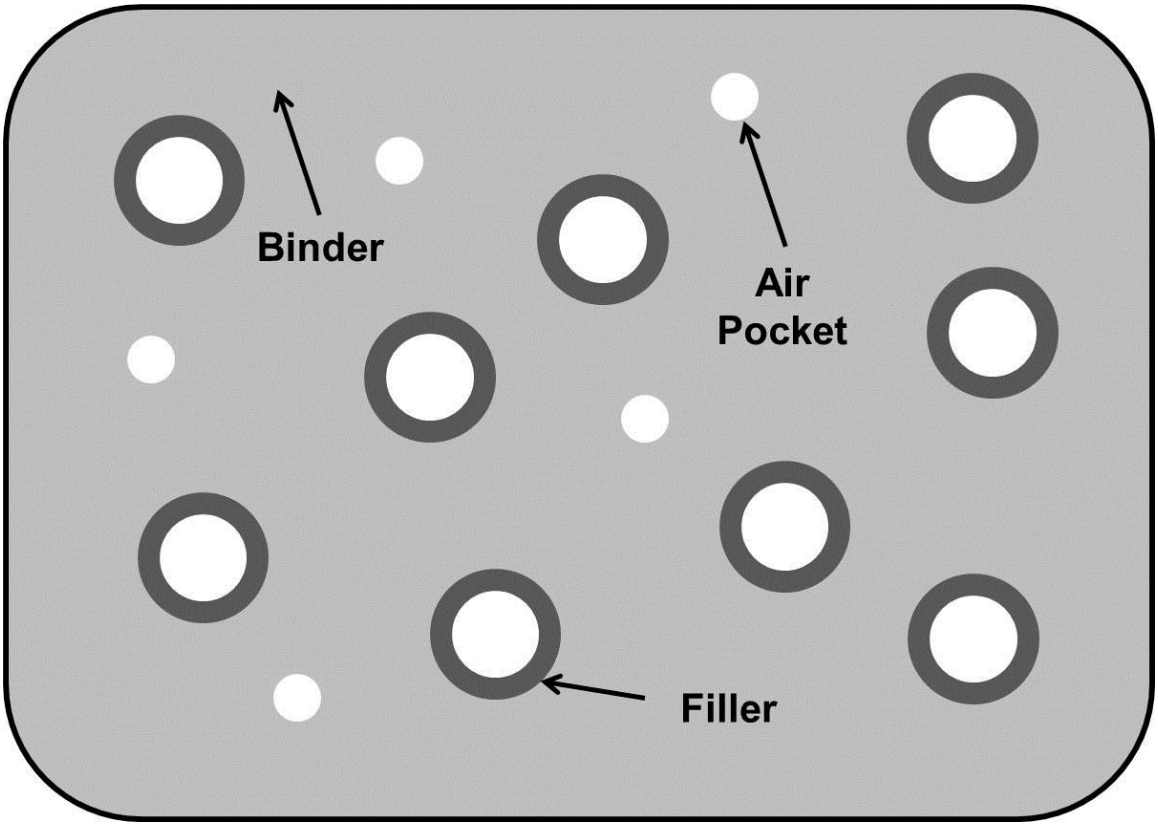


Figure 1.1 Scheme to illustrate structure and composition of syntactic foams.

The unique filler-binder structure enables syntactic foam to have some valuable properties, such as low density, low coefficient of thermal expansion, high strength-to-weight ratio, low moister absorptivity, and good resistance to hydrostatic pressure [4, 5]. These properties are highly influenced by several factors including the type, volume fraction, size, and distribution of fillers, matrix binder, filler/matrix interface, and processing conditions, and thus can be tailored to specific applications [6, 7].

A typical manufacturing process of syntactic foams consists of mixing of filler and binder, filling the mold or structure with the mixture, curing and post-treatment [8]. The major challenge lies in the mixing stage where a careful choice of processing parameters is required. Generally, the viscosity of the mixture should be maintained in a

certain range. The viscosity should not be too high. Otherwise, the mold filling step will be influenced, resulting in cavities or incomplete filling. To assist in the filling step, vacuum is frequently used when the mixture is cast into the mold.

Syntactic foam has been extensively applied in the fields of marine, construction, aerospace, automobile, electronics, medicine, energy, etc. [9-11]. It is also worth noting that the high flexural modulus-to-weight feature makes syntactic foam very suitable to serve as the core material used in the construction of sandwich structures [9, 12].

### *1.1.2 Matrix/Binder*

The matrix binders of syntactic foam can be thermosetting resins, such as epoxy, unsaturated polyester, phenolic resin, polyurethane, silicone, and polybenzoxazine, or thermoplastics like polyethylene and polypropylene [12-15]. For the thermosetting materials, it is generally recommended for the binders to possess the following properties [8]:

1) Low viscosity
2) Easily controlled gelation time
3) Small exothermal effect during curing
4) Low curing shrinkage
5) Good adhesion and wettability to the filler
6) Compatibility with modifiers and fillers, including diluents, plasticizers, dyes, and flame retardants

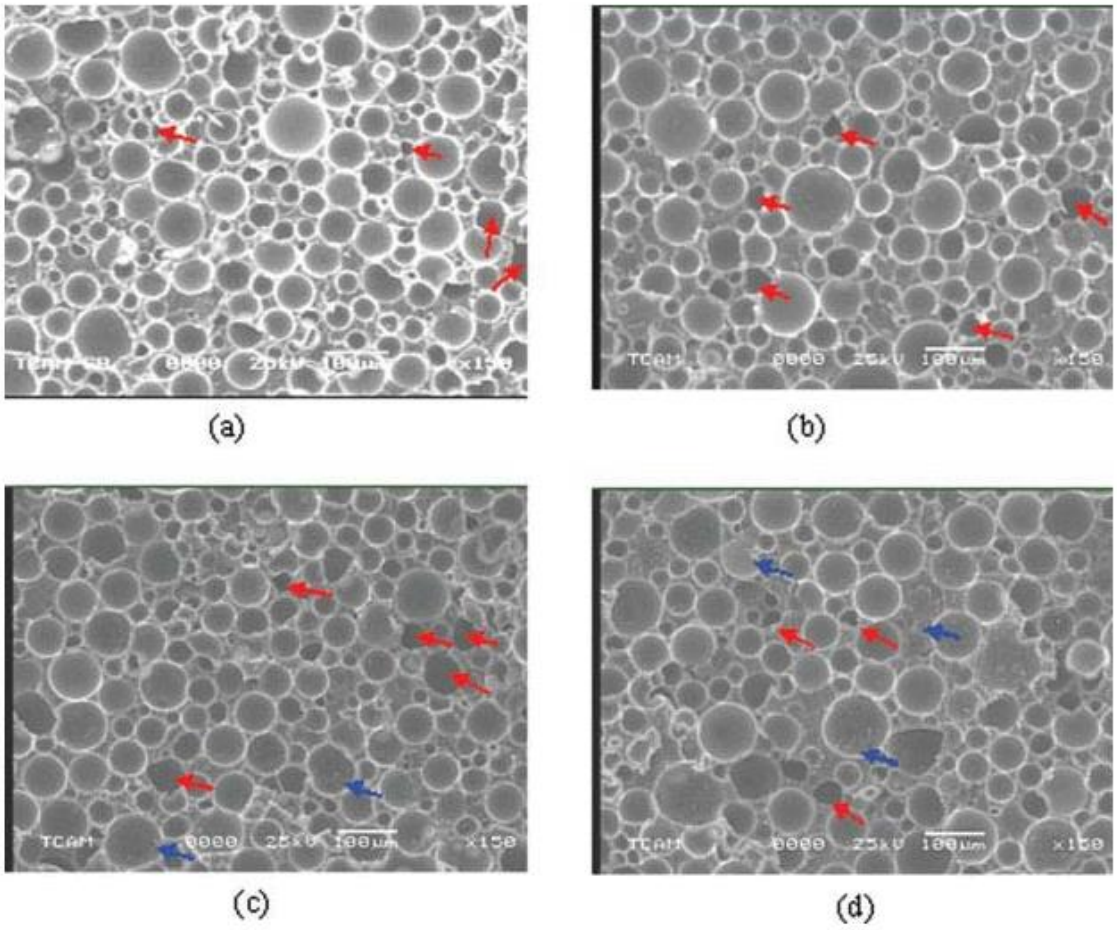


Figure 1.2 Microstructure of hollow glass microspheres filled epoxy syntactic foam showing voids and nanoclay clusters for (a) neat, (b) 1 wt% nanoclay, (c) 2 wt% nanoclay, and (d) 3 wt% nanoclay [16].

Among all of these choices, epoxy resin is the most popular one as the binder material in syntactic foam and extensively serves in structural and composites applications, especially for construction and aerospace industrials, because it can provide a unique combination of properties which are unattainable with other resins [17]. Uncured epoxy is available in wide range of physical forms from low-viscosity liquid to high-melting solids, enabling it to be amenable to various processes. Some very

attractive features are found in cured epoxy solid including but not limited to high strength, satisfactory adhesion to substrates, low shrinkage, good electrical insulation, high chemical resistance, and low toxicity [18]. Another appealing characteristics of epoxy is that it has an easy curing process without evolution of any volatiles or by-products, thus introducing no voids, compared with other resins like melamine and phenolic [19]. However, epoxy resin suffers from several deficient properties, for example, inherent brittleness and high material cost, hindering its further application in many areas [20]. An example on the hollow glass microspheres filled epoxy syntactic foams with nanoclay reinforcement is presented in Figure 1.2 [16].

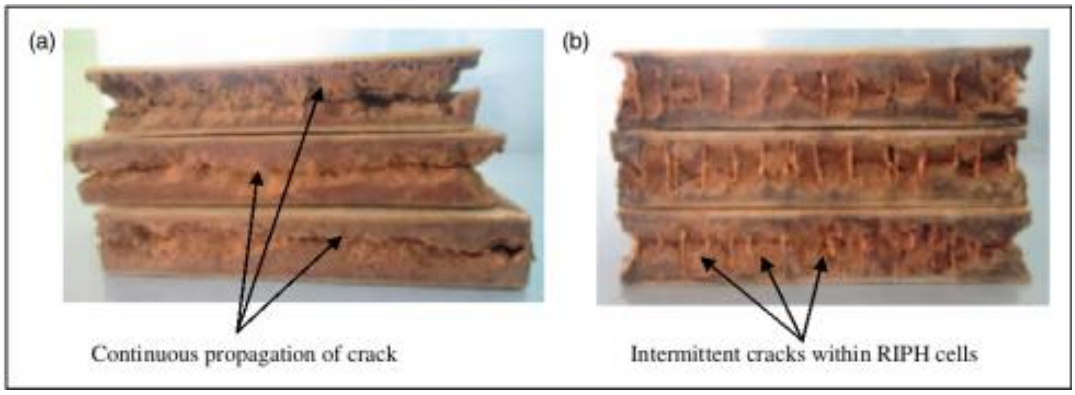


Figure 1.3 Fractures of phenolic resin matrix syntactic foam containing dry fly ash cenospheres and E-glass fiber reinforcing additives [12].

Phenolic resin is another widely employed thermosetting binder in the manufacture of syntactic foams. It is produced by the reaction of phenol and phenol substitutive with formaldehyde. Phenolic resin can be generally classified into two categories [21]. When the formaldehyde is excess with an alkaline catalyst, the resin is named as resole which possesses functional groups of hydroxymethyl group and dimethylene ether bridge.

Resole can be cured by the application of heat or acid through methylol condensation. On the other hand, when the phenol and phenol substitute are excess with an acidic catalyst, the resin is named as novolac which has no functional groups and must be cured by adding extra curing agent. Uncured phenolic resin is commercially available in either solid or liquid state. When cured, phenolic resin possesses high hardness and high stability, but a very low fracture strain [22]. It is also fire retardant due to the crosslinked structure with high concentration of benzene rings. Because of this, many fire resistant coatings contain phenolic resin as the major organic component [23]. An example to show the use of phenolic resin matrix syntactic foam containing dry fly ash cenospheres and E-glass fiber reinforcing additives for light weight structural applications is presented in Figure 1.3 [12].

### *1.1.3 Fillers*

The hollow or foamed microspheres are usually made of glass, metal, ceramics, phenolic resin, epoxy, polystyrene, polyurethane, polyvinyl chloride, etc. [24-26]. Generally, the fillers are required to be spherical, noncohesive, strong, intact, resistant to moisture and chemicals, and hydrolytically stable [8].

Hollow glass microsphere is most commonly used as the filler in syntactic foam. This is because it usually has high strength and significant difference in elasticity compared with polymer matrix. Since the processing techniques and sources of the raw materials have been well established for many years, the price of hollow glass microspheres are generally considerably cheaper than that of hollow polymeric microspheres. An example using hollow glass microspheres as the fillers in syntactic foam is shown in Figure 1.4 [3].

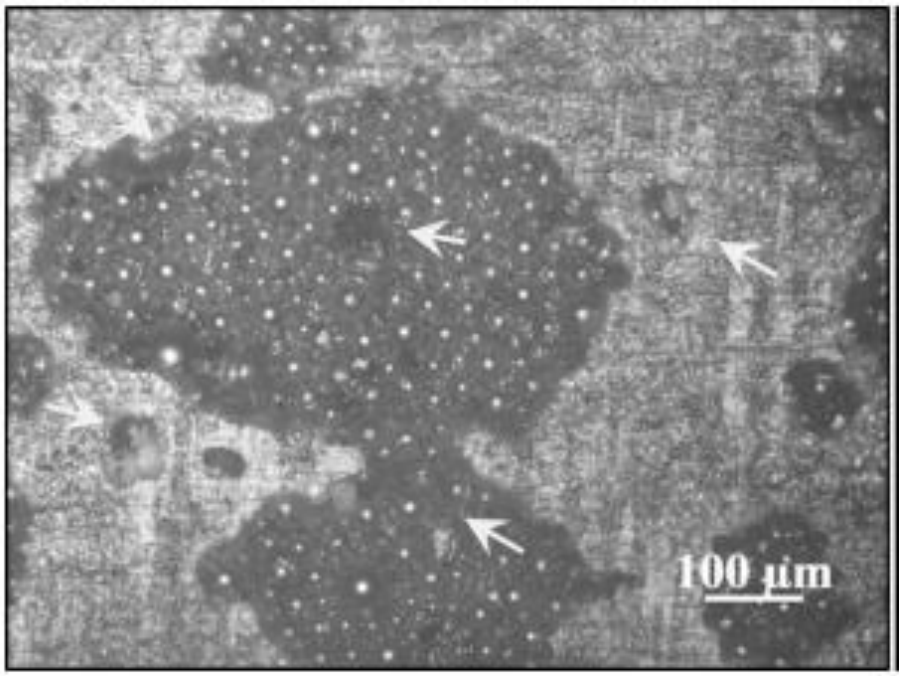


Figure 1.4 Micrographs of syntactic foams containing hollow glass microspheres as fillers [3].

However, the stiff and brittle nature of hollow glass microspheres usually results in poor processability and has side effects on performance of the foam, especially when brittle binder material, such as epoxy, is employed [4]. Moreover, since the density of glass is relatively high, hollow glass microsphere is less effective in weight reduction when applied to syntactic foam.

Polymeric fillers, in contrast, are less brittle and elastically deformable. When added in the binder material, they can enhance the material processability, improve the compatibility between microsphere and matrix resin, effectively reduce the density of syntactic foam, and toughen the syntactic foam [14]. Since the polymeric fillers usually give a very similar elasticity as the binder, the mechanical strength of syntactic foams made of these fillers are generally weaker than that of hollow glass microsphere filled

ones. However, when considering the density reduction effect, one can find a significant improvement in specific mechanical strength of syntactic foams with polymeric fillers. That is why these foams are more likely to be used in lightweight structural and floating applications.

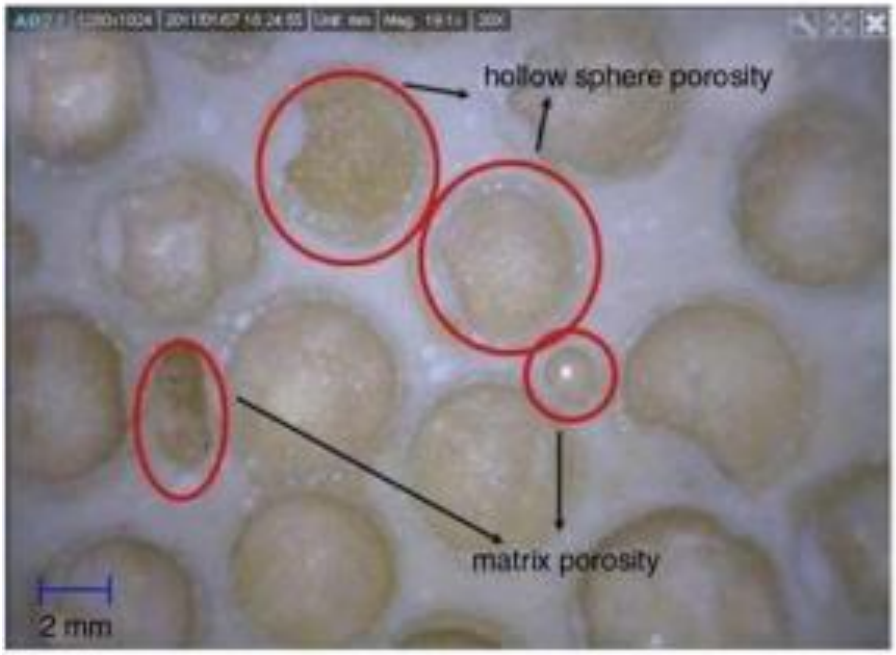


Figure 1.5 Micrograph of syntactic foam containing hollow epoxy microspheres as the fillers [27].

Samsudin and Bakar [27] reported a study that focused on the development of epoxy syntactic foam containing hollow epoxy microspheres as fillers. The hollow epoxy microspheres were created using an innovative approach that the expandable polystyrene microspheres were first coated with epoxy resin and then served as the sacrificial templates at high temperature which shrank the polystyrene beads and thus produced hollow structure. It was found that the hollow epoxy fillers had an excellent

adhesion with the binder material. The deformation pattern of the syntactic foams made in this study was observed to be very similar to those of the other types of syntactic foams. Huang and Nutt [28] fabricated phenolic resin syntactic foam with hollow phenolic microspheres which was reinforced by chopped carbon fibers. It was found that the syntactic foam can be substantially strengthened by relatively small amount of short carbon fibers. The relationship of syntactic foam density to foam density was seen to follow a power-law behavior.

Among all of the hollow polymeric microspheres mentioned above, expandable thermoplastic microsphere (ETP) is a very promising class but its application in syntactic foam has not been well explored. The usage of ETP in syntactic foam will be discussed in details in 1.2.2.

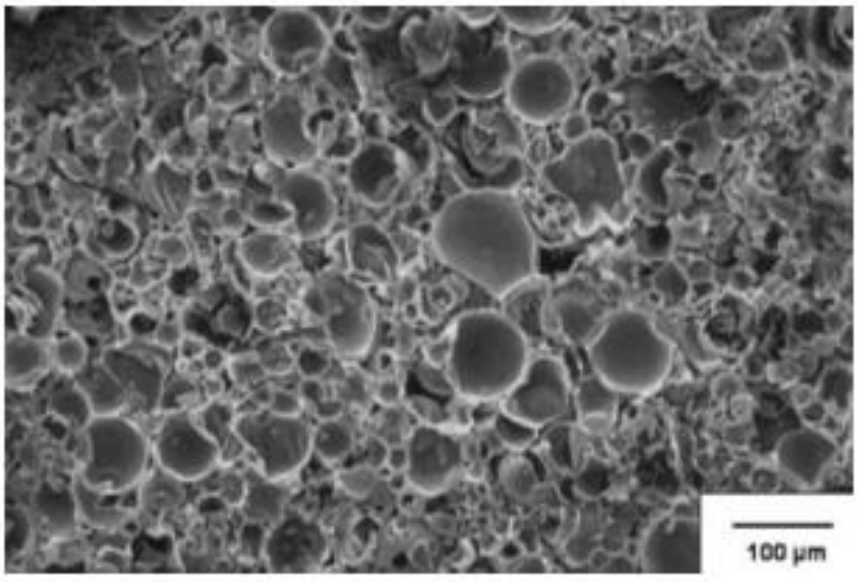


Figure 1.6 Micrograph of the fractured section of syntactic foam containing hollow phenolic microspheres as fillers [28].

## 1.2 Expandable Thermoplastic Microsphere

### *1.2.1 Expandable Polystyrene*

Among many types of ETP, expandable polystyrene (EPS) is the most widely employed in the industrial applications. It is the raw material used for molding foamed polystyrene products that are extensively used as buffering or thermal insulation materials in construction and packaging. EPS is manufactured in the form of very small polystyrene microsphere with a weight-average molecular weight between 160,000 and 260,000 and contains physical blowing agent, usually pentane or butane [29]. The unexpanded microsphere has a diameter ranging from 0.2mm to 3.0mm. The microsphere can be up to 25 to 40 times larger in volume with a closed-cell cellular structure when expanded at elevated temperature [30].

The manufacturing process of unexpanded EPS usually contains polystyrene polymerization, physical blowing agent impregnation, drying and sieving, as shown in Figure 1.7. Solid polystyrene microspheress are first produced using emulsion or suspension polymerization with styrene monomers. The bead size and molecular weight are controlled by the amount of additives and catalysts and reaction parameters, such as reactor temperature and agitation speed. Since the polystyrene polymerization process is an exothermal reaction, special cares to the control of reactor temperature and pressure should be addressed. The physical blowing agent, such as pentane or butane as mentioned above, are then impregnated into the soft polystyrene beads under pressure. When the impregnation step is completed, the entire system is dumped into de-watering bath. After dewatering, the produced beads are transported into dryers to further remove the residual water. The dried EPS microspheres are finally screened through a sieving system to have the desired sizes. Common sizes of unexpanded EPS

microspheres include Large “A”, Medium “B”, Small “C”, and Cup Grade “T”. Usually, for large quantity, the unexpanded EPS microspheres are stored in specially designed low hydrocarbon permeability liners. Even with such special care, the blowing agent that is quite volatile can be dissipated over time. A low storage temperature is also recommended since the emission rate of blow agent is in proportion to the storage temperature.

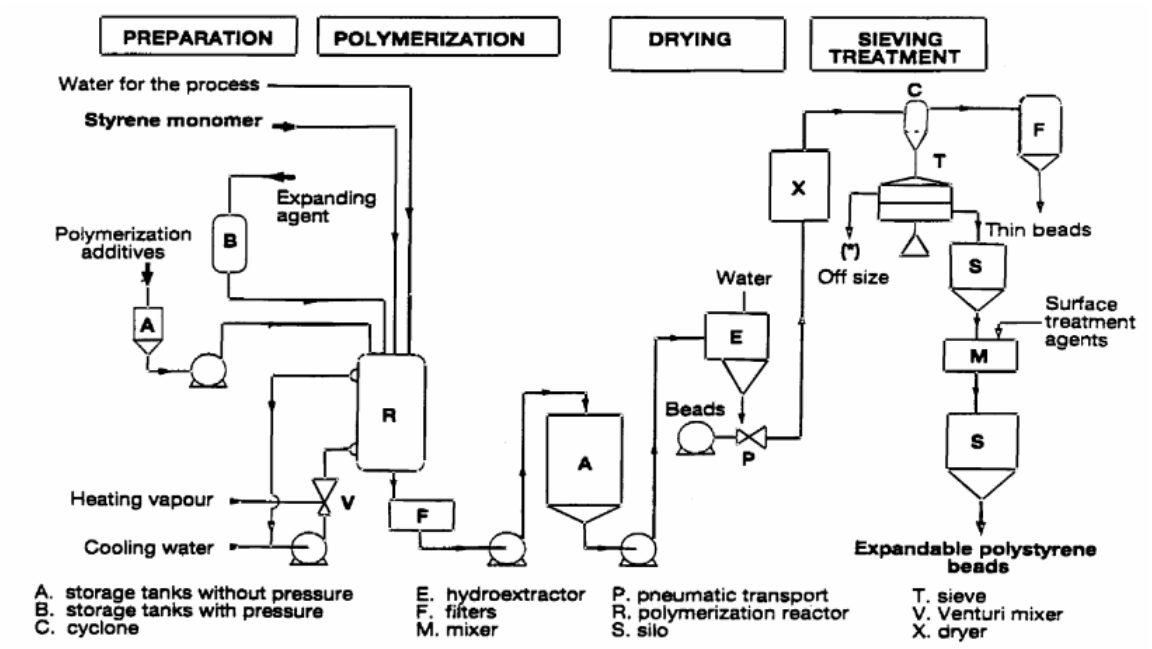


Figure 1.7 Manufacturing unit of expandable polystyrene [31].

Expanded EPS or EPS foam exhibits several appealing features that meet the requirements of a number of applications such as construction, package, flotation, and transportation. These features include but are not limited to low density, good thermal insulation property, satisfactory mechanical properties and good water resistance. The process to manufacture the EPS foams generally include three steps, namely, pre-

expansion, stabilization, and block molding, as presented in Figure 1.8. A prepuff particle with desired size and density is first generated in a pre-expansion vessel from unexpanded EPS. The vessel is equipped with inlets for steam and air, agitation blades, and automatic feeding system. The unexpanded EPS microspheres are quickly expanded to the required density via controlling the bead feed rate, steam and air flow, agitation speed. The expansion time control should be emphasized because an extended period in pre-expander results in a subsequent collapse of the foamed microspheres. After the pre-expansion step and a short drying, the produced prepuff is then transferred to holding bins to reach ambient temperature. This process can take as long as days to stabilize the expanded beads to further eliminate residual water and dissipate the excess blowing agent. The stabilization step is necessary for the following block molding step. The prepuff is molded into different geometries in a specially designed stainless metal molds with openings to have steam entered and condensed water escaped. Vacuum chamber is usually installed on the block molds to assist the steam penetration during molding. After being molded, the EPS foamed blocks are allowed to stabilize for at least one day at room temperature or higher. Such molding process can also be achieved with specially designed injection molding machine which allows automatic fill, mold, and ejection completed as one cycle.

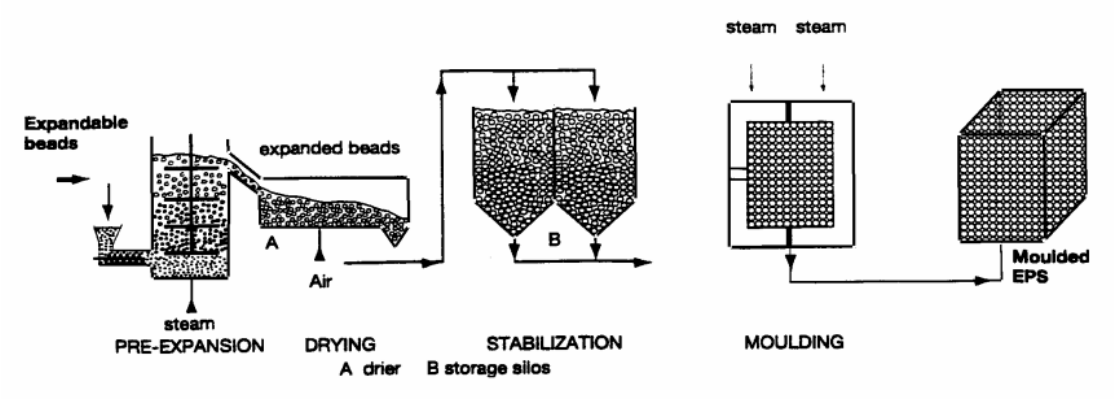


Figure 1.8 Manufacturing unit of molded expanded polystyrene foams [31].

*1.2.2 EPS-filled Syntactic Foam*

Despite only a few reports found, EPS-filled syntactic foam has shown its high potential to serve as a novel class of engineering materials, especially for lightweight structural applications. Here are some examples.

Brooks and Rey [32] prepared EPS-polyurethane syntactic foam which was designed as automobile crash pad. The unexpanded EPS microspheres were first well-blended with polyurethane system and then the fillers were foamed by the heat generated from the curing of matrix. An impact resistance test was conducted to study the performance of the syntactic foamed products. It is found that the EPS-filled polyurethane syntactic foam can absorb much larger amount of impact energy as the result of collapse of discrete rigid foamed polystyrene microspheres, compared with conventional polyurethane pad. Moreover, since the EPS is much cheaper than that of the polyurethane, the cost of pad is considerably lowered.

Lawrence and Pyrz [14] produced EPS-filled syntactic foam with polyethylene as the matrix material using a single screw extruder. The low density polyethylene with low

melting point was chosen as to maintain the cellular structure of the fillers. The morphology of the syntactic foam is presented in Figure 1.9. It is discovered that the extruded EPS-polyethylene foam possessed higher specific creep than neat polyethylene. Moreover, compared with the neat polymer, the syntactic foam was of a much larger stress relaxation modulus over density squared, indicating the EPS-filled polyethylene is a better choice for the structural beam applications.

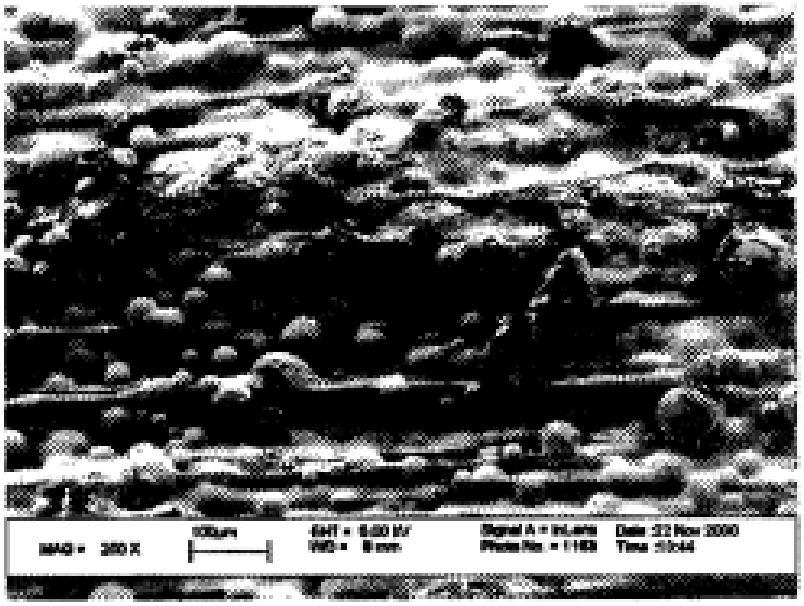

Figure 1.9 Micrographs of EPS-polyethylene syntactic foams [14].

Expanded thermoplastic microspheres can also be incorporated in inorganic matrix. A study conducted by Aglan and Ahmad [33] added Expancel microspheres which were made from acrylic copolymer containing isopentane as the fillers into Portland white cement. It is found that a 2.5-fold increase in indirect tensile strength and 30% increase in thermal resistance can be achieved by incorporating only less than 1% (w/w) expanded Expancel into Portland white cement. Moreover, the water diffusion in cement

can be considerably improved with the addition of Expancel, resulting in an improved hydration process. It is also revealed that the nanoscale roughness of the cement increases with proximity to an Expancel using atomic force microscopy as shown in Figure 1.10.

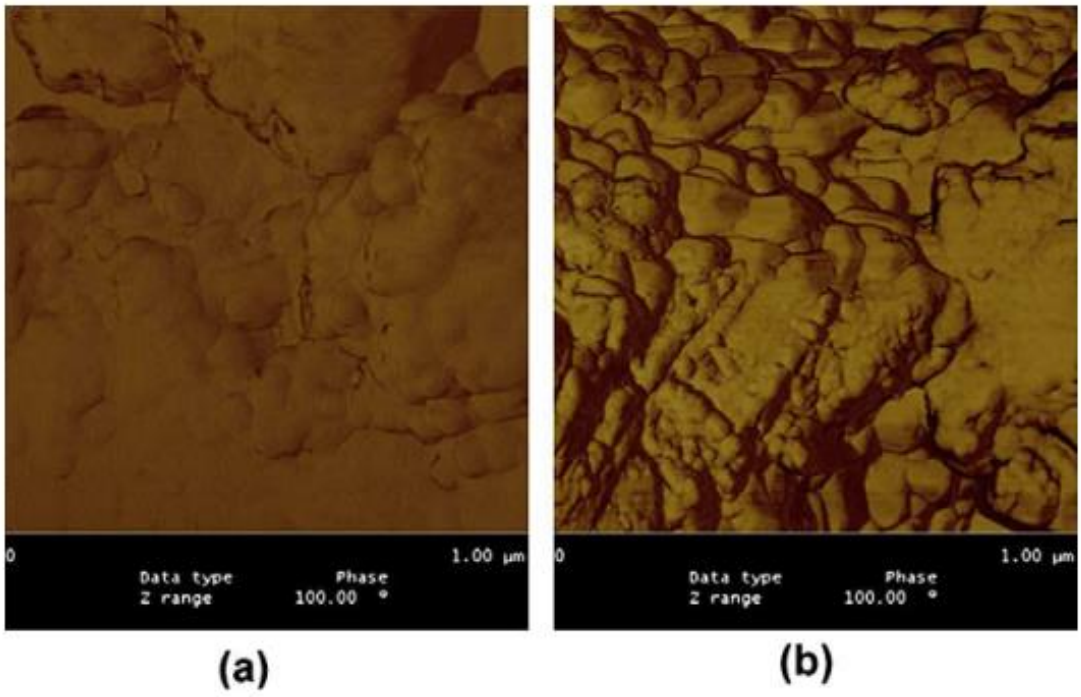


Figure 1.10 (a) Atomic force micrograph of neat white Portland cement (b) atomic force micrograph of white Portland cement with 0.1% Expancel microspheres. Micro-graph taken in an area a few millimeters away from a microsphere [33].

Kim and Kim [34, 35] proposed a new epoxy toughening mechanism by introducing thermally treated EPS microspheres. They deduced and then experimentally proved, as shown in Figure 1.11 and Figure 1.12, respectively, that the residual compressive stress around dispersed microspheres via thermal treatment is the major toughening mechanism rather than the cavitation. It is found that the epoxy samples containing

thermally treated EPS microspheres has a considerable higher specific fracture energy and critical stress intensity factor than those of neat epoxy, indicating an effective toughening phenomenon occurred.

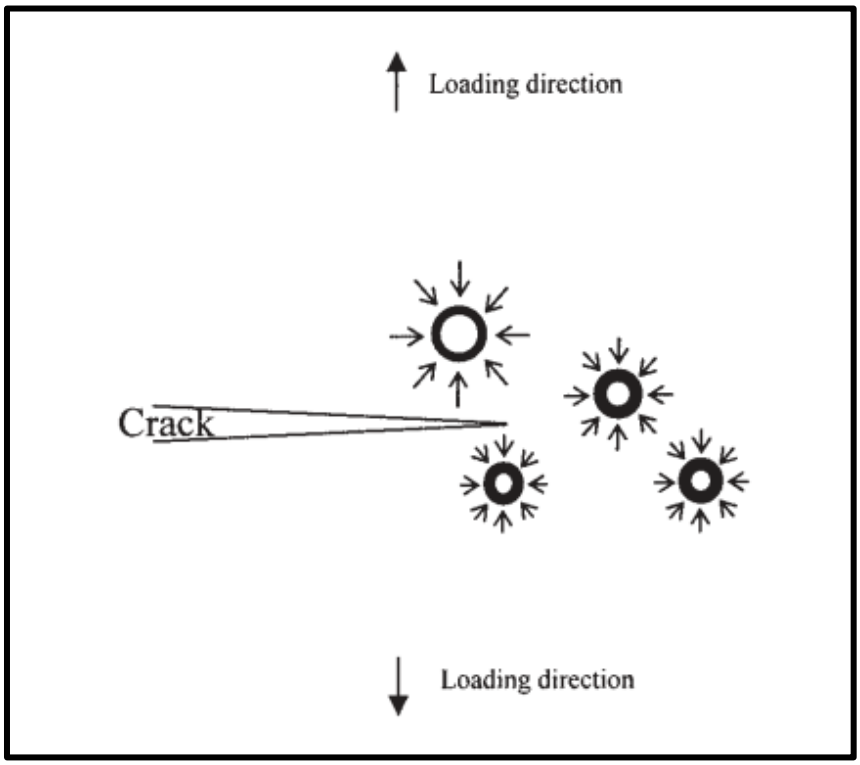


Figure 1.11 Residual compressive stresses around micro-spheres in the vicinity of the crack tip before loading [35].

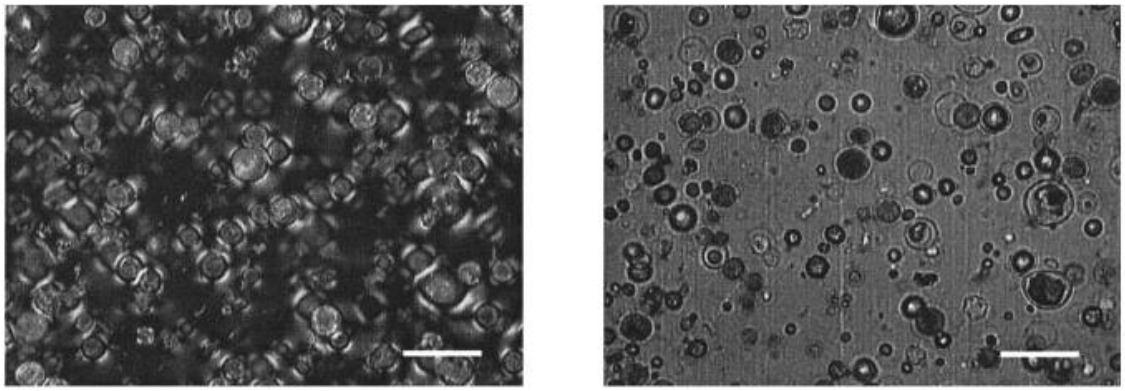


Figure 1.12 A thin section of EPS-filled epoxy sample showing heat treatment effect: (a) polarized and (b) unpolarized. The polarized image displays strong fringe patterns around microspheres representing residual stresses [34].

Shutov [36] studied the reinforcing effect of expanded EPS microspheres in polyurethane elastomer. It is found that, with the increase of the EPS loading, the density of the syntactic foam decreases while the tensile strength first increases then decreases and reaches the maximum at approximately 10% (w/w). A same tendency was obtained for the specific tensile strength.

Peng and Peng [37] extruded microcellular polylactic acid (PLA) parts using EPS or supercritical nitrogen. All of the foamed parts had a decent reduction of density ranging from 10% to 20%. As shown in Figure 1.13, it is found that the PLA parts with EPS as the pore generators has a better surface quality compared with that made by nitrogen. In Figure 1.14, the nitrogen-blown PLA foam was measured to have higher tensile modulus and strength than those with EPS. However, a much higher strain at break was observed for the PLA syntactic foam with high loading of EPS.

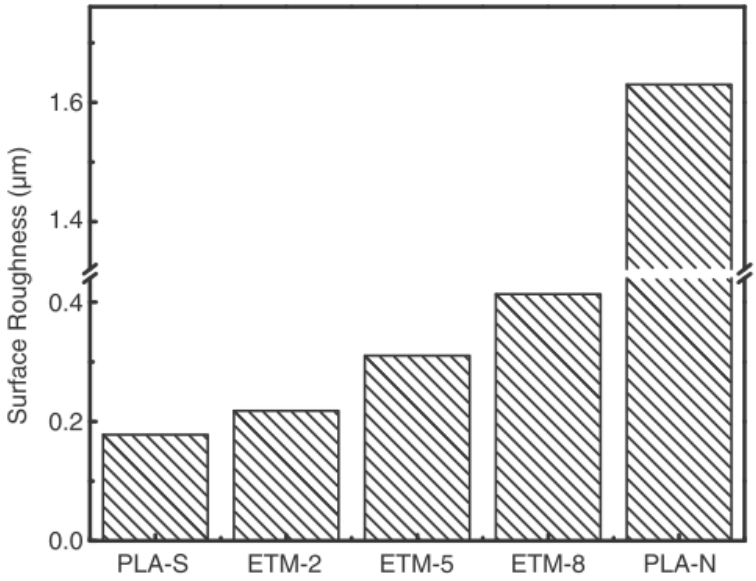


Figure 1.13 Two-dimensional surface roughness of solid and microcellular PLA parts with different loadings of EPS or foamed with supercritical nitrogen [37].

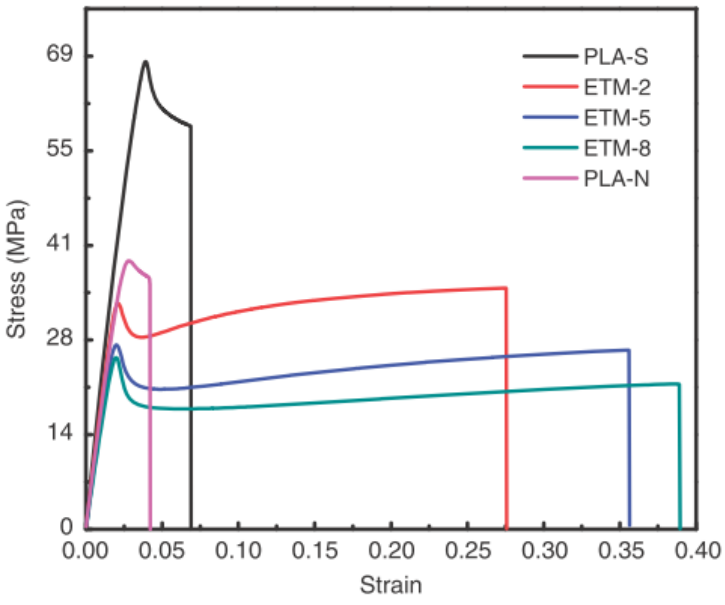


Figure 1.14 Mechanical properties of solid and microcellular PLA parts with different loadings of EPS or foamed with supercritical nitrogen [37].

## 1.3 Fire Retardation of EPS Foam

### *1.3.1 Burning Characteristics*

Applications of EPS foams have been restricted in recent years due to some fire safety considerations. Since EPS foams are made of polystyrene, usually having pentane as blowing agent, they are easily ignited with a limiting oxygen index of only 18 [30]. Once the foam is ignited, the flame can spread along the foams rapidly and sustain itself even when the fire source is removed. Moreover, during combustion of EPS foams, toxic heavy black smoke is generated with an obvious material dipping phenomenon. The smoke can irritate human respiratory system and enable asphyxia. The burning dripping material can flow and ignite other combustible materials. In addition, especially when the foam blocks or slabs are used for housing thermal insulation layers, a disastrous collapse of foam structure occurs in fire, resulting in the shedding of painting and decorating layers at building outer walls. This usually hinders firefighting and rescuing actions due to the destruction of working surfaces, leading to a severe life and property loss [38].

A number of tragedies have happened in recent years due to EPS fire. In September 1991, a fire occurred in a chicken processing factory constructed from insulated EPS panel, located in North Carolina. Of the 90 staff present at the time of the blaze, 25 were killed and a further 54 injured. In 2010, EPS foam in exterior insulation panels ignition caused by welding in Shanghai, China, produced a horrific fire, claiming the lives lost of 58 and injuring more than 70 others [39]. An EPS foam accelerated fire in Roubaix, France, in May, 2012, leaving one dead, 10 injured and 94 homes uninhabitable. Therefore, fire-retardant EPS foamed articles are highly desired.

*1.3.2 Fire Retardation*

Currently, three processes are available for the manufacture of fire retardant EPS foam products, including copolymerization [40-42], pre-blending [43-45], and particle coating [46-49]. Although these methods can improve the fire retardancy of conventional EPS foams to some extent, no satisfactory products have been successfully made using current technologies.

In the copolymerization method, the fire retardant agent is added into styrene monomer suspension as the second monomer or directly covalently bonded with styrene oligomers via chemical reaction during emulsion polymerization stage of unexpanded EPS beads preparation. This method enables the fire retardant agent to be distributed uniformly on the backbone of polymer chains, leading to the improvement of fire retardancy of end products. Pre-blending method works in a similar way as the copolymerization method except that no chemical reactions occur to form covalent bonds between polystyrene and fire retardant agent. The fire retardant agent is simply physically distributed in the unexpanded EPS beads. In the particle coating method, a fire retardant coating is prepared and coated on the surface of unexpanded or pre-expanded EPS beads to empower fire retardancy. The major issue of copolymerization method and pre-blending method is that the fire retardant agent used is typically the high efficient compound containing halogen or phosphorus, such as hexabromocyclododecane and 9,10-dihydro-9-oxa-10-phospha-phenanthrene-10-oxide, because only a small amount of fire retardant can be added. Otherwise, the following foaming process will be hindered. However, since these compounds can cause environment issues and damages to human body when ignited, their uses are now restricted by laws and regulations in some of the countries [50].

The particle coating method is used to coat fire retardant coating on the pre-expanded EPS beads to impart the fire retardancy. A relatively large amount of fire retardant can be incorporated in the EPS-coating system. Therefore, some halogen-free inorganic fillers, including but not limited to aluminum hydroxide, magnesium hydroxide, clay and graphite, that typically need to reach a high filler loading (larger than 50% w/w) to impart fire retardancy, can be used in this method. Several issues are limiting the further application of this method. First, the resultant mixture of pre-expanded beads and coating material typically has a considerably high viscosity. This leads to processing issues, such as high processing cost, large difficulty in uniformly dispersion of component, uneven coating on foamed EPS beads, and hindrance in post-foaming process. Second, the most widely used coating material matrix resins are mainly formaldehyde-based thermosetting polymers, including phenol-formaldehyde resin, urea-formaldehyde resin, and melamine-formaldehyde resin. It has been proven that formaldehyde is slowly released to the atmosphere from these resins [51, 52]. Many comprehensive studies have revealed that formaldehyde can result in long recognized irritation, induce nasal tumors in rodents, and increase the risk of certain cancers in human being [53, 54]. Third, the addition of large loading of inorganic fillers usually leads to a considerable decrease of mechanical strength and extensibility of the coating material [55]. This eventually results in a poor mechanical performance of prepared fire retardant EPS foam products. Therefore, fire-proof environment-friendly EPS foams that have good mechanical performance and can be produced in an economic industrial-scale process are desirably awaited in the polymer industry.

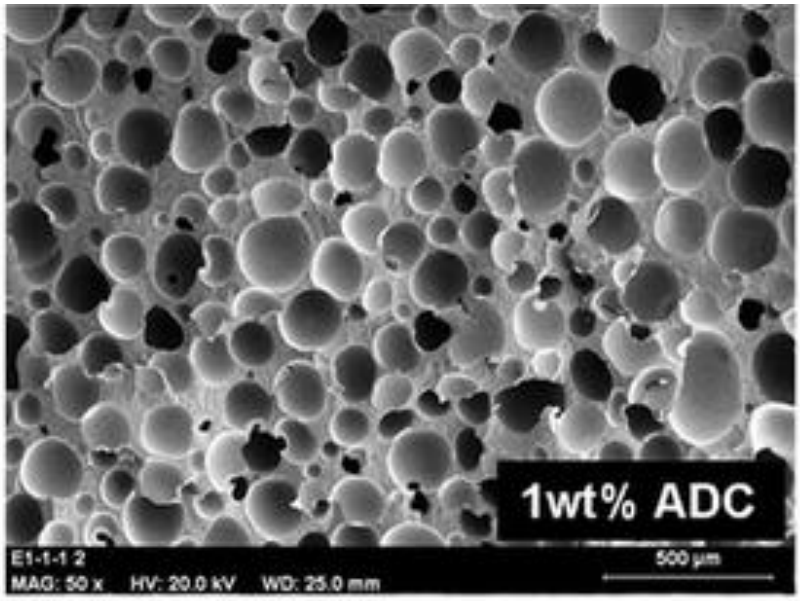


Figure 1.15 Micrograph of polyurethane foam blown by azodicarbonamide [56].

## 1.4 Modeling of Physically Foamed Plastics

### *1.4.1 Physically Foamed Plastics*

Usually, the cellular structure in foamed plastics is generated by a blowing agent that is embedded in the polymer melt to form a gaseous phase. A great variety of blowing agents are currently available to produce foams with different morphologies and are generally categorized into two major types, chemical blowing agents (CBA) and physical blowing agents (PBA) [1].

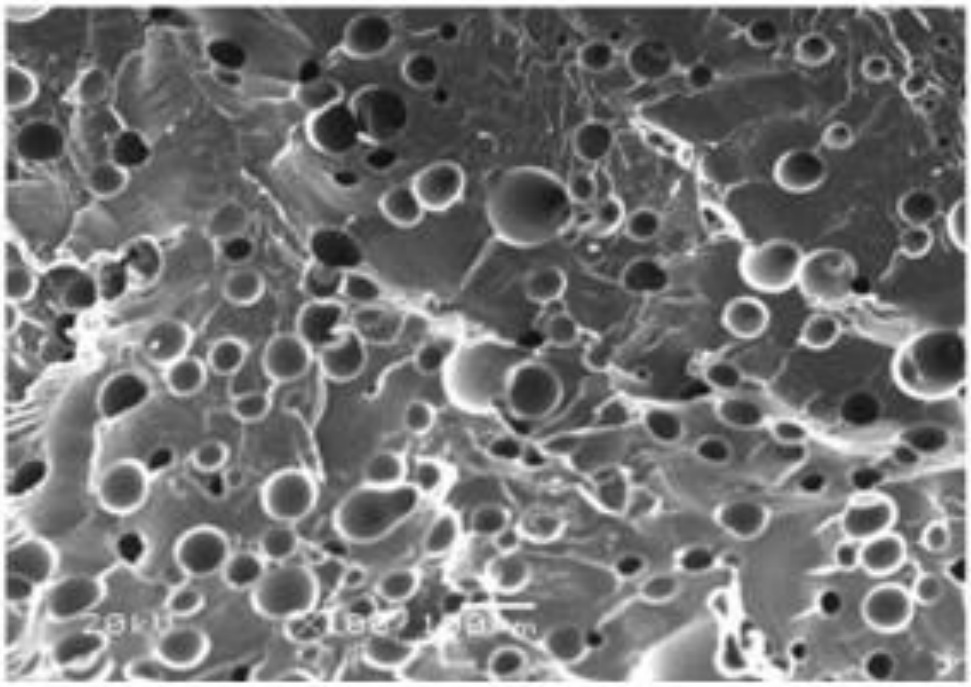

Figure 1.16 Micrograph of poly(ethylene terephthalate) foam blown by supercritical nitrogen [57].

For chemically foamed plastics, the foaming process occurs through the heat-induced CBA decomposition that releases gas. Saiz-Arroyo and Rodríguez-Pérez prepared polyurethane foams with a chemical blowing agent of azodicarbonamide as shown in Figure 1.15 [56]. The physically foaming process is triggered by converting the PBA from liquid state to gas state, usually with sudden increase of system temperature or decrease of system pressure. Xi and Turng extruded foams made of poly(ethylene terephthalate) with a physical blowing agent of supercritical nitrogen [57]. The results are presented in Figure 1.16

### *1.4.2 Previous Modeling Efforts*

Numerical modeling of the foaming process is crucial to understand the fundamental aspects of the process and can provide important quantitative references for a further process optimization. Many efforts have been made to numerically simulate the physically foaming process. Most of these models are focused on the PBA-thermoplastics system triggered by a sudden decrease of system pressure.

Early work can be dated back to 50's and 60's in the last century. A single bubble model was used as the basic model to investigate the physically foaming process [58-61]. Most of these studies focused on the growth of a single bubble in an infinite sea of liquid [62-64]. The diffusion-induced bubble growth in viscous liquid with both mass and momentum conservations was analyzed. Later, Street [65] took the viscoelasticity of matrix liquid into consideration by incorporating a three-constant Oldroyd fluid model. A rigorous model with non-linear viscoelastic fluid model was formulated by Venerus [66]. In this work, the surface tension and inertial effects were studied. Many other researchers had also contributed to the development of the single bubble model [67-69]. The single bubble model has considerably improved the understanding of the bubble expansion in the foaming process. However, since a swarm of bubbles grow simultaneously in the actual foaming process, the practical application of this model is very limited.

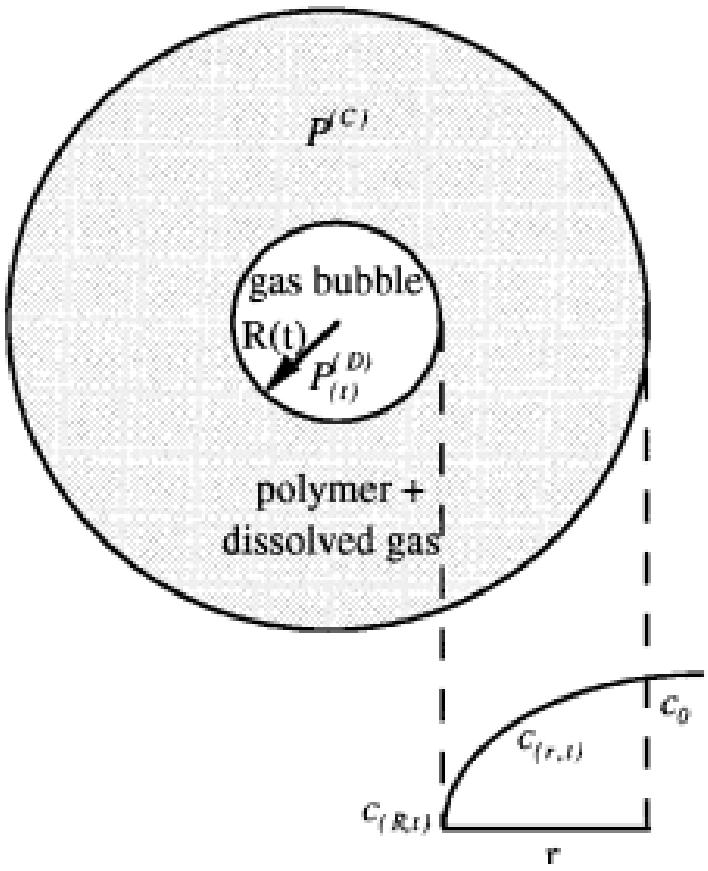


Figure 1.17 Scheme of bubble growth in IVA [70].

In order to simulate the bubble growth of a large amount of bubbles in close proximity to each other in a gas/polymer solution, the cell model was introduced by Amon and Denson [71]. It divided the gas/polymer solution into many spherical unit cells that contained equally limited amount of dissolved PBA. Arefmanesh and Advani [72] approximated the dissolved gas concentration gradient in the unit cell as a polynomial profile to simplify the calculation involved. Later, they extended this work by considering the viscoelastic property of polymer [73] and non-isothermal effects [74]. The effects of dissolved PBA content and gas loss to surrounding were studied by Ramesh [75] to simulate a more realistic situation.

In the physically foaming process, cell nucleation and cell growth are competing for the limited PBA dissolved in the polymer melt. An influence volume approach (IVA) was proposed by Shafi and Joshi [70, 76] to simultaneously consider these two processes, as shown in Figure 1.17. The cell model was used to simulate the bubble growth process and the cell nucleation rate was quantitatively expressed by a classic heterogeneous nucleation theory. Since the IVA model was able to characterize the interaction between cell nucleation and growth in the foaming process, it can quantitatively simulate the experimental data. After the initial work, many researchers have extended or modified IVA model to simulate the foaming phenomena in different material systems [77-93].

### 1.5 Microwave Heating Technique

Although different techniques may be used for volumetric heating, microwave heating stands out as an effective, fast and environmentally friendly method with low cost. When microwave is penetrating a bulk material, the electromagnetic energy is absorbed by the material and transformed to kinetic energy and potential energy of the molecules, thus heating the inner and outer parts of the material simultaneously and homogeneously [94].

Compared with convective heating and conduction heating, microwave heating possesses several advantages including rapid volume heating, no overheating spot on surface, controllable heating rate and energy input, energy saving, and low operation cost [95-97]. Moreover, microwave heating features with a special self-limiting heating phenomenon that the materials are less susceptible to microwave heating once the

polymerization or crosslinking reaction occurs and thus the heating will automatically focus on the unreacted part [98].

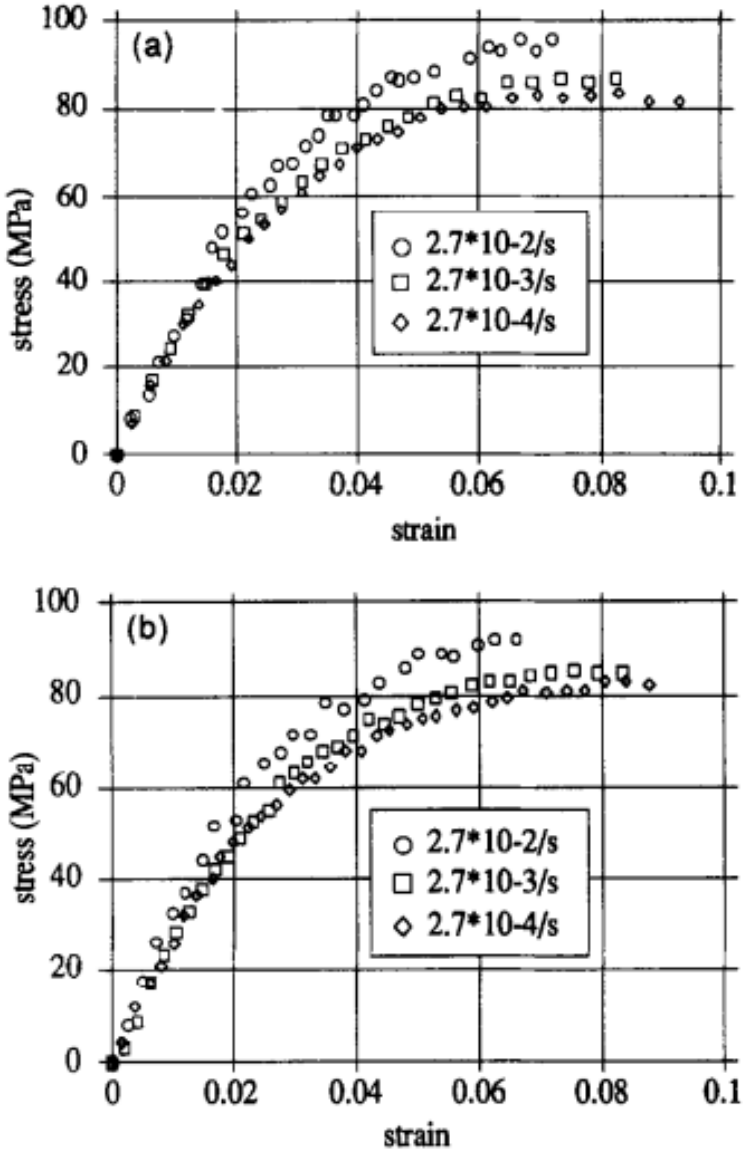


Figure 1.18 Stress-strain relationship in tension of studied resins: (a) microwave cured resin; and (b) thermal cured resin [99].

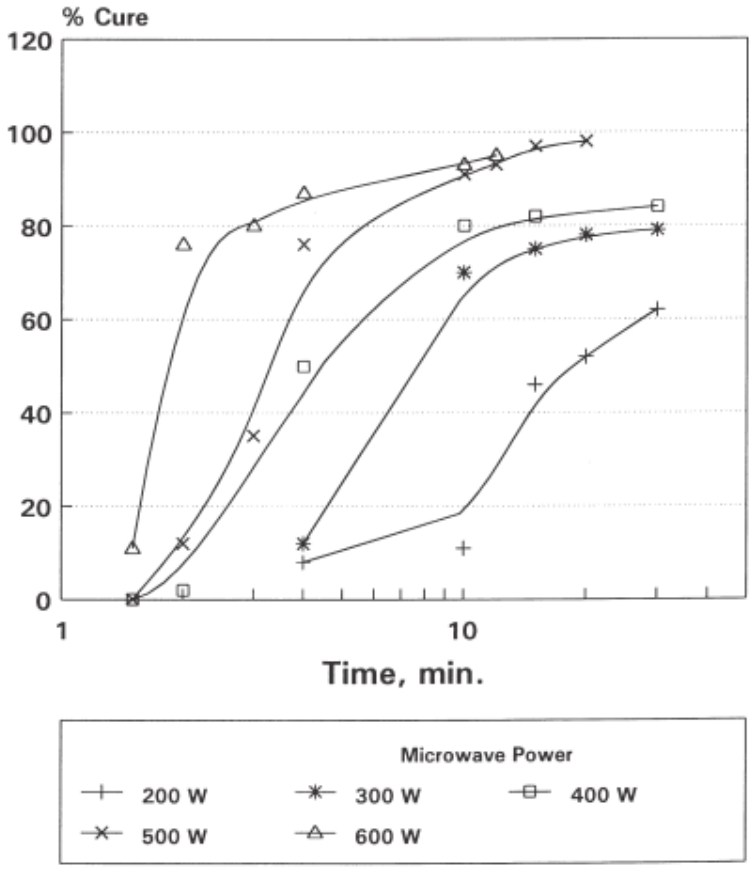


Figure 1.19 Influence of input microwave power over the curing behaviors of epoxy resins [100].

Due to the appealing features mentioned above, microwave has been widely used to cure thermosetting materials [101-106]. Bai and Francois [99] compared the mechanical properties of the epoxy samples cured by microwave or thermal heating methods. As shown in Figure 1.18, it is found that the epoxy samples cured by microwave or thermal heating demonstrate very similar tensile behaviors. However, with the consideration that the time taken by microwave heating is much less than that by thermal heating, it can conclude that the microwave curing method outweighs the conventional thermal curing. Boey and Chia [100] studied the influence of microwave

power over the curing behaviors of epoxy resins. It is observed that, with an increase of microwave power input, the initial curing rate and the required time for 100% cured increased significantly, as presented in Figure 1.20. However, one should notice that when a too high microwave power is chosen, the curing process is less controlled, resulting in the generation of burnt marks.

### 1.6 Challenges and Motivations

Little progress has yet been made to effectively process EPS-contained syntactic foam. Currently, three processing techniques with limited capabilities are available to make syntactic foam containing expanded EPS microspheres.

The first technique is to directly blend expanded EPS microspheres with matrix resin [36]. However, since the expanded EPS microspheres have much lower density than the resin, it is difficult to achieve homogeneous mixing at high EPS loading. The problem exacerbates due to the high viscosity of the resin, and the expanded EPS can be easily deformed or even shredded by high shear forces in the mixing stage.

In the second technique, the EPS microspheres are expanded inside the matrix using the heat generated during the curing process [32]. Although it can lessen the mixing difficulty in the first technique, this process can only be applied to a very limited number of thermosetting resins that are specially formulated for this purpose with small EPS loading.

The last technique, which is also considered the most promising one, is to use thermal energy to expand the EPS microspheres in the mixture of unexpanded EPS and uncured resin. Existing efforts [33, 34, 107], however, have been limited to the use of

convection and conduction for heat transfer. The major issue with these thermal processes is that the temperature inside the foaming material is not uniform and the desired thermal history for foaming and curing is difficult to obtain. In the resulting material, the extent of foaming is typically low and the foamed microspheres are largely non-uniform.

Besides the difficulties in processing of EPS-filled syntactic foams, fundamental understandings in the expansion of EPS microsphere which plays a vital role to optimize the existing processes are still missing. Although many modeling efforts have been made, to simulate the foaming process with physical blowing agent, they are almost exclusively focusing on the systems foamed by sudden reducing the system pressure. These models cannot be directly employed to simulate the foaming process of EPS microsphere because the EPS expansion process is triggered by a sudden increase of system temperature. Moreover, usually the models mentioned in 1.4.2 do not take the geometry of foaming plastics into consideration since the foaming process occurs in extrusion or injection molding machine and the bubble size is far smaller than that of the machine chamber. However, the geometry of EPS microsphere must be considered when EPS expansion process is simulated because the shape and size of foamed EPS directly impact the morphology and property of resulting syntactic foams. Therefore, a model that is specially formulated for the EPS expansion is still awaited to enhance the fundamental understandings of this foaming process.

To address the emerging issues mentioned above, in this thesis work, a novel microwave expansion process was developed to produce thermoset-matrix syntactic foam containing expandable thermoplastic microspheres. This process was designed to have unexpanded ETP microspheres directly foamed in uncured thermoset matrix via microwave heating. This design demonstrated the capability to considerably decrease

the processing difficulty and effectively expand ETP of high loadings, fulfilling the requirement of industrial-scale production of syntactic foam filled with foamed polymeric microspheres.

The microwave expansion process was first validated by producing epoxy-based syntactic foam with expandable polystyrene (EPS) microspheres. The engineering aspect of this study focused on the development and optimization of the process, the establishment of process-structure-property relation, and the extension of the process application to broader areas. Moreover, in an effort to address the fundamental aspect, the expansion process of EPS microsphere was modeled based on continuum mechanics. The modeling work can considerably contribute to the understanding in the basics of EPS expansion process, providing important references for the simulation and optimization of similar processes.

# CHAPTER 2

# MICROWAVE PROCESSING OF SYNTACTIC FOAM FROM AN EXPANDABLE THERMOSET/THERMOPLASTIC MIXTURE*

## 2.1 Introduction

As demonstrated in Chapter 1, while hollow glass microspheres are commonly used as the microballoons in syntactic foam, their abrasive and brittle properties usually result in poor processability and have adverse effects on the foam performance, especially when a brittle binder such as epoxy is employed [28]. Polymeric microballoons or foamed microspheres, in contrast, are less brittle and elastically deformable. When added in the matrix, they can enhance the processability, improve the compatibility between the microspheres and the matrix, and toughen the syntactic foam [14]. Among known foamable microspheres, expandable polystyrene (EPS) is a promising choice, but its application in syntactic foam has not been well explored.

EPS is the raw material used for molding foamed polystyrene products that are usually used as buffering or thermal insulation materials in construction and packaging. It is manufactured in the form of small polystyrene microspheres containing physical blowing agents, usually pentane or butane [29]. The solid microspheres can be expanded into foams with a closed-cell cellular structure when exposed to elevated temperature [30].

However, little progress has yet been made to effectively process EPS-contained syntactic foam. Currently, three processing techniques with limited capabilities are available to make syntactic foam containing expanded EPS microspheres. The first

technique is to directly blend expanded EPS microspheres with resin [36]. However, since the expanded EPS microspheres have much lower density than the resin, it is difficult to achieve homogeneous mixing at high EPS loading. The problem exacerbates due to the high viscosity of the resin, and the expanded EPS can be easily deformed or even shredded by high shear forces generated during mixing. In the second technique, the EPS microspheres are expanded inside the matrix using the heat generated during the curing process [32]. Although it can lessen the mixing difficulty in the first technique, this process can only be applied to a limited number of thermosetting resins that are specially formulated for this purpose with low EPS loading. The last technique, which is also considered the most promising one, is to use thermal energy to expand the EPS microspheres in the mixture of unexpanded EPS and uncured resin. Existing efforts [33, 34, 107], however, have been limited to the use of convection and conduction for heat transfer. The major issue with these thermal processes is that the temperature inside the foaming material is not uniform and the desired thermal history for foaming and curing is difficult to obtain. In the resulting material, the extent of foaming is typically low and the foamed microspheres are largely non-uniform.

One effective method for increasing the heating uniformity in the EPS/resin foaming material is to apply volumetric heating. In this case, the heat is directly generated inside the foaming material, and non-uniform thermal effects from conduction and convention are minimized. Although different techniques may be used for volumetric heating, microwave heating stands out for the current application. When microwave is penetrating a bulk material, the electromagnetic energy is absorbed uniformly by the molecules in the material, thus heating the inner and outer parts of the material simultaneously [94]. Compared with convection heating and conduction heating, microwave heating has several advantages including rapid volume heating, no

overheating spot on surface, controllable heating rate and energy input, energy saving, and low operation cost [95-97]. Moreover, microwave heating features with a special self-limiting heating phenomenon that the materials are less susceptible to microwave heating once the polymerization or crosslinking reaction occurs, and thus the heating will automatically focus on the unreacted part [101].

In Chapter 2, a microwave expansion process is designed and developed to produce syntactic foam from an expandable thermoset/thermoplastic material. Expandable polystyrene microspheres and epoxy resin were chosen as a model material system for feasibility study and demonstration. The new foaming technique can process syntactic foam with high EPS loading and effectively expanded microspheres. A feasible process window for foaming was proposed and evaluated. Optimized process conditions were then determined. Flexural properties and toughening effects of the EPS/epoxy syntactic foam were subsequently studied. Finally, an effort was made to apply the microwave expansion process to mold syntactic foamed parts of relatively sophisticated geometry.

## 2.2 Conceptual Process Design

In microwave processing of syntactic foam from an expandable thermoset/thermoplastic mixture, the major control parameters are microwave input power, pre-cured epoxy viscosity, and microwave heating time. Since these three parameters (power, viscosity, and time) are generally independent with each other, the feasible process window determined by them is expected to be a hexahedron in 3D Cartesian coordinates, shown in Figure 2.1 (A). For illustration purposes, the boundaries of the process window are drawn as flat surfaces. However, in actual cases, the

boundaries can be nonlinear and the corresponding surfaces of the hexahedron can be curved.

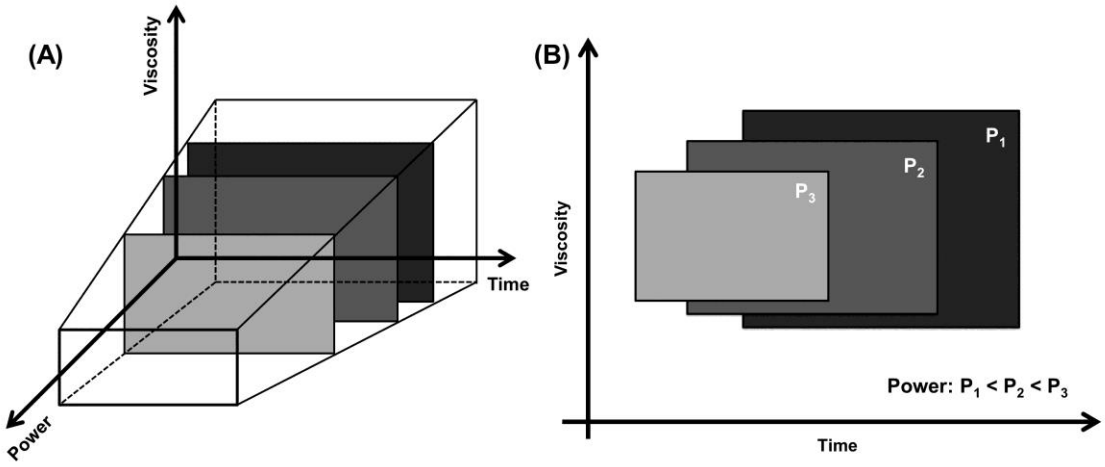


Figure 2.1 Feasible process window for microwave processing of syntactic foam from an expandable thermoset/thermoplastic mixture: (A) viscosity, time, and power as primarily controlling parameters and (B) viscosity and time as primarily controlling parameters when power is fixed.

The microwave input power is controlled by the microwave generating device employed in the process. The minimum power can be approximated by the ratio of the required energy for effectively expanding the thermoplastic microspheres over the pot life of the resin. The pot life here is used to estimate the longest curing time. To refine the minimum power, one may also consider the microwave absorptivity in the estimation. The maximum microwave input power can be determined by the factors related with the device and manufacturing process. For industrial-scale microwave ovens, the highest power can reach several hundreds of kilo-watts [94]. However, in most cases, an

extremely high input power is generally not preferred since it increases the difficulty in process control and the risk to generate defects in products.

In order to help illustrate the other two parameters, a 2D scheme is drawn in Figure 2.1 (B). The shadowed rectangles on the Cartesian plane represent the projections of cross-sections of the 3D process window in the direction of the power axis in Figure 2.1 (A). From $P_1$ to $P_3$, the power input increases. The viscosity in the vertical axis refers to the pre-cured resin viscosity while the time in the horizontal axis refers to the microwave heating time.

In the new syntactic foaming process, a pre-curing stage is needed for two reasons. First, with the expansion during microwave heating, the density of the microspheres decreases dramatically and thus the buoyancy will drag the foamed microspheres toward the upper surface of the mold, resulting in inhomogeneous distribution of microspheres. Pre-curing helps increase the viscosity and prevent separation due to buoyancy. Second, especially for the EPS and epoxy model system used in this study, a pre-cured resin is needed to prevent the dissolution of the microspheres in the resin during heating by partially cross-linking the resin. A relatively stable pre-cured resin can be prepared using a two-stage hardener addition method. To do so, one divides the required amount of hardener into two parts. The first part is mixed with the base resin first and cured for a prolonged time to reach desired viscosity. The second part is then added and mixed to form the pre-cured resin mixture. Due to the partial cross-linking of this resin mixture, the dissolution of the microspheres can be largely suppressed. Details on this approach will be further discussed in the Results and Discussion section.

From the above discussion, it is seen that the lower bound of the pre-cured resin viscosity should be set to suppress the buoyancy and inhibit the dissolution of the

microspheres. On the other hand, when the pre-cured resin viscosity is too high, it will be extremely difficult to remove the air pockets that are introduced during mixing and trapped in the resin. Therefore, a maximum viscosity should exist to prevent this problem happening.

With fixed microwave input power, the microwave heating time is proportional to the microwave energy input. The minimum heating time or energy input can be estimated based on the energy needed to effectively expand the expandable thermoplastic microspheres. With the consideration of microwave energy absorption efficiency, the energy used in actual cases should be considerably larger than the minimum value. The maximum microwave heating time or input energy is determined by the resin decomposition activation energy at which the material begins to decompose. Since heat loss exists in practical manufacture, a compensation factor, usually measured by experiments, should be multiplied with the decomposition activation energy to obtain the maximum heating energy. Dividing this maximum energy by the fixed power yields the maximum heating time for successful foaming.

It should be noticed from Figure 2.1 (B) that as the microwave input power increases from $P_1$ to $P_3$, the process window in the 2D Cartesian plane shrinkages and moves toward the left side. This can be explained as follows. In the viscosity axis, the maximum resin viscosity at higher microwave power is supposed to be lowered. This is because the difficulty for air bubbles to escape from the mixture increases as the resin curing process is accelerated. For the minimum viscosity, a higher value is resulted due to the increased expanding rate of microspheres. In the time axis, the process window shifts to the left side with the increase of microwave power because the heating time to achieve the required amount of energy decreases.

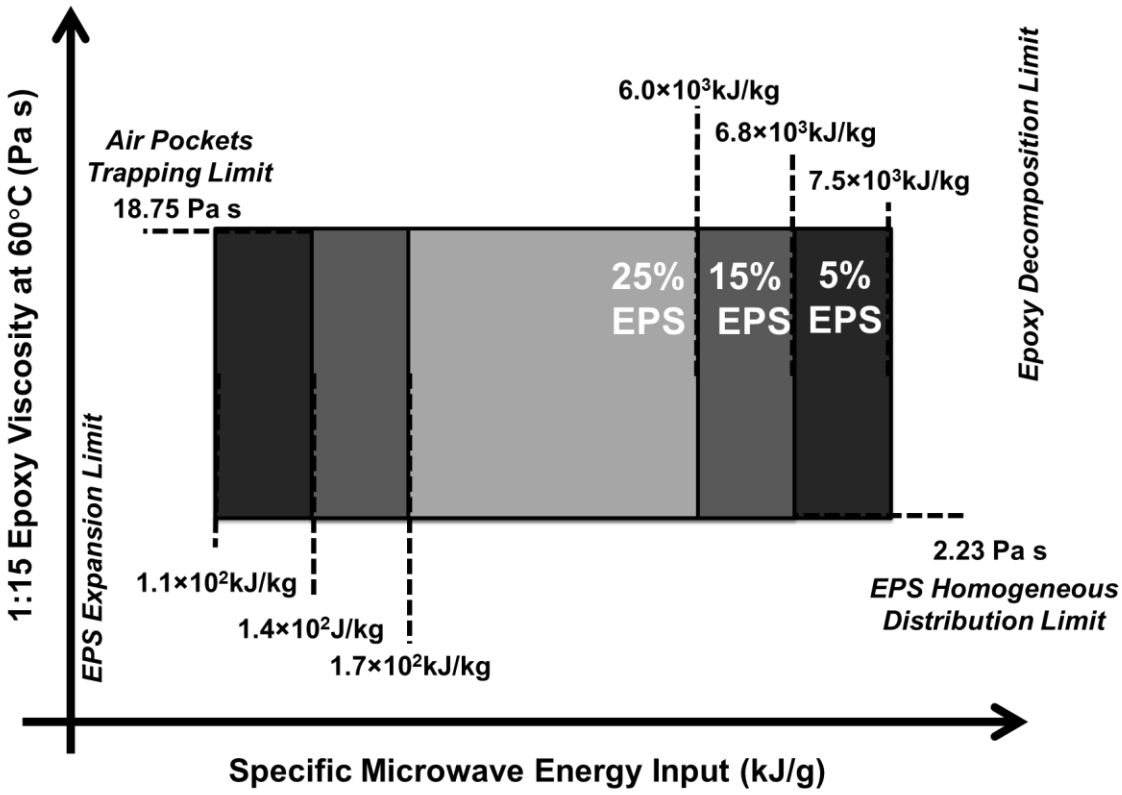


Figure 2.2 Feasible process window for microwave processing of syntactic foam from an expandable epoxy/EPS mixture, with varying EPS loading and fixed microwave power at 100W.

In this study, the microwave power was fixed at 100W to have a controllable expansion process. Since the microwave heating time is proportional to the microwave energy input at fixed microwave power, the specific microwave energy and pre-cured epoxy viscosity were set to be the two governing parameters for the process window (Figure 2.2). For easy understanding, the process boundaries are referred to as air pockets trapping limit, EPS homogeneous distribution limit, epoxy decomposition limit, and EPS expansion limit, respectively. With the variation of the composition of EPS-

epoxy syntactic foam, the corresponding values of these limits are different. Details on the determination of these limits via experiments and estimations will be further discussed in the Results and Discussion section.

## 2.3 Experimental

### *2.3.1 Materials*

Araldite®LY 8601 (base resin) / Aradur® 8602 (hardener), obtained from Huntsman Advanced Materials Americas LLC (Woodlands, TX), was chosen as the model epoxy system in this study. This low-viscosity, two-component system is widely used in vacuum infusion processes for advanced composites manufacturing. The base resin contains diglycidyl ether of bisphenol-A (DGEBA) as the major component with monofunctional epoxy compounds as diluents. The hardener consisted of aliphatic amines as resin curatives and substituted imidazole as an accelerator. The recommended mixing ratio of hardener to base is 1 to 4 by weight. Cup grade unexpanded EPS microspheres DYLITE® F271T were obtained from Nova Chemicals Corporation (Moon Township, PA). The unexpanded EPS contains 5.3-5.9% by weight of pentane as a blowing agent. The average diameter of unexpanded EPS microspheres was measured to be 388.6$\pm$17.8$\mu$m.

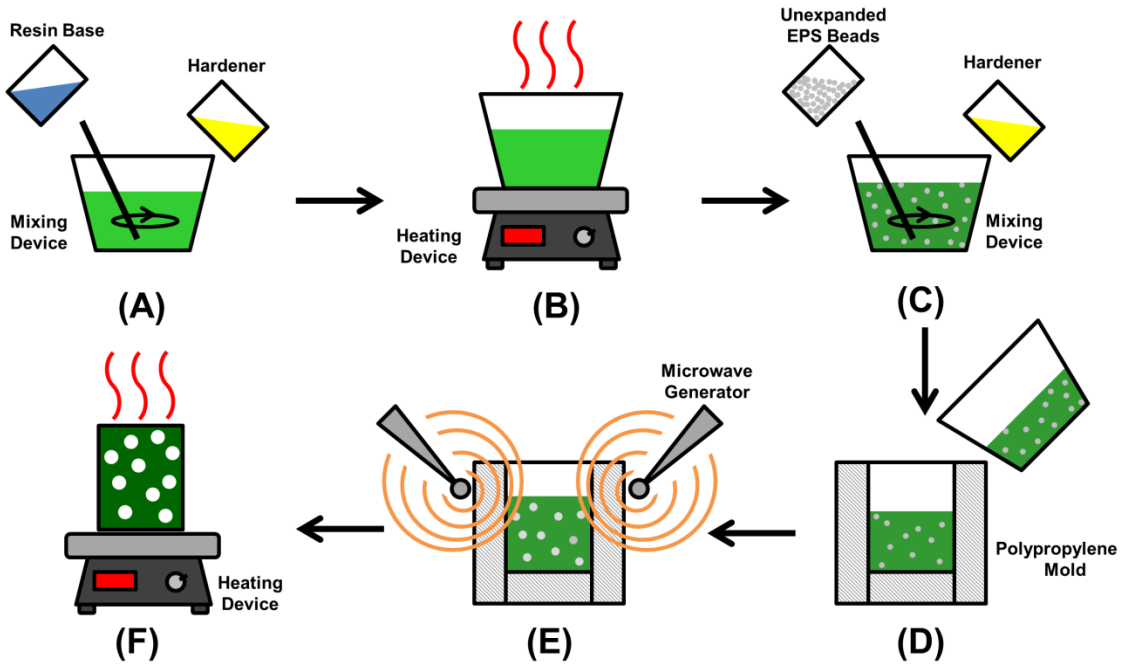


Figure 2.3 Experimental setup for microwave expanding of epoxy-EPS syntactic foam: (A) mixing epoxy base and the first-part hardener, (B) pre-curing, (C) mixing unexpanded EPS microspheres, the second-part hardener, and the pre-cured epoxy, (D) transferring foaming feed to a polypropylene mold, (E) microwave heating, and (F) post-curing.

### *2.3.2 Syntactic Foam Processing*

The experimental setup for microwave expansion of EPS/epoxy syntactic foam is shown in Figure 2.3. The two-stage hardener addition method was employed to prevent the dissolution and inhomogeneous distribution of EPS microspheres. In this method, the hardener is split into two parts and added separately during the preparation of the feed material. The base resin was firstly mixed with the first-part hardener with a hardener to base resin ratio of 1 to 15 by weight. The mixture was then pre-cured at 60°C for 24 hr to achieve the desired viscosity. The feed material was subsequently

made by blending the pre-cured resin mixture, unexpanded EPS microspheres, and the second-part hardener. After being de-gassed under vacuum, the feed was placed inside a polypropylene mold and transferred into a 950W 2.45GHz Magic Chef MCD795SW microwave oven (MC Appliance Corporation, Wood Dale, IL). The specific energy input was optimized and found to be 30% to 50% of the epoxy decomposition limit. Under these processing conditions, the feed material was adequately foamed and cured in several minutes, and the foamed sample gained sufficient rigidity for demolding. Post curing can be conducted either inside or outside the mold. In this work, all samples were post-cured outside the mold at 60°C for 24hr.

*2.3.3 Characterization*

Rheological properties of pre-cured epoxy (before addition of the second-part hardener) were characterized on a controlled-stress parallel-plate rheometer with 25mm diameter steel plates (model: AR2000EX, TA Instruments, New Castle, DE). The steady peak hold mode with a steady shear rate of $1s^{-1}$ was employed to study the curing kinetics. The steady-state flow mode was employed to determine the viscosity as a function of steady shear rate and degree of pre-curing.

Thermal properties of EPS and epoxy were evaluated by differential scanning calorimetry (DSC, model Q2000, TA Instruments, New Castle, DE). The expansion temperature of EPS was determined by a temperature ramp at a heating rate of 10°C/min. The expansion energy of EPS and curing energy of pre-cured or uncured epoxy were determined using an isothermal process at 100°C.

Optical microscopy images were captured by an Olympus BX51 optical microscope installed with an Olympus UC30 digital camera (Olympus Corporation of the Americas, Center Valley, PA) under the reflective mode. The syntactic foam surfaces were polished with sandpapers before the observation. An image analysis software (Olympus Stream Image Analysis) was used to measure the size of EPS microspheres from optical microscopy images. All other optical images were captured by a Canon EOS Kiss X5 Digital SLR camera (Canon U.S.A. Company, Melville, NY).

Flexural mechanical properties of syntactic foams were measured by a DDL 650M mechanical testing machine (TestResources, Inc, Shakopee, MN) with a 4500N load crosshead. Testing samples were molded and machined into a dimension of 12mm (width) $\times$ 60mm (length) $\times$ 6mm (depth) for edgewise placement. The support span length was set to be 38mm. A 10mm/min crosshead speed was adopted for the test.

### 2.4 Results and Discussion

In this section, estimation of process window boundary limits of the microwave expansion process is firstly demonstrated. The relation between density and composition of syntactic foam is then illustrated. The results from flexural mechanical tests are subsequently presented and analyzed to explore some appealing features of the foams serving as lightweight structural materials. Finally, a molded foam part with relatively sophisticated geometry is shown to demonstrate the capability of the microwave expansion process to be used as a molding technique.

*2.4.1 Estimation of Process Window Limits*

Rheological properties of 1:15 epoxy were measured to assist in determination of the EPS homogeneous distribution limit and the air pockets trapping limit. The 1:15 epoxy represents the mixture of base resin and hardener with a weight ratio of 1 to 15. This ratio was chosen because it had a slow viscosity increase in a sufficiently long pre-curing period. The rheological data are provided in Figure 2.4. Figure 2.4 (A) shows the curing kinetics at 60°C under a steady shear rate of $1s^{-1}$. The viscosity had a gradual and slow increase for the initial 30hrs and experienced a sudden rise afterwards. Compared with direct curing of the conventional 1:4 epoxy, the two-stage hardener addition method provides better controllability over the pre-curing process. The inset graph in Figure 2.4 (A) shows the viscosity of the 1:15 epoxy can be continuously varied within a long time period from 6hr to 38hr. Therefore the desired viscosity for EPS foaming can be readily obtained. It was found that if the pre-curing stage lasts shorted than 8hr, the foamed EPS microspheres tend to move toward the upper surface of the mold during microwave expansion. On the other hand, if the pre-curing time is longer than 36hr, air pockets can be easily trapped during mixing of the feed material. Therefore, the viscosity limits for homogeneous EPS distribution and for air pockets trapping were determined to be 2.23 Pa·s and 18.75 Pa·s, respectively. These are the corresponding viscosities after pre-curing for 8 hr and 36 hr.

Figure 2.4 (B) shows viscosity as a function of shear rate for 1:15 epoxy samples undergoing different pre-curing time at 60°C. Three different pre-curing times were employed. At the pre-curing temperature of 60°C, the 1:15 epoxy samples pre-cured for 8hr, 24hr, and 36hr show constant viscosities within the examined shear rate range, indicating that the viscosity is not a function of shear rate within this range. The viscosities are also low, especially for the 8hr and 24hr samples. This low and constant

viscosity is considered an appealing feature to enhance the processability of pre-cured epoxy mixture in syntactic foam manufacture.

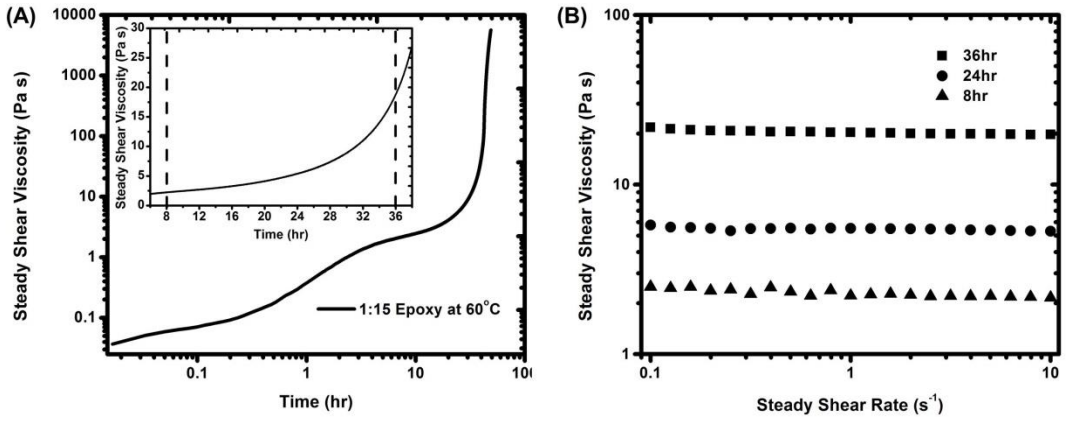


Figure 2.4 Rheological characterization of 1:15 epoxy: (A) curing kinetics at 60°C (inset graph: curing kinetics at 60°C from 6hr to 38hr) and (B) viscosity as a function of steady shear rate for samples undergoing different pre-curing time at 60°C.

Thermal properties of EPS and epoxy were characterized using DSC. The DSC thermograms are shown in Figure 2.5. The data were used to aid in the estimation of the EPS expansion limit and the epoxy decomposition limit. The heat flow of unexpanded EPS in a temperature ramp from 20°C to 150°C with a heating rate of 10°C/min is shown in Figure 2.5 (A). Two endothermic peaks were found. The first peak appearing at 64.04°C is related to the gasification of blowing agent. The second peak is at 99.34°C that is very close to the known glass transition temperature (Tg) of polystyrene. It is known that the unexpanded EPS should be heated above Tg for effective expansion. Therefore, 100°C was set to be a testing temperature for isothermal expansion of EPS. The specific heat absorbed during EPS expansion is found to be 309.4kJ/kg, as

indicated in Figure 2.5 (B). For comparison purposes, isothermal curing of epoxy was also conducted using DSC. The specific heat released for achieving full curing is 5334.2 kJ/kg for the 1:4 epoxy (Figure 2.5(C)). The value reduces to 3211.2kJ/kg for the 24hr pre-cured 1:15 epoxy mixed with the second-part hardener (Figure 2.5 (C)). The difference arises from the different degrees of curing of the two samples at the start of the experiment.

The following additive rule is used to estimate the EPS expansion limit $E_{EEL}$:

$$E_{EEL} = \varphi_{EPS}\left(E_{EPS\ Expasion} + C_{p\ EPS}\Delta T\right) + (1 - \varphi_{EPS})\left(C_{p\ Epoxy}\Delta T\right) \quad (2.1)$$

where $\varphi_{EPS}$ is weight fraction of EPS, $E_{EPS\ Expasion}$ is specific energy needed to expanded EPS (309.4kJ/kg), $C_{p\ EPS}$ is heat capacity of EPS (1.3kJ/kg°C), $C_{p\ Epoxy}$ is heat capacity of epoxy (1.23kJ/kg°C), and $\Delta T$ is temperature difference between EPS expansion temperature and room temperature. The heat capacity data are from reference [18].

To estimate the epoxy decomposition limit $E_{EDL}$, the following equation is employed:

$$E_{EDL} = F_t(1 - \varphi_{EPS})E_{Decomp} + E_{EEL} \quad (2.2)$$

where $F_t$ is a factor for heat transfer efficiency (fixed at 5 for estimation [108]), and $E_{Decomp}$ is the epoxy decomposition activation energy ($1.56\times10^3$kJ/kg for DGEBPA/ aliphatic amine system [109]).

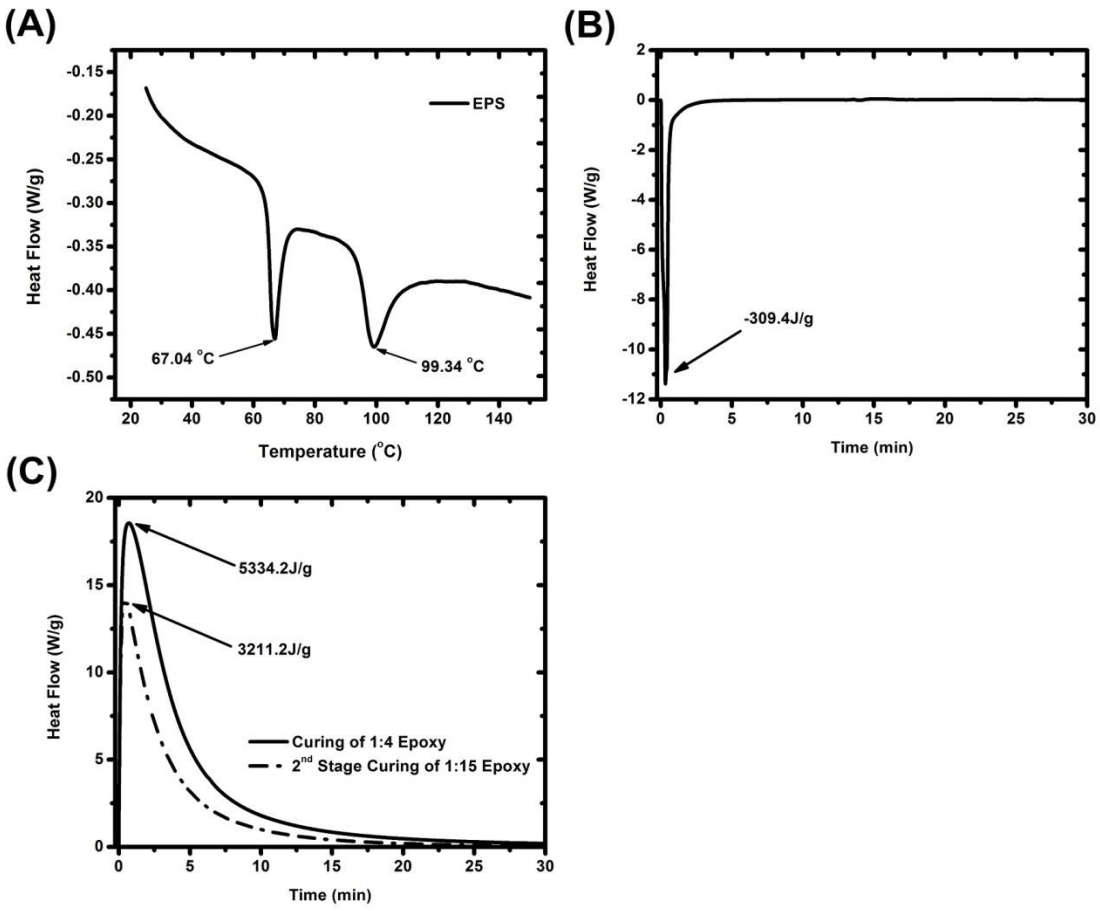


Figure 2.5 Thermal analysis of EPS and 1:15 epoxy: (A) heat flow of EPS in temperature ramping and (B) heat flow of EPS in isothermal dwell (100°C), and (C) heat flow of epoxy in isothermal dwell (100°C) (exothermic direction points upward).

A summary of the estimated EPS expansion limit and epoxy decomposition limit for EPS/epoxy syntactic foams with varying EPS weight fractions are given in Table 2.1.

Morphologies of EPS/epoxy syntactic foams processed within/beyond the process window are shown in Figure 2.6. All the samples contained 5% (w/w) EPS. The foam prepared under optimized condition is presented in Figure 2.6 (A). The expanded EPS microspheres were effectively foamed and homogeneously distributed, and no burning

marks were observed. Figure 2.6 (B) shows the sample made via directly mixing unexpanded EPS microspheres and the 1:4 epoxy without a pre-curing stage. EPS microspheres were dissolved in the resin, resulting in a transparent and gel-like solid. The sample shown in Figure 2.6 (C) was prepared using the 1:15 epoxy with insufficient pre-curing time. Due to the low feed viscosity, the buoyancy dragged foaming EPS to the upper surface of the mold, leaving an inhomogeneous distribution of microspheres. In Figure 2.6 (D), the syntactic foam was expanded using a specific microwave energy that is considerably higher than the epoxy decomposition limit. Obvious burning marks can be observed on the external surface and internal body of the sample, indicating that decomposition occurred. In contrast, Figure 2.6 (E) shows a sample obtained using insufficient microwave energy. In this case, no expansion was found for the EPS. Additionally, Figure 2.6 (F) shows a sample from an over pre-cured 1:15 epoxy resin. One can observe a large number of air pockets trapped inside the sample. This again can be attributed to the undesirably large viscosity.

Table 2.1 Summary of estimated EPS expansion limit and epoxy decomposition limit for EPS-epoxy syntactic foams with varying EPS weight fractions.

| Sample | EPS Expansion Limit (kJ/g) | Epoxy Decomposition Limit (kJ/g) |
|---|---|---|
| **5% (w/w) EPS-Epoxy** | **0.11** | **7.52** |
| **15% (w/w) EPS-Epoxy** | **0.14** | **6.77** |
| **25% (w/w) EPS-Epoxy** | **0.17** | **6.02** |

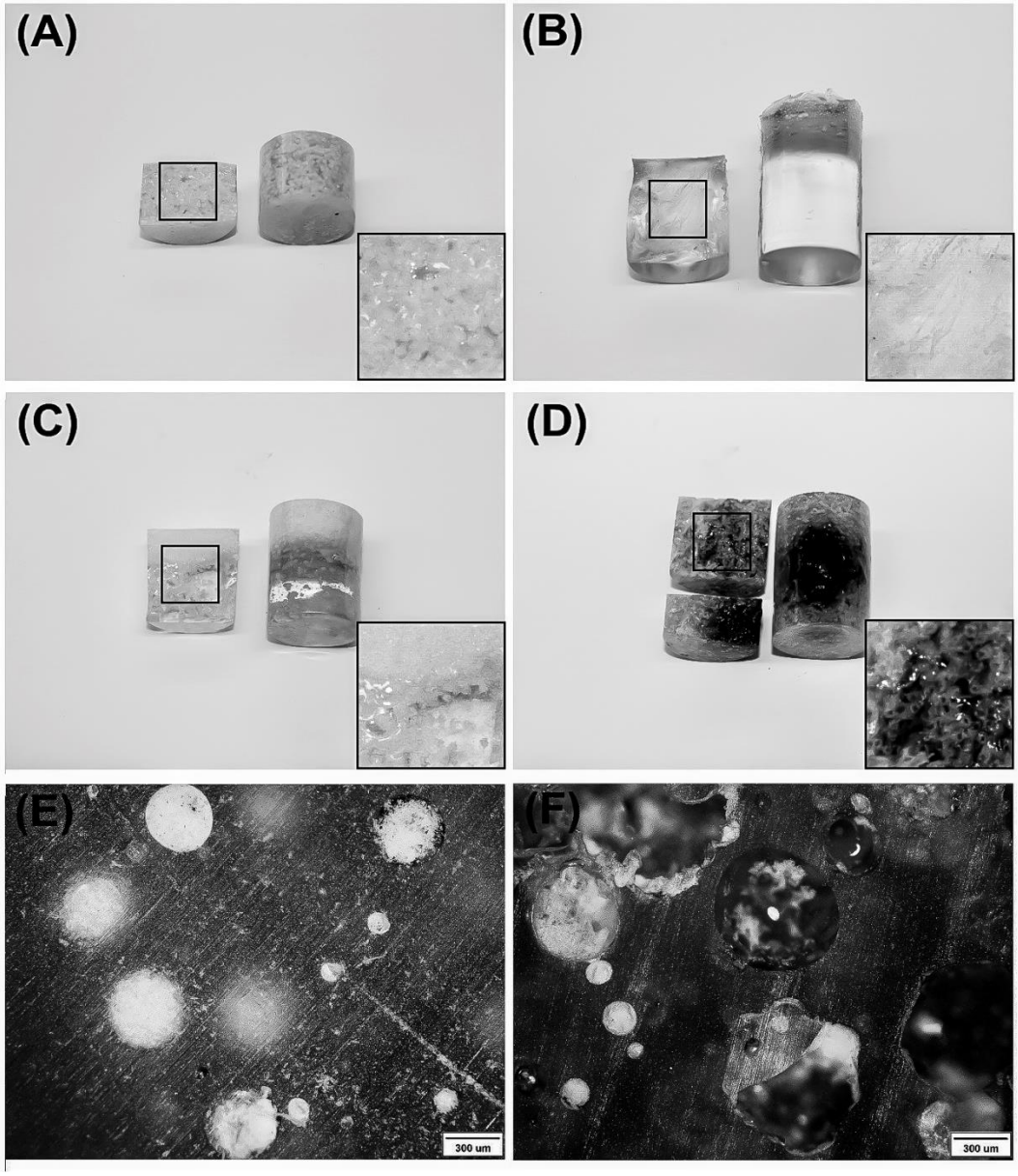


Figure 2.6 Optical images of 5% (w/w) EPS-epoxy syntactic foams processed under different conditions: (A) using the optimized condition (B) directly mixing unexpanded EPS microspheres with the 1:4 epoxy without pre-curing, (C) using the 4hr pre-cured 1:15 epoxy, (D) using a specific microwave energy input of 12kJ/g, (E) using a specific microwave energy input of 0.08kJ/g, and (F) using the 38hr pre-cured 1:15 epoxy.

*2.4.2 Syntactic Foam Density and EPS Volume Fraction*

The microwave expansion process has a capability to effectively expand EPS microspheres in the syntactic foam with high EPS loading. In this study, the highest loading of EPS that was attempted is 45% by weight. Although the loading can be further increased, the viscosity of the foaming feed becomes considerably high, requiring a heavy-duty industrial blender to achieve good mixing. Since density is one of the most important characteristics of syntactic foam, the relation between density and EPS loading was also established.

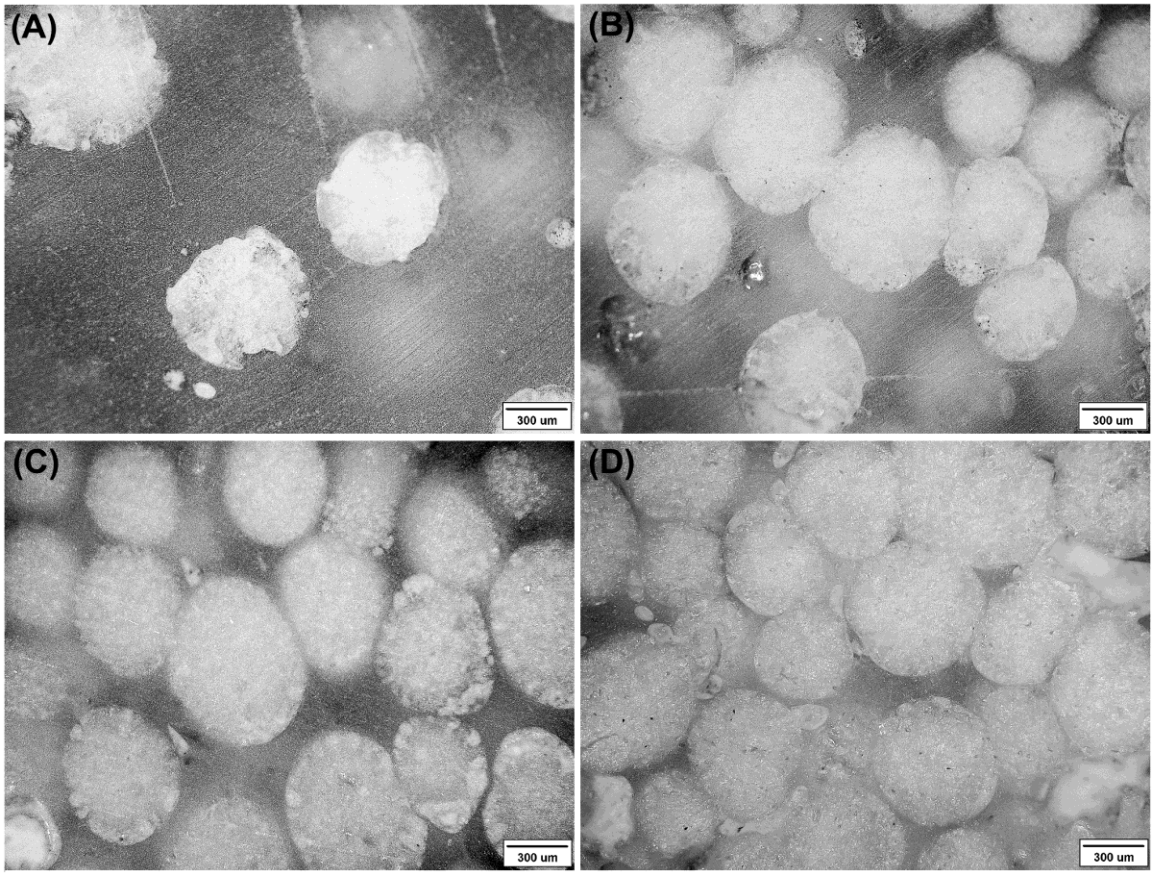


Figure 2.7 Optical microscopy images of EPS-epoxy syntactic foam with EPS weight fraction of (A) 5%, (B) 25%, (C) 35%, and (D) 45%.

Figure 2.7 shows the morphologies of EPS/epoxy syntactic foams with varying EPS loadings. The microscopy image of cross-section of the foam containing 5% (w/w) EPS is presented in Figure 2.7 (A). Foamed EPS microspheres are isolated from each other in the epoxy matrix. The distance between individual microspheres decreases as the EPS loading increases to 25% (Figure 2.7 (B)). Some microspheres began to contact with each other. When the loading of EPS further increases to 35%, some microspheres are distorted into polyhedron shapes (Figure 2.7(C)) due to the compression generated from expansion of neighboring microspheres. This usually happens in syntactic foams with deformable polymer microspheres when the volume fraction of microspheres reaches a critical value [110]. In the syntactic foam with 45% (w/w) EPS loading, almost all EPS microspheres contact with each other and develop into polyhedron-shaped morphologies.

Table 2.2 Sizes and densities of unexpanded EPS and expanded EPS.

| | **Unexpanded EPS** | **Expanded EPS** |
|---|---|---|
| **Diameter ($\mu m$)** | **388.6±17.8** | **681.2±12.2** |
| **Normalized Diameter** | **1.00** | **1.75** |
| **Density (g/cm$^3$)** | **0.980±0.038** | **0.182±0.011** |

Note: The normalized diameter is calculated by dividing the diameter of corresponding EPS with that of unexpanded one.

Table 2.2 summarizes the diameters and densities of unexpanded EPS and expanded EPS. The size of unexpanded EPS is 388.6±17.8μm. After microwave expansion inside the epoxy matrix, the size was enlarged to 681.2±12.2μm, 1.75 times larger than the original one. More effective expansion of EPS is achieved in the microwave expansion process as compared with the conventional thermal foaming

process where an expansion ratio of less than 1.3 are typically reported for EPS [34, 107].

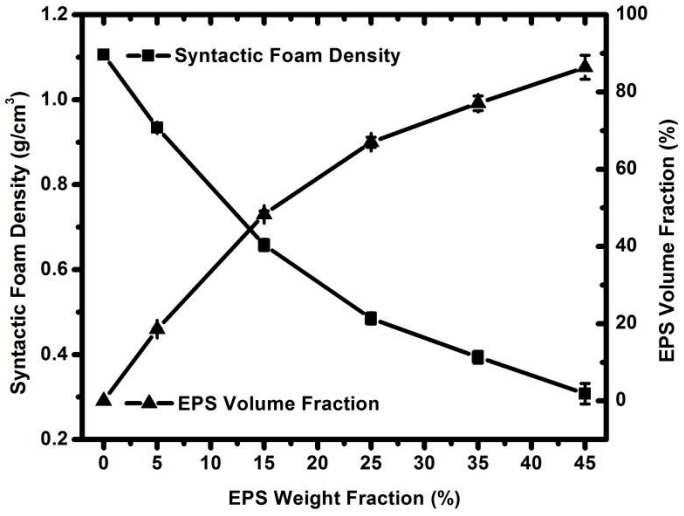


Figure 2.8 Syntactic foam density and EPS volume fraction as a function of EPS weight fraction.

To calculate the EPS volume fraction as a function of EPS loading, one can employ the following equation:

$$\eta_{EPS} = \frac{\rho_{Epoxy} - \rho_{Foam}}{\rho_{Epoxy} - \rho_{Expanded\ EPS}} \tag{2.3}$$

where $\eta_{EPS}$ is EPS volume fraction, $\rho_{Epoxy}$ is neat epoxy density, $\rho_{Foam}$ is EPS/epoxy syntactic foam density, and $\rho_{expanded\ EPS}$ is density of EPS expanded in epoxy.

The relation between syntactic foam density and EPS volume fraction is shown in Figure 2.8 and summarized in Table 2.3. As expected, the foam density keeps

decreasing and the expanded EPS volume fraction keeps increasing as the EPS loading increases from 0% to 45%. At 45% EPS loading, the syntactic foam can have a low density of 308±24kg/m$^3$ and a high EPS volume fraction of 86.4%±3.1%. It should also be noticed that the densities of syntactic foams with 4% or more EPS are lower than the density of water (approximately 1g/cm$^3$), showing a potential in marine applications.

Table 2.3 Densities and EPS volume fractions of neat epoxy and EPS/epoxy syntactic foams.

| | Neat Epoxy | 5% (w/w) EPS-Epoxy | 15%(w/w) EPS-Epoxy | 25%(w/w) EPS-Epoxy | 35%(w/w) EPS-Epoxy | 45%(w/w) EPS-Epoxy |
|---|---|---|---|---|---|---|
| **Density (g/cm$^3$)** | **1.106±0.004** | **0.934±0.007** | **0.658±0.013** | **0.485±0.013** | **0.394±0.014** | **0.308±0.024** |
| **Normalized Density** | **1.00** | **0.84** | **0.59** | **0.44** | **0.36** | **0.28** |
| **EPS Volume Fraction** | **0.0%±0.0%** | **18.6%±0.2%** | **48.5%±1.0%** | **67.2%±1.5%** | **77.1%±1.9%** | **86.4%±3.1%** |

Note: The normalized density is calculated by dividing the density of corresponding syntactic foam with that of neat epoxy.

*2.4.3 Syntactic Foam Mechanical Property*

Besides density, mechanical properties, especially specific flexural property, represent another vital factor that considerably influences the performance of syntactic foam serving as lightweight structural materials.

The flexural strength $\sigma_M$ and flexural modulus $E$ can be calculated from a 3-point bend test using the following two equations according to ASTM D790-10:

$$\sigma_M = \frac{3P_M L}{2bd^2} \tag{2.4}$$

$$E = \frac{L^3 m}{4bd^3} \tag{2.5}$$

where $P_M$ is maximum load, $L$ is support span length, $b$ is width of the beam, $d$ is depth of the beam, and $m$ is slope of the initial linear portion of the load-deflection curve.

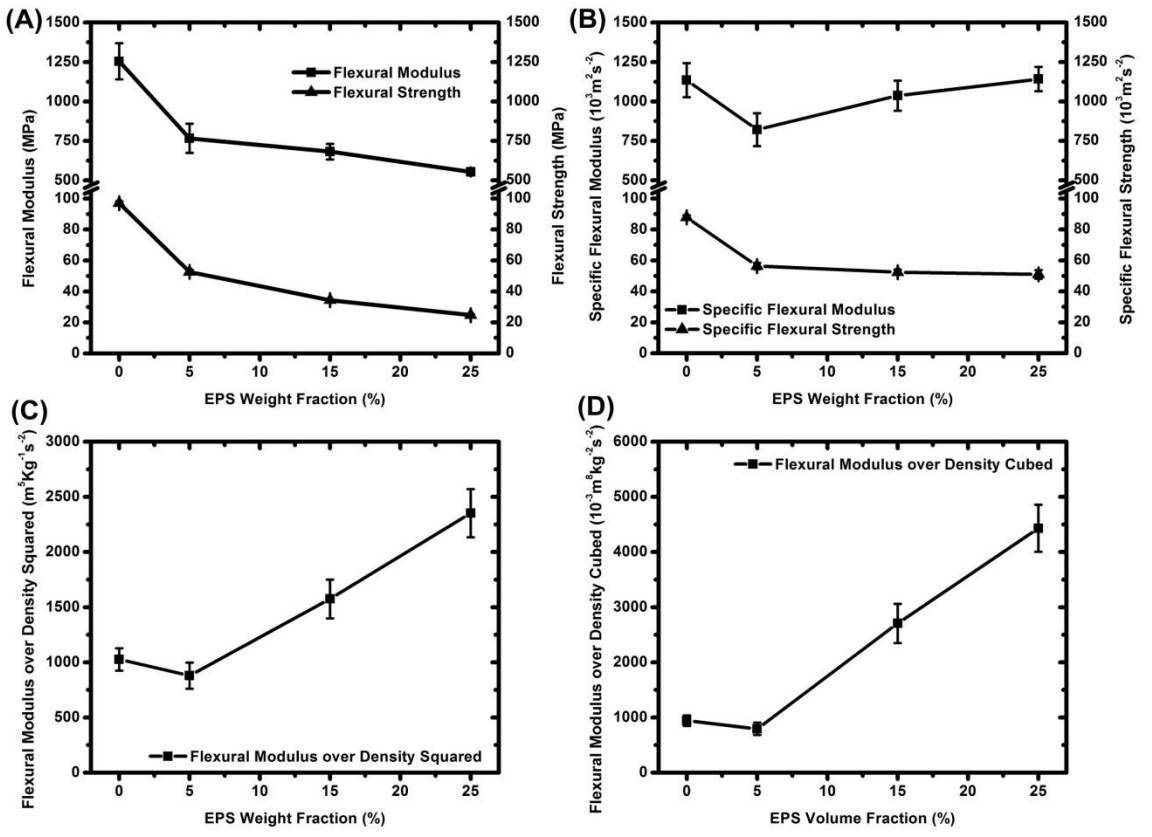


Figure 2.9 Flexural properties of EPS-epoxy syntactic foam as a function of EPS weight fraction: (A) flexural modulus and strength, (B) specific flexural modulus and strength, (C) flexural modulus over density squared, and (D) flexural modulus over density cubed.

The results of flexural strength and modulus as a function of EPS loadings are shown in Figure 2.9 (A) and summarized in Table 2.4. The flexural strength and modulus

of syntactic foam decrease as the EPS loading increases. This is understandable because the mechanical strength of foamed EPS is expected to be lower than that of neat epoxy. However, for syntactic foam the most important properties are specific properties rather than absolute properties since such foams are usually used in lightweight structural applications. The specific flexural properties are calculated by dividing the measured values by density. The results after this conversion are shown in Figure 2.9 (B) and summarized in Table 2.5. The specific flexural strength of syntactic foam retains about 60% of that of neat epoxy. In contrast, the specific flexural modulus is closer to that of the neat epoxy; at 25% EPS loading, the foam has specific modulus comparable to that of the neat epoxy.

Table 2.4 Summary of flexural properties of neat epoxy and EPS-epoxy syntactic foams.

| Sample | Neat Epoxy | 5% (w/w) EPS-Epoxy | 15% (w/w) EPS-Epoxy | 25% (w/w) EPS-Epoxy |
|---|---|---|---|---|
| **Flexural Strength (MPa)** | **97.0±1.1** | **52.6±1.5** | **34.4±0.4** | **24.7±0.7** |
| **Normalized Flexural Strength** | **1.00** | **0.54** | **0.35** | **0.25** |
| **Flexural Modulus (MPa)** | **1254.3±114.3** | **766.4±92.1** | **682.3±49.5** | **554.4±22.8** |
| **Normalized Flexural Modulus** | **1.00** | **0.61** | **0.54** | **0.44** |

For syntactic foams used as structural beams, the flexural modulus over density squared or cubed is also highly influential. If the weight is fixed, the beam performance can be optimized by maximizing the flexural modulus according to the beam geometry [14]. The normalized moduli are plotted in Figure 2.9 (C) and (D) and summarized in Table 2.5. Except at 5% EPS loading, syntactic foams with 15% and 25% EPS loadings both have much larger flexural moduli over density squared or cubed than those of neat epoxy. Especially at 25% EPS loading, the flexural modulus over density squared or

cubed is 2.29 times or 4.71 times larger than the corresponding one of neat epoxy, indicating that the syntactic foam can outperform the net polymer in structural applications.

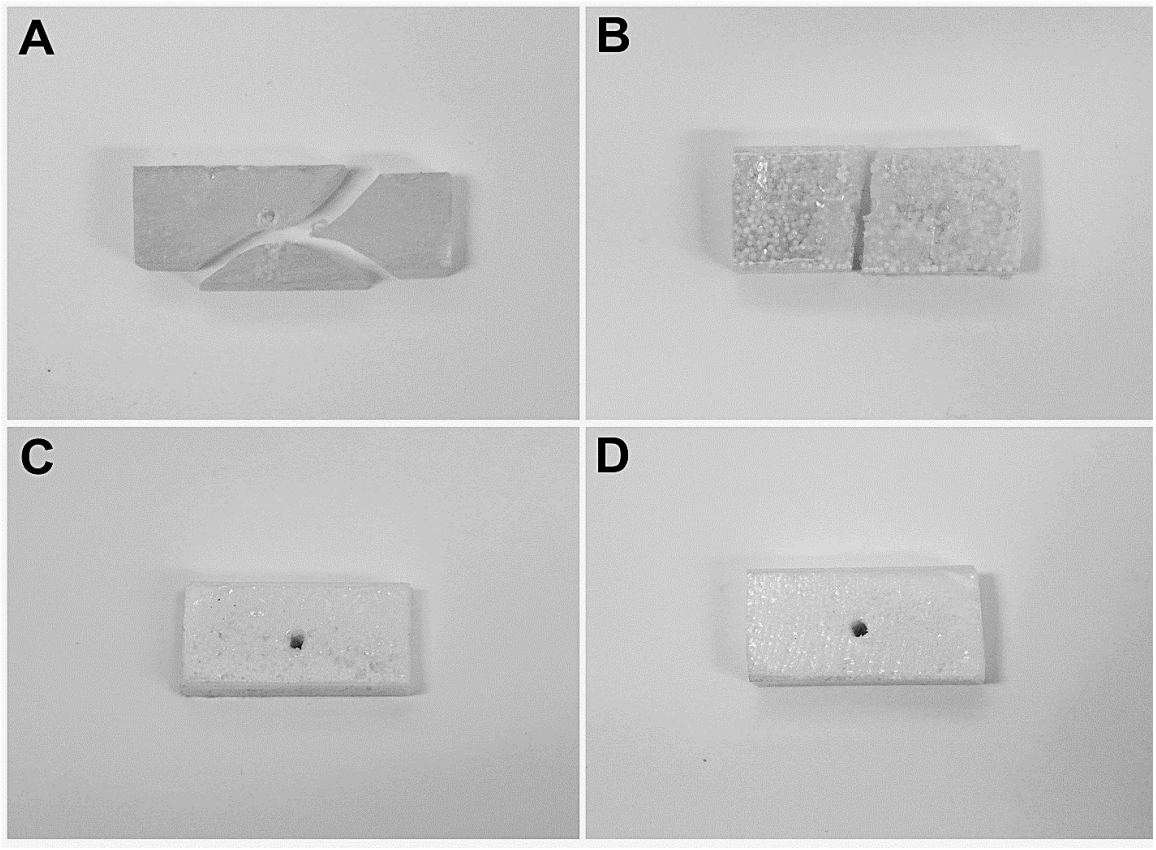


Figure 2.10 Optical images of samples penetrated by a steel nail with a diameter of 2mm: (A) neat epoxy, (B) 5% (w/w) EPS/epoxy, (C) 15% (w/w) EPS/epoxy, and (D) 25% (w/w) EPS/epoxy.

Table 2.5 Summary of specific flexural properties of neat epoxy and EPS-epoxy syntactic foams.

| | Neat Epoxy | 5% (w/w) EPS-Epoxy | 15% (w/w) EPS-Epoxy | 25% (w/w) EPS-Epoxy |
|---|---|---|---|---|
| **Specific Flexural Strength ($10^3 m^2 s^{-2}$)** | **87.8±1.3** | **56.4±2.0** | **52.4±1.7** | **51.0±2.8** |
| **Normalized Specific Flexural Strength** | **1.00** | **0.64** | **0.60** | **0.58** |
| **Specific Flexural Modulus ($10^3 m^2 s^{-2}$)** | **1134.5±107.9** | **821.0±104.5** | **1036.5±95.3** | **1142.0±76.6** |
| **Normalized Specific Flexural Modulus** | **1.00** | **0.72** | **0.91** | **1.01** |
| **Flexural Modulus over Density Squared ($m^5 kg^{-1} s^{-2}$)** | **1026.2±101.6** | **879.5±118.2** | **1574.5±175.3** | **2352.2±218.5** |
| **Normalized Flexural Modulus over Density Squared** | **1.00** | **0.86** | **1.53** | **2.29** |
| **Flexural Modulus over Density Cubed ($10^{-3} m^8 kg^{-2} s^{-2}$)** | **941.0±96.9** | **793.2±112.2** | **2705.1±353.5** | **4430.8±426.2** |
| **Normalized Flexural Modulus over Density Cubed** | **1.00** | **0.84** | **2.87** | **4.71** |

Furthermore, the toughening effect of expanded EPS microspheres was also observed in a nail penetration test. A steel nail with a diameter of 2mm was hammered into neat epoxy and syntactic foam bars. Results are presented in Figure 2.10. The neat epoxy sample is immediately shattered into three pieces. The 5% (w/w) EPS-epoxy foam has clean crack propagating through the body, breaking the sample into halves. For the syntactic foams with 15% and 25% EPS loadings, no cracks are found in the samples and the bodies still remains integrated. A possible EPS toughening mechanism

was proposed by Kim and Kim [34, 35]. They explained that the cracks are stopped by the compressive residual stresses generated via the expansion of EPS during heating.

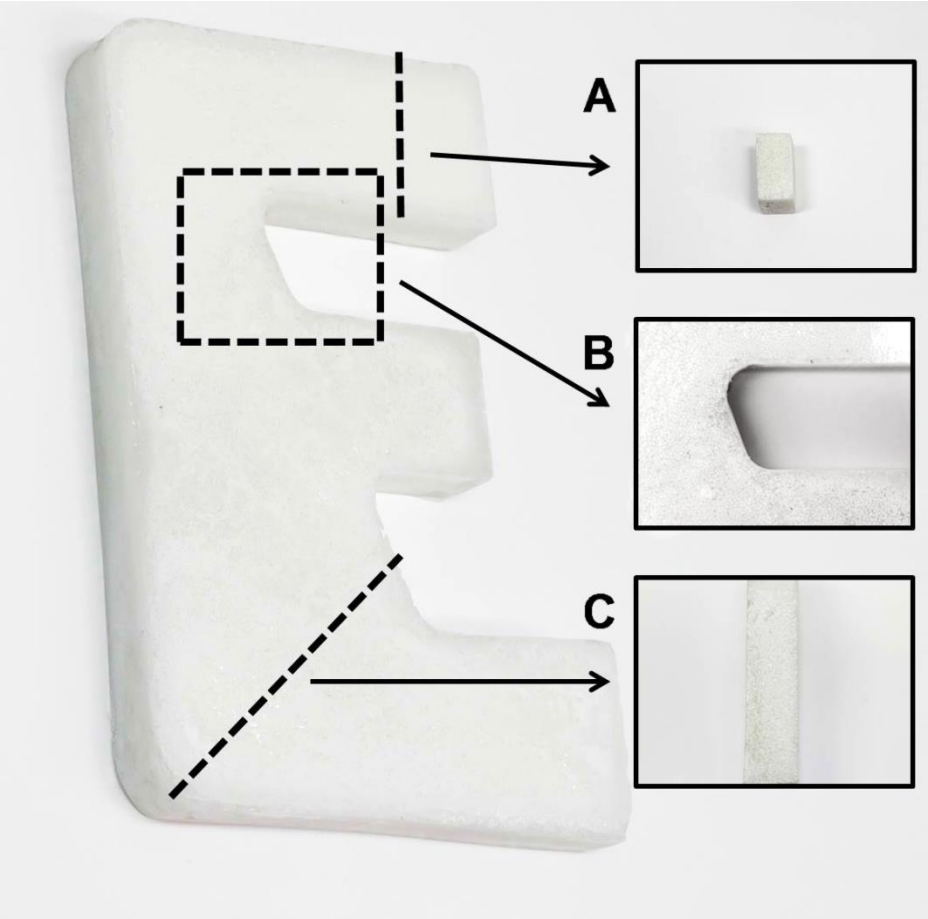


Figure 2.11 EPS-epoxy syntactic foamed letter “E” part molded via microwave expanding process: (A) cross-section of upper arm, (B) magnified image of upper curving section, and (C) cross-section of lower curving section.

*2.4.4 Microwave Expansion Molding*

The microwave expansion process was adapted to molding a foamed part with a relatively complex shape. Specifically, a letter “E” shaped part with 15% EPS loading

was molded, as shown in Figure 2.11. A dosed amount of feed material was placed inside the mold, and after mold closure microwave energy was applied. It was found that the syntactic foamed part can duplicate well the internal contour of the mold. Moreover, the surfaces of the molded part are smooth. This indicates an effective holding stage during molding. It is reasonable to deduce that the positive pressure generated from the expansion of EPS microspheres works as the main driving force in such a molding process. Magnified images of cross-sections of the part are shown in Figure 2.11 (A) and (C). One can observe the homogeneous distribution of foamed EPS. Figure 2.11 (B) presents the magnified image of upper curving section. The transition between straight line and curvature line is continuous, and the surface is very smooth.

## 2.5 Conclusions

A novel microwave expansion process was designed and developed to produce thermoset-matrix syntactic foam containing expandable thermoplastic microspheres. Expandable polystyrene microsphere and epoxy resin were chosen as the model material system for feasibility study and demonstration. The microwave power was fixed to be 100W to ensure a controlled process. A two-stage hardener addition method was employed to prevent the dissolution and inhomogeneous distribution of EPS microspheres. The specific microwave energy and the pre-cured epoxy viscosity at room temperature are found to be the two governing parameters in the process. The proposed process window is delimited by four limits: EPS homogeneous distribution limit, air pockets trapping limit, EPS expansion limit, and epoxy decomposition limit. The values of these limits were obtained from rheological measurements and thermal analyses.

The experimental results demonstrated that the microwave expansion process is able to effectively expand EPS microspheres in EPS/epoxy syntactic foam even with high EPS loading. Mechanical tests showed that the specific flexural strength and modulus of syntactic foam are comparable with those of neat epoxy. By comparison, the flexural moduli over density squared or cubed of the foam are much higher, especially at high EPS loadings, than those of neat epoxy. The foamed EPS microspheres can also effectively toughen the syntactic foam, preventing propagation of cracks. Finally, the microwave expansion process is also capable of molding syntactic foamed parts of relatively sophisticated geometry with smooth surfaces.

# CHAPTER 3

# PROCESSING OF COMPOSITE POLYSTYRENE FOAM WITH A HONEYCOMB STRUCTURE*

## 3.1 Introduction

As introduced in Chapter 1, EPS is the raw material used for molding foamed polystyrene products. Polystyrene or EPS foam parts are then made by thermally molding these expanded particles into various geometries. Such EPS foam is lightweight and possesses excellent buffering, water proof, heat retention and thermal insulation properties [29]. Because of these appealing features, it has been extensively employed in construction, package, marine, and automobile [33, 34, 36, 107].

Although some properties of EPS foam can be altered by changing the cellular structure [111], it is difficult to improve the performances in other aspects since the foam is made of one single component. This greatly restricts applications of EPS foam in many fields. Among them, poor fire retardation is one of the major issues [1].

EPS foam is a notorious fire hazard in buildings [112]. It can be easily ignited with a limiting oxygen index of only 18 [30]. During combustion of the foam, toxic black smoke will be generated with burning dripping material that can flow and ignite other combustibles. Moreover, disastrous collapse of the foam structure can further occur in fire, hindering firefighting and rescuing actions [38]. Previous efforts in improving the fire-retardation properties of EPS foam have almost exclusively focus on incorporating fire-retardant ingredients into unexpanded EPS microspheres via copolymerizing or blending methods [112, 113]. However, in order to retain the foamability of EPS microspheres, only a small amount of fire-retardant material can be practically added in these methods,

resulting in unsatisfactory fire-resistant performance. For a similar reason, most environmentally friendly fire retardants such as aluminum hydroxide and magnesium hydroxide cannot be used as effective additives in EPS microspheres since high loading is needed [114]. On the other hand, halogenated based fire-retardant materials are extensively used due to their high fire-retardation enhancement capability, but they are environmentally unfriendly and toxic to the human body [50]. Their uses are now restricted by laws and regulations in some countries [55].

In the work presented in Chapter 2, a microwave expansion process was developed to produce EPS-filled syntactic foam [115]. In this process, unexpanded EPS microspheres were directly foamed in uncured thermoset matrix using a microwave heating method. This design enables the microwave expansion process to effectively expand EPS of high loadings. Based on this feature, one can deduce that if the EPS loading is extremely high, the matrix will form a thin barrier layer that wraps each foamed microsphere, resulting in a honeycomb-like structure. This will provide an alternative solution to improve properties of EPS foam. When the matrix material is replaced by a specially formulated fire-retardant compound, the unique honeycomb-like structure in the composite foam is able to serve as a barrier to stop the fire. Moreover, a large amount of those environmentally friendly inorganic fire retardants can now be incorporated into the foam because the composition of the barrier layer has limited influence over the foamability of unexpanded EPS microspheres.

Based on this idea, in Chapter 3, an expandable suspension process is designed and developed to produce EPS composite foam with a honeycomb-like barrier structure. An attempt to explore the influence of such a unique structure on the mechanical and fire-retardant properties of the resulting foam was made. In the following sections, the process setup and procedure was first described. The formulation and rheological behavior of the expandable suspension were then discussed. Next, the morphology of

the composite foam was correlated with the suspension viscosity. The physical and mechanical properties were subsequently presented and analyzed. Finally, the fire-retardant characteristics of the composite foam, including flame resistance, local burning characteristics, and high temperature structure integrity, were evaluated.

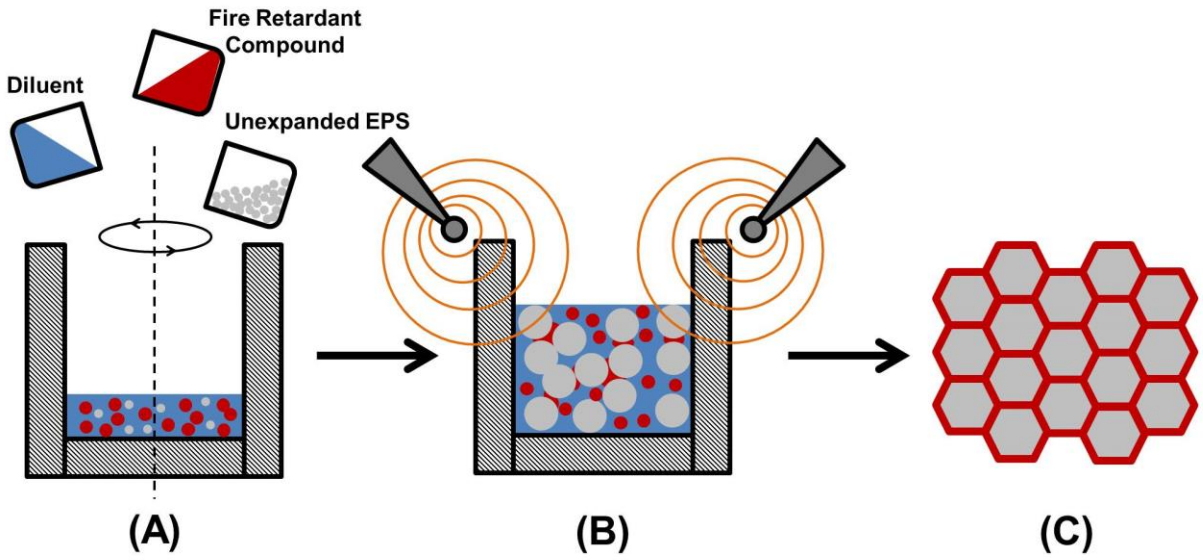


Figure 3.1 Process setup and procedure to produce composite EPS foam from an expandable suspension.

## 3.2 Experimental

### *3.2.1 Materials*

Unexpanded EPS microspheres with an average diameter of 965.6±27.3μm were acquired from IASCO-Industrial Arts Supply Company (Minneapolis, MN). The unexpanded EPS contains approximately 5% by weight of pentane as blowing agent. A phenolic resin system, Cellobond® J2027L (base liquid) and Phencat® 382 (catalyst), was generously provided by Momentive Specialty Chemicals Inc. (Forest Park, GA). The

ratio by weight between the base liquid and the catalyst is 19:1. Aluminum hydroxide (particle size:10-50μm), boric acid (particle size: 10-35μm) and sodium dodecyl sulfate were obtained from Sigma-Aldrich Corporation (St. Louis, MO) and used as received. BYK-P® 104S was generously provided by BYK Additives Inc. (Louisville, KY). Milled glass fibers, 1/32" long, were obtained from Fiber Glast Developments Corporation (Brookville, OH). Cyclohexane was from Alfa Aesar (Ward Hill, MA).

### *3.2.2 Foam Processing*

The experimental setup and procedure for the expandable suspension process to produce composite polystyrene foam with a honeycomb-like barrier structure is described in Figure 3.1. A stable and compatible expandable aqueous suspension was first prepared by mixing fire-retardant compound, unexpanded EPS microspheres, and diluent. The formulation is summarized in Table 3.1. During the preparation, these components were added in a sequence of first diluent, then fire retardant compound and finally unexpanded EPS, and blended until a homogeneous light yellow liquid suspension was formed. The expandable suspension was then transferred into a glass or polypropylene mold and fully expanded using a 1000W 2.45GHz Oster OGB81101 domestic microwave oven (John Oster Manufacturing Company, Boca Raton, FL). Microwave power was fixed at 1000W. The actual expansion time may vary with the size and geometry of the sample. For example, 3min expansion time was required to effectively foam the sample in a closed cylindrical glass mold with a diameter of 100mm and a height of 15mm containing 3.5g of unexpanded EPS microspheres. Details on process window estimation and expansion time determination of this microwave expansion method were discussed in the previous publication [115]. After the microwave

expansion, the resulting foam gained sufficient rigidity for demolding. Post-curing can be subsequently conducted either inside or outside of the mold for 4hr at 60°C.

Table 3.1 Expandable suspension formulation.

| Component | Component Ratio | Component Composition | |
|---|---|---|---|
| Fire Retardant Compound | 10 part | Phenolic Resin | 51% (w/w) |
| | | Aluminum Hydroxide | 35% (w/w) |
| | | Boric Acid | 7% (w/w) |
| | | 1/32” Glass Fiber | 5% (w/w) |
| | | BYK-P 104S | 2% (w/w) |
| Diluent | 1 part | Water | 95% (w/w) |
| | | Sodium Dodecyl Sulfate | 5% (w/w) |
| EPS | 8 part | Expandable Polystyrene | 100% (w/w) |

*3.2.3 Characterization*

Thermal properties of EPS were characterized by differential scanning calorimetry (DSC, model Q2000, TA Instruments, New Castle, DE). A temperature ramp test in a nitrogen atmosphere at a heating rate of 10°C/min was used to determine the expansion temperature of unexpanded EPS microspheres. The expansion energy of EPS was determined using an isothermal process at 110°C.

Rheological properties of the expandable suspension were characterized on a controlled-stress rotational rheometer with 21mm diameter parallel steel plates (model: Thermo Mars II, Thermo Fisher Scientific, Inc., Waltham, MA). A steady-state flow mode

was employed to determine the viscosity as a function of steady shear rate at room temperature.

Optical microscopy images were captured by a Motic® SMZ-168 Stereo Zoom Microscope (Speed Fair Co., Ltd., Hong Kong, China) installed with an Olympus UC30 digital camera (Olympus Corporation of the Americas, Center Valley, PA) under the reflective mode. All other optical images were captured by a Canon EOS 5D Mark II Digital SLR camera (Canon U.S.A. Company, Melville, NY).

An Instron 5667 universal testing machine (Instron Corporation, Norwood, MA) with a 10kN load cell was used to conduct uniaxial compression, compressive creep, and three point bending tests. For uniaxial compression and compressive creep tests [116], the samples were cut into cubic shape with a dimension of 15mm × 15mm × 15mm. The pre-set compressive strain in the uniaxial compression was chosen as 0.5mm/mm. The holding compressive stress in the compressive creep test was set to be 0.25MPa. For three point bending test [117], the samples were cut into a dimension of 60mm (length) × 25mm (width) × 15mm (depth). The pre-set flexural strain was set to 0.05mm/mm. A crosshead rate of 5mm/min was used for all tests.

Fire resistance test was performed by applying an external fire source in contact with one corner of the composite foam and the neat foam, respectively. The foam overall appearances were captured with a digital camera at 0s, 5s, and 15s after the beginning of the test. Local burning characteristics of the composite foam was observed with an optical microscopy by recording the morphological changes after the foam contacting the fire for 0s, 1s, 3s, 5s, 10s, and 15s.The structural stability of the foam at high temperature was examined by placing the composite foam and the neat foam on a hot

stage surface at a temperature of 350°C. The changes of the foam appearance after 0.0min, 1.0min, 2.0min, 2.5min, and 3.0min were recorded for comparison.

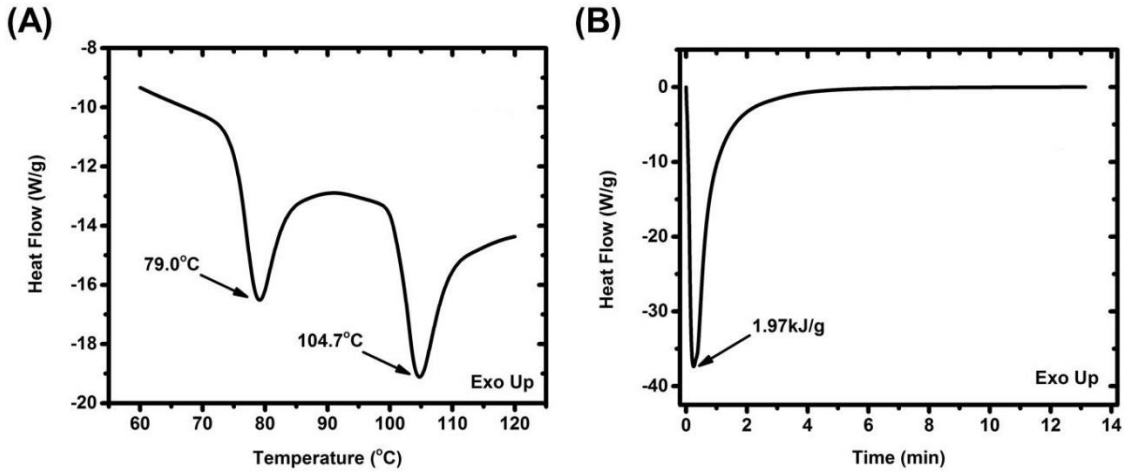


Figure 3.2 Thermal analysis of EPS: (A) heat flow of EPS in temperature ramping and (B) heat flow of EPS in isothermal dwell (110°C).

### 3.3 Results and Discussion

In the following sections, the thermal property of EPS is first presented. Next, the formulation and rheological behavior of the expandable suspension are discussed. Foam morphology is subsequently shown and correlated with the suspension viscosity. The density and foamed EPS volume fraction are also presented. The results from uniaxial compression, creep, and flexural tests are then analyzed to explore the influence of the honeycomb-like structure over the mechanical performance of the composite foam. Finally, the fire retardant characteristics of the composite foam, including flame resistance, local burning characteristics, and high temperature structure integrity, is illustrated and discussed.

### *3.3.1 EPS Thermal Property*

Thermal properties of EPS were characterized using DSC. The results are shown in Figure 3.2 (A). Two endothermal peaks are observed. The first peak appears at 79.0°C that is related with the gasification of pentane serving as a physical blowing agent in the unexpanded EPS microsphere. The second peak is at 104.7°C that corresponds to the glass transition temperature of polystyrene [118]. The unexpanded EPS microspheres can be effectively foamed when the expanding temperature is larger than the glass transition temperature [1]. The heat flow as a function of time in an isothermal dwell test is presented in Figure 3.2 (B). It is found that the expansion of EPS microsphere is an endothermic process with specific expansion energy of 1.97kJ/g.

### *3.3.2 Expandable Suspension Formulation and Rheology*

In the new process developed, the composite EPS foam is produced by foaming an expandable aqueous suspension using microwave heating. The formulation of such suspension is presented in Table 3.1. The weight ratio of fire-retardant compound, diluent, and unexpanded EPS microsphere was chosen as 10:1:8. The resulting expandable suspension was found to remain stable in the time scale much longer than that needed to complete the foaming process.

The recipe of fire retardant compound was modified from reference [119]. Phenolic resin was selected as the thermosetting binder because of its inherent fire-resistance after curing and good compatibility with EPS microspheres and inorganic fillers [120]. Aluminum hydroxide in particle form was chosen as inorganic fire-retardant additive due to its high effectiveness, low price, and smoke suppression capability [55]. Boric acid acted as an fire-retardant enhancer since it can react with aluminum hydroxide at high

temperature to form a glass structure [113]. Milled glass fibers (1/32” long) were added to the mixture as a mechanically reinforcing component. BYK-P® 104S is a commercial liquid additive containing low molecular weight unsaturated polycarboxylic acid polymer. It can be used to improve compatibility and wettability between inorganic and organic phases.

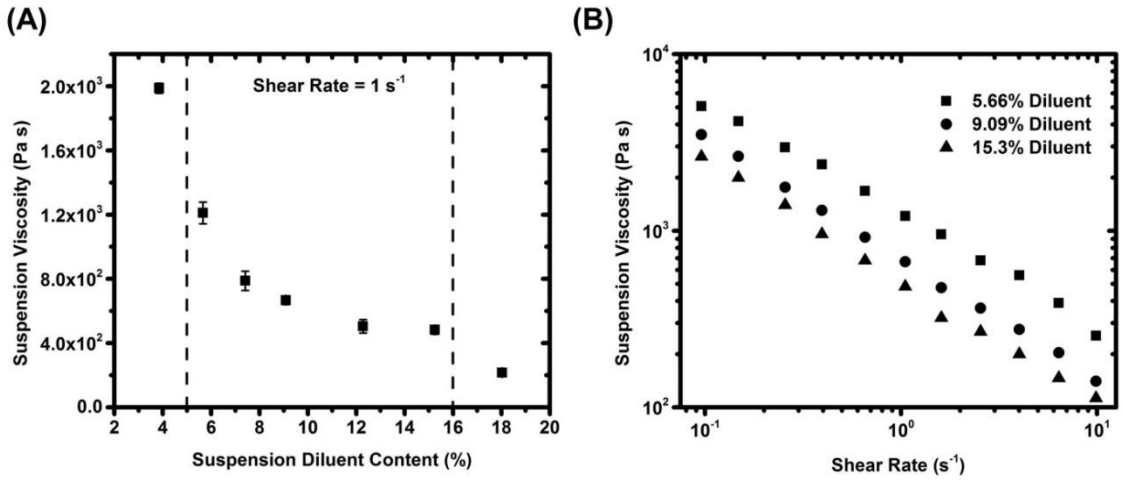


Figure 3.3 Suspension (containing only fire retardant compound and diluent) viscosity as a function of (A) diluent content and (B) shear rate.

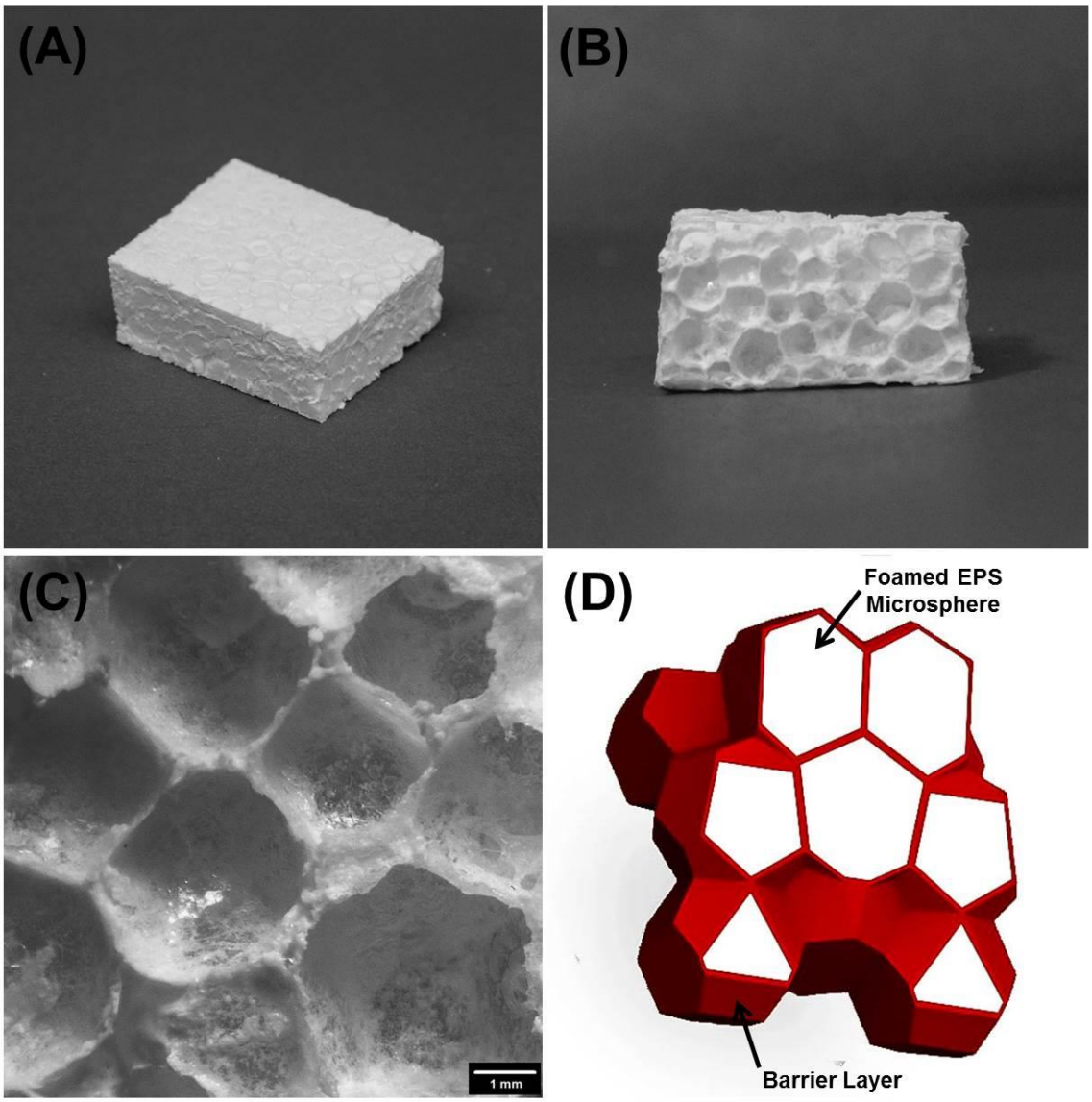


Figure 3.4 Composite EPS foam: (A) overall appearance, (B) morphology of honeycomb-like structure after dissolution of polystyrene, (C) morphology of barrier material, and (D) 3D pictorial model with cross-section.

The diluent made of 5% surfactant aqueous solution was used to control the viscosity and increase the stability of the suspension. Sodium dodecyl sulfate was chosen as the surfactant. The viscosity of the suspension contained only fire retardant

compound and diluent as functions of diluent content and shear rate is presented in Figure 3.3. In Figure 3.3 (A), the suspension viscosity decreases with increase of diluent. The shear rate was chosen to be $1s^{-1}$ because it was in the order of the mixing rate during suspension preparation. As discussed in the previous work, a minimum suspension viscosity is required to offset the buoyancy effect during EPS expansion [115]. It was also found the EPS microspheres cannot be effectively expanded at a too high suspension viscosity while, when the suspension viscosity was too low, the honeycomb-like barrier structure became incomplete. Details will be further discussed in the next section. Therefore, a recommended diluent content is from 5% to 16% by weight. In Figure 3.3 (B), it can be observed that the suspensions with different diluent contents follow a shear thinning behavior as the shear rate increases, corresponding to a typical rheological feature of aqueous suspension containing solid particles under steady shear [121].

### *3.3.3 Foam Morphology*

The expandable suspension was expanded via microwave heating into composite EPS foam. Post-curing at 60°C for 4hr was subsequently used to completely cure the phenolic resin. Optical images of the resulting foam are presented in Figure 3.4. In Figure 3.4 (A), it is found that the overall appearance of the composite foam is almost identical to that of the neat one. The only difference is that the composite foam is light yellow because of the color of the cured phenolic resin. The honeycomb-like barrier structure can be clearly observed after dissolving the EPS in the composite foam with cyclohexane, shown in Figure 3.4 (B). A magnified image of such barrier structure is presented in Figure 3.4 (C). Each individual foam particle is encapsulated by a very thin

composite barrier layer made of the fire-retardant compound. Moreover, due to the interaction of adjacent microspheres during expansion, the EPS microspheres developed into polyhedron geometries, similar to those found in neat EPS foams [110]. This shaped the cured barrier layers into a honeycomb-like structure. A pictorial model, presented in Figure 3.4 (D), with a cross-section cutting through the composite foam, is made to assist in the further illustration of 3D morphology of this unique honeycomb-like barrier structure.

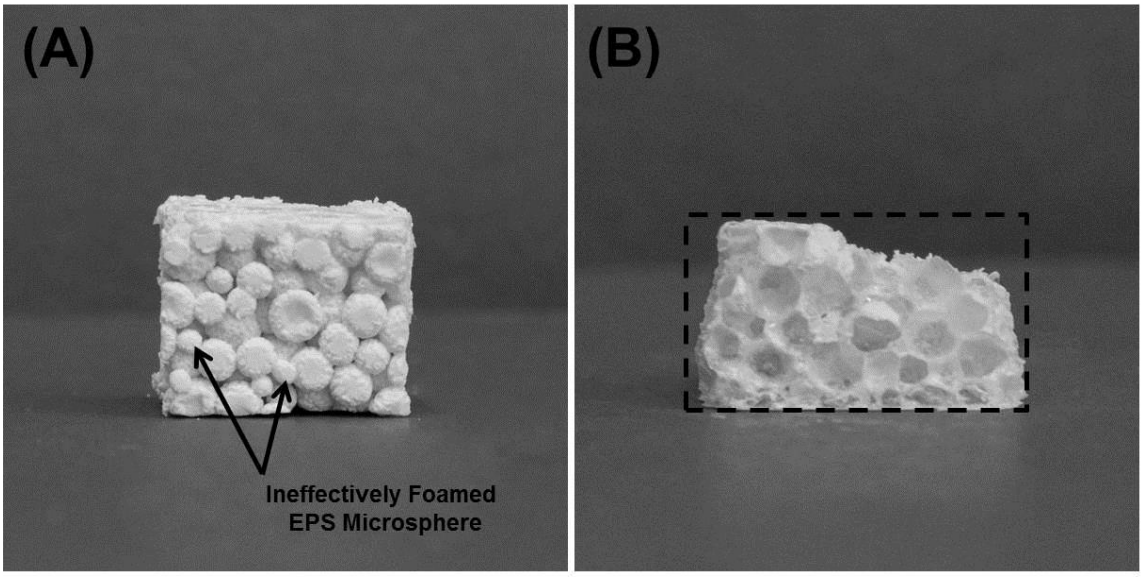


Figure 3.5 Composite EPS foam produced with a diluent weight content of: (A) 3.85% and (B) 19.4%.

As mentioned above, the diluent content of the expandable suspension can considerably influence the morphology of the composite foam. Results are shown in Figure 3.5. In Figure 3.5 (A), it can be observed that when the diluent concentration was very low (3.85%), corresponding to a high suspension viscosity (1984Pa·s), the EPS

microspheres cannot be effectively foamed, leaving unexpanded solid particles inside of the composite foam. As can be seen in Figure 3.5 (B), an incomplete barrier structure was formed when the water content was too high (19.4%) or the suspension viscosity was too low (151Pa·s). The black dash line outlines the shape of the composite foam before the dissolution of foamed polystyrene particles. It can be seen that some of the fire-retardant barrier layers in the top are missing, resulting in an inhomogeneous structure.

### *3.3.4 Foam Density and EPS Volume Fraction*

Table 3.2 summarizes the density and EPS volume fraction of the neat and the composite EPS foams. Here "neat EPS foam" refers to the foam made directly from foaming of EPS microspheres with no other component contained. To calculate the foamed EPS volume fraction in composite foam, the following equation was used:

$$\eta_{EPS} = \frac{\rho_{FRMixture} - \rho_{FRFoam}}{\rho_{FRMixture} - \rho_{NeatFoam}} \times 100\% \qquad (3.1)$$

where $\eta_{EPS}$ is the volume fraction of foamed EPS in the composite foam, $\rho_{FRMixture}$ is the density of fire-retardant compound after curing ($1.69\times10^3$kg/m$^3$), $\rho_{FRFoam}$ is the density of the composite EPS foam, and $\rho_{NeatFoam}$ is the density of the neat EPS foam.

The density of the neat EPS foam made in this work is 43.1±1.2kg/m$^3$ that is approximately half of the composite foam density as 93.6±2.0kg/m$^3$. The measured neat and composite foams were made using the same amount of fully expanded EPS microspheres from the same glass mold. Moreover, it is found that the foamed EPS

microspheres occupy as high as 96.9±2.3% of volume fraction in the composite foam in accordance with the fact that the barrier layer in the honeycomb-like structure is very thin.

Table 3.2 Summary of density and foamed EPS volume fraction of neat and composite EPS foams.

| Sample | Foam Density ($kg/m^3$) | Foamed EPS Volume Fraction (%) |
|---|---|---|
| Neat PS Foam | 43.1 ± 1.2 | 100.0 ± 0.0 |
| Composite PS Foam | 93.6 ± 2.0 | 96.9+ ± 2.3 |

*3.3.5 Foam Mechanical Property*

Mechanical properties, especially compressive and flexural properties, represent another important factor that considerably influences the performance of EPS foam. In this work, uniaxial compression, compressive creep, and three point bending tests were conducted to evaluate the mechanical performance of the composite polystyrene foam. Results of these tests are summarized and presented in Figure 3.6 and Table 3.3. The mechanical properties of the neat EPS foam are found to be comparable with data from commercialized products [1].

The flexural stress, modulus, and strain were calculated using the following equations [35, 117, 122]:

$$\sigma = \frac{3Pl}{2bd^2} \qquad (3.2)$$

$$E = \frac{l^3 m}{4bd^3} \qquad (3.3)$$

$$\varepsilon = \frac{6Dd}{l^2} \quad (3.4)$$

where $\sigma$ is the flexural stress, $E$ is the flexural modulus, $\varepsilon$ is the flexural strain, $P$ is the load, $l$ is the support span length, $b$ is the width of sample, $d$ is the depth of sample, $m$ is the slope of the tangent to the initial straight line portion of the load-deflection curve, and $D$ is the deflection of the center of the sample.

Table 3.3 Summary of mechanical properties of neat and composite EPS foams.

| | Sample | Compressive Modulus (MPa) | Compressive Stress at Pre-set Strain (MPa) |
|---|---|---|---|
| **Uniaxial Compression Test** | Neat PS Foam | 3.35±0.22 | 0.337±0.008 |
| | Composite PS Foam | 5.80±0.62 | 0.387±0.008 |
| | **Sample** | **Creep Compliance after 1 min ($10^{-5}$ $Pa^{-1}$)** | **Creep Compliance after 5 min ($10^{-5}$ $Pa^{-1}$)** | **Creep Compliance after 10 min ($10^{-5}$ $Pa^{-1}$)** |
| **Compressive Creep Test** | Neat PS Foam | 3.23±0.11 | 5.55±0.19 | 6.74±0.22 |
| | Composite PS Foam | 2.16±0.25 | 4.27±0.39 | 5.57±0.44 |
| | **Sample** | **Flexural Modulus (MPa)** | **Flexural Stress at Pre-set Strain (MPa)** |
| **Three Point Bending Test** | Neat PS Foam | 5.16±0.17 | 0.253±0.022 |
| | Composite PS Foam | 6.57±0.57 | 0.304±0.026 |

In Figure 3.6 (A), it can be seen that, in the uniaxial compression, the compressive modulus of the composite foam (5.80±0.62Mpa) is considerably higher than that of the neat foam, while the compressive stress at the pre-set strain (0.5mm/mm) of the neat foam (0.337±0.008MPa) is slightly lower than that of the composite foam (0.387±0.008MPa). Moreover, although the yielding strains of the neat and composite

foams are identical, the yielding stress of the composite one is larger due to its higher compressive modulus.

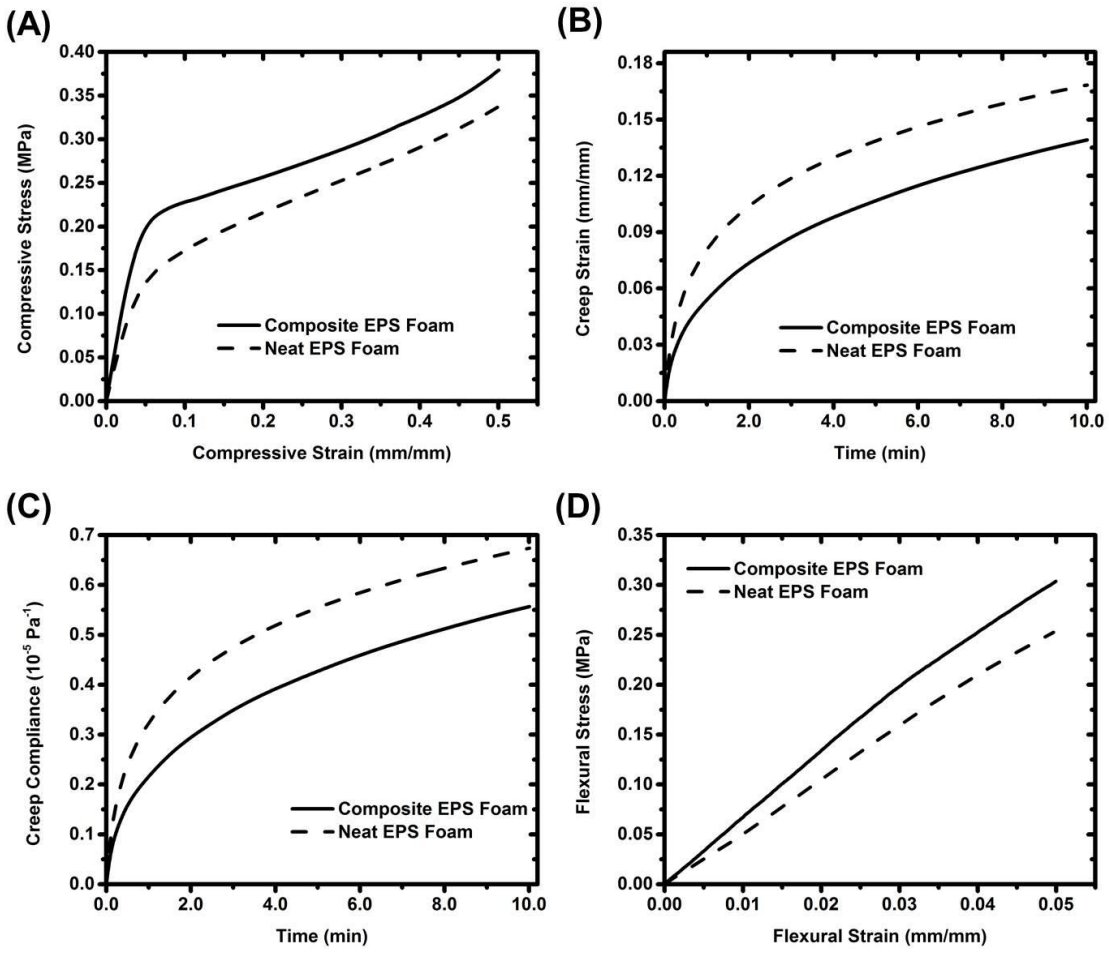


Figure 3.6 Representative curves of neat EPS foam and composite EPS foam under (A) uniaxial compression test (pre-set strain 0.5mm/mm), (B) compressive creep test (holding stress 0.25MPa), (C) compressive creep test (creep compliance as a function of time), and (D) three point bending test (pre-set strain 0.05mm/mm).

Results of compressive creep test are shown in Figure 3.6 (B) and (D). The holding stress was chosen to be 0.25MPa. It can be observed that the creep strain of the composite foam is lower than that of the neat foam. The curve of creep compliance as a function of time also follows a similar trend. Table 3.3 quantitatively illustrates this result, indicating that the composite foam is more durable when experiencing external stress compared with neat foam.

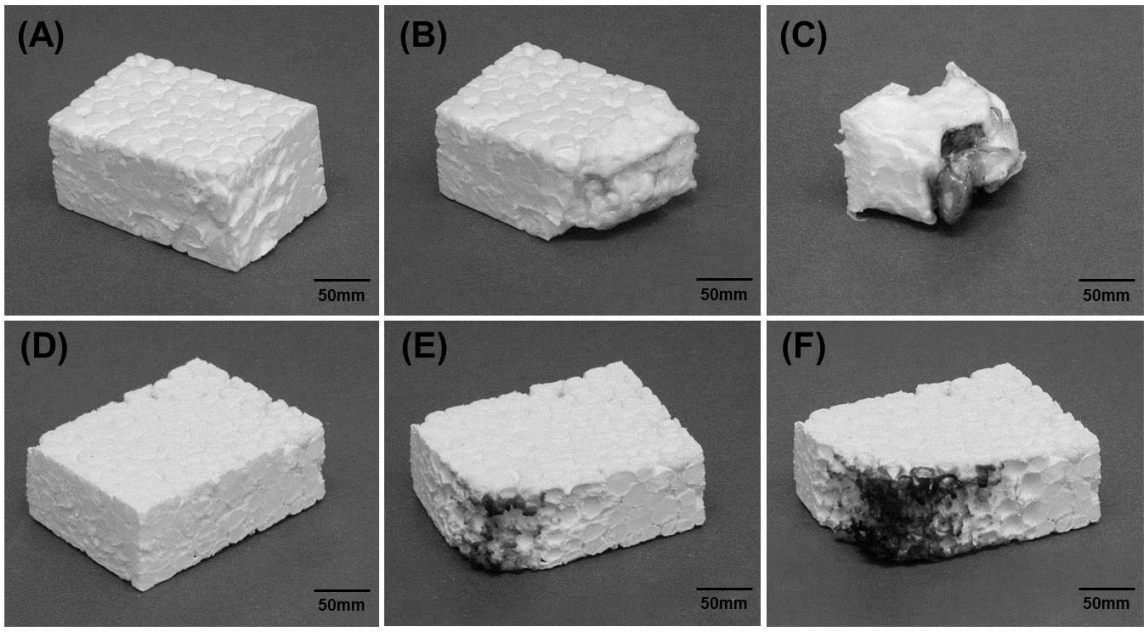


Figure 3.7 Comparison of burning characteristics of neat EPS foam (A-C) and composite EPS foam (D-F): before burning (A & D), after burning for 5s (B & E), and after burning for 15s (C & F).

The representative curves of both composite and neat EPS foams are presented in Figure 3.6 (C). The flexural modulus of the composite foam is found to be 6.57±0.57MPa which is higher than that of the neat foam (5.16±0.17MPa). Similarly, the flexural stress

at pre-set strain (0.05mm/mm) of the composite foam (0.304±0.026MPa) is calculated to be larger than that of the neat foam (0.253±0.022MPa).

Therefore, it is concluded that the existence of the honeycomb-like barrier structure can considerably improve the mechanical performance of the composite EPS foam in comparison with the neat one.

### *3.3.6 Foam Fire Retardation*

In this section, the fire retardation characteristics of the composite EPS foam with a honeycomb-like barrier structure is evaluated and compared with the neat EPS foam. The results on fire resistance test are shown in Figure 3.7. The composite foam and the neat foam before burning are shown in Figure 3.7 (A) and 7 (D), respectively. No obvious difference of appearances was found for the two foams in their initial state. During burning, an external fire source stayed in contact with one corner of the foam. Figure 3.7 (B) shows the composite foam after being burned for 5s. The polystyrene component was melted and retracted when contacting with the flame, leaving a hollow honeycomb-like structure. No dripping and nearly no black smoke were found. The overall shape of the foam stayed unchanged. When the external fire was removed, no flame was sustained on the foam. The neat polystyrene foam burnt for 5s is shown in Figure 3.7 (E). The polystyrene retracted and the foam structure was collapsed. Melt dripping and black smoke were observed. When the external fire was removed, the flame sustained itself on the neat foam. The composite foam and the neat foam burned for 15s are shown in Figure 3.7 (C) and 3.7 (F), respectively. The composite foam was found to be nearly fire-proofing. No dripping and nearly no smoke were observed. The honeycomb structure was kept with no collapse or observable shrinkage. The flame was

self-extinguished when the external fire source was removed. On the contrary, the neat EPS foam burned vigorously with burning dripping materials. Heavy black smoke was generated. The structure completely collapsed with shrinkage of the dimension. When the external fire was removed, the flame sustained itself and spread rapidly.

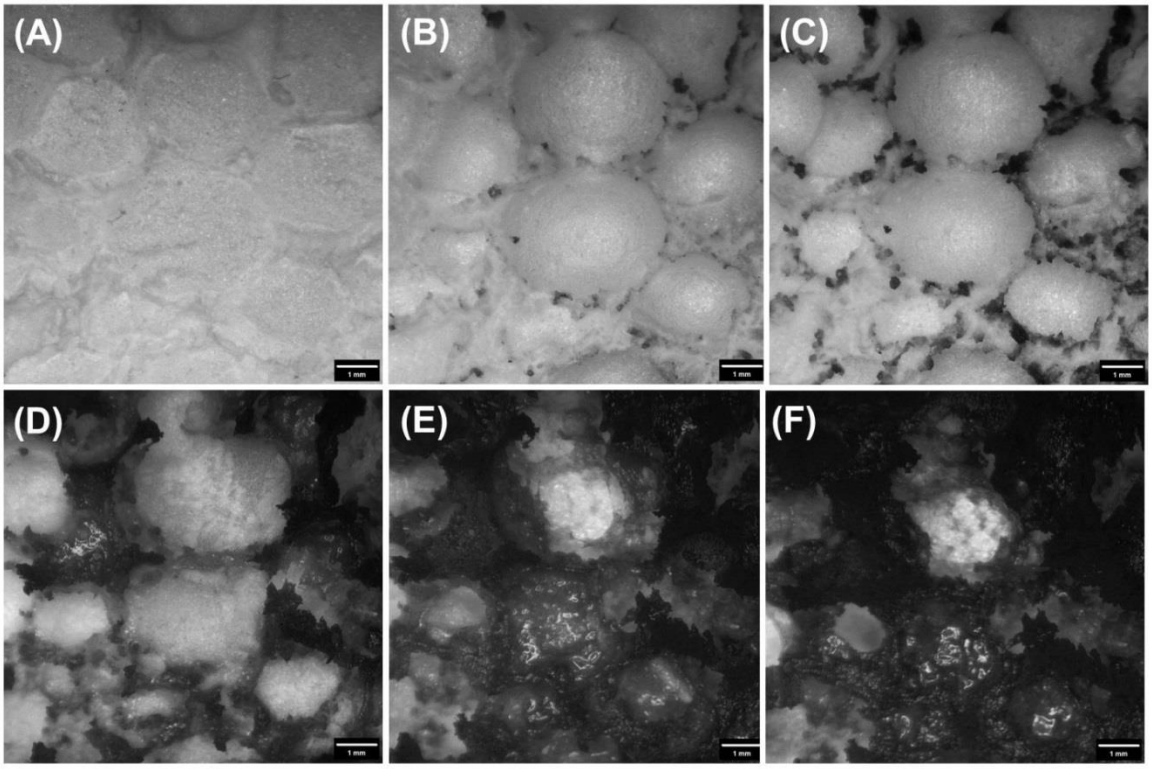


Figure 3.8 Local burning characteristics of composite EPS foam after contacting with fire flame for: (A) 0s, (B) 1s, (C) 3s, (D) 5s, (E) 10s, and (F) 15s.

To further study the fire retardation of the composite foam, local burning characteristics was observed with an optical microscopy, shown in Figure 3.8. In Figure 3.8 (A), before the burning test, the boundary between the foamed EPS microsphere and the fire-retardant barrier layer was difficult to distinguish. As the composite foam surface contacted with flame from 1s to 5s, shown from Figure 3.8 (B) to Figure 3.8 (D),

the polystyrene was melted and gradually retracted, leaving a hollow honeycomb structure. At the same time, the barrier layer began to turn dark because of the carbonization of phenolic resin and decomposition of fire-retardant fillers, but the overall barrier structure remained almost unchanged. When the composite foam was burnt from 10s to 15s, shown from Figure 3.8 (E) to Figure 3.8 (F), polystyrene at the surface completely disappeared but the polystyrene beneath the hollow honeycomb-like barrier still remained almost untouched. The barrier structure became darker, indicating a further progress of resin carbonization and filler decomposition. However, the overall structure was kept integrated and no obvious collapse or dimensional change was observed either.

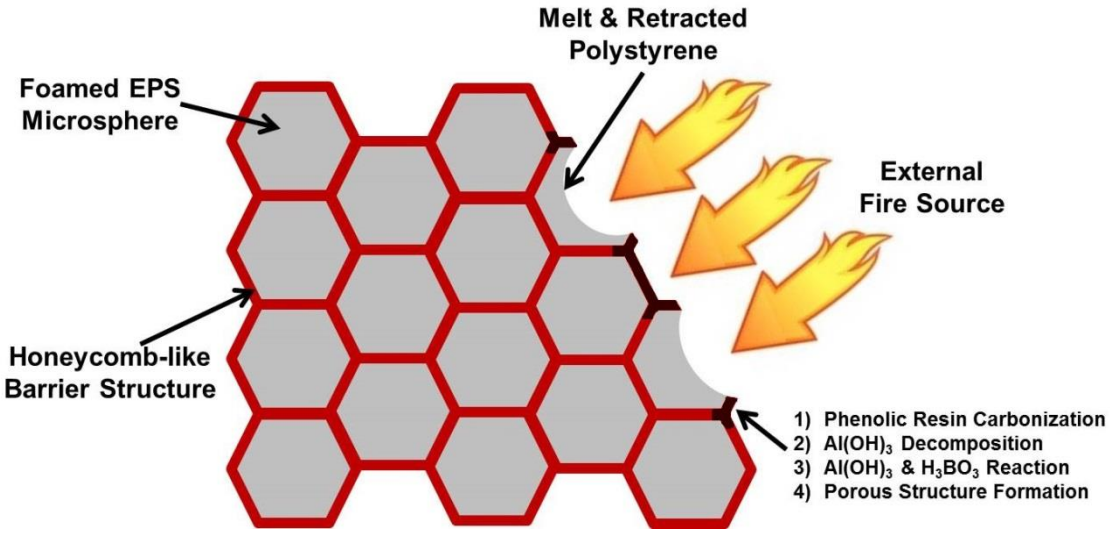


Figure 3.9 Illustration of fire-retardation mechanism of composite EPS foam.

An illustrative scheme is drawn in Figure 3.9 to have a further explanation on the fire-retardation mechanism of the composite EPS foam. When the foamed EPS particle is touched by an external fire source, the polystyrene is melted and retracted, leaving a

hollow honeycomb barrier structure contacting with the flame. In the barrier layer, the phenolic resin begins to be carbonized and the aluminum hydroxide starts to decompose. This process absorbs a large amount of energy and, at the same time, releases a great deal of water [123]. As the temperature continues to increase, aluminum hydroxide reacts with boric acid to form a glassy structure that can bear high temperature [50]. Since the honeycomb-like structure can remain a certain extent of rigidity even at high temperature, the foam structure can be kept integrated during the combustion. Moreover, during the hydroxide compound decomposition, a porous barrier structure that can effectively suppress the release of toxic smoke also forms [114]. Therefore, it can be concluded that the formed honeycomb-like barrier structure can considerably improve the fire-retardation of the composite EPS foam, by effectively stopping the fire path into the foam, suppressing the release of toxic smoke and retaining the integrity of the foam structure.

At last, the structure integrity when the foam contacted with a high-temperature surface was investigated. This test is important because usually, during the fire, the foam will not only directly contact with the flame but also with hot surfaces. The results are presented in Figure 3.10. Before the test, shown in Figure 3.10 (A), the composite foam and the neat foam were placed on a hot stage surface and then the surface temperature was raised to 350°C. As the contacting time went by from 1min to 3min, presented from Figure 3.10 (B) to Figure 3.10 (E), the neat polystyrene foam quickly shrank from a cuboid to a slice and finally into a melt with a disastrous collapse of the foam structure while only limited dimension shrinkage at the bottom was observed in the composite foam. The difference between the composition foam and the neat foam during the test can be explained as follows. As presented in Figure 3.10 (F), when contacting with the hot surface, the foamed polystyrene at the bottom surface was melted and

retracted, leaving a hollow honeycomb-like barrier structure. Since the hollow barrier remained structural integrity and sufficient rigidity to support the stand of the entire composite foam, it can prevent the foamed polystyrene to directly contact with the hot source, thus minimizing the dimensional shrinkage of the foam.

Based on the results from the above tests, it can be concluded that the composite polystyrene foam with a honeycomb-like barrier structure has improved fire-resistant properties over the neat polystyrene foam.

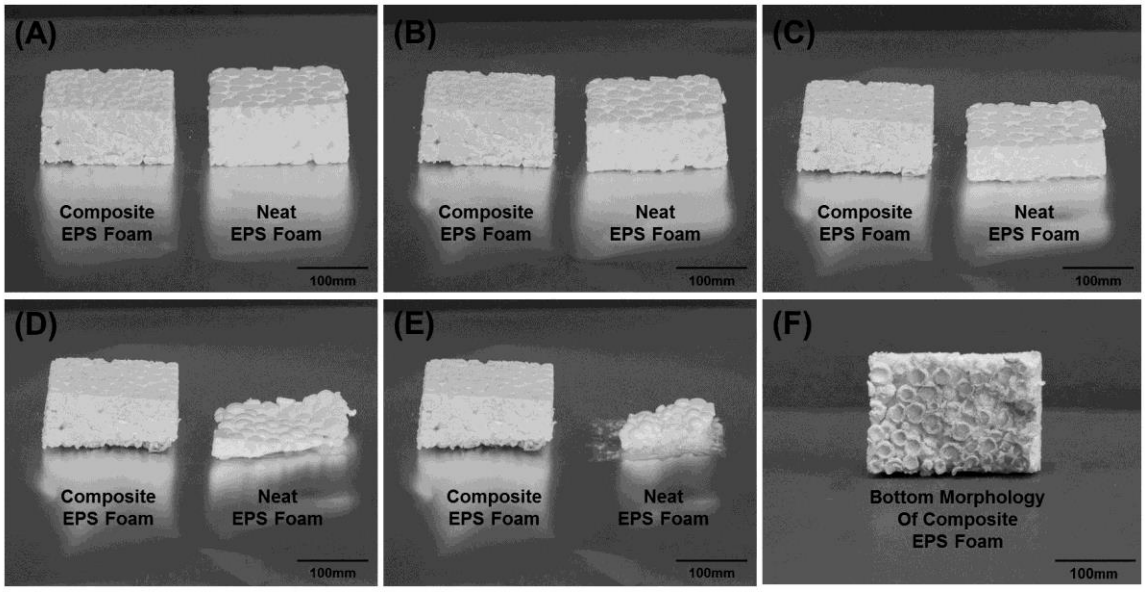


Figure 3.10 Comparison of dimensional change of neat EPS foam and composite EPS foam after contacting with hot surface (350$^{o}$C) for (A) 0.0min, (B) 1.0min, (C) 2.0min, (D) 2.5min, and (E) 3.0min; (F) shows the bottom surface morphology of the composite EPS foam after contacting with the hot surface for 3.0min.

### 3.4 Conclusions

A novel expandable suspension process was designed and developed to produce composite EPS foam with improved fire-retardant performance. This process converts an expandable suspension containing a fire-retardant compound, unexpanded EPS microspheres and a diluent, into a composite foam with a honeycomb-like barrier structure. The expandable suspension process is featured with incorporation of high loadings of environmentally friendly and low-cost inorganic fire-retardant agents without undermining the foamability of EPS microspheres.

The optical observation confirmed the formation of the honeycomb-like structure that encapsulates each individual foam microsphere in the composite foam. The diluent content was found to highly influence the suspension viscosity and the foam morphology. With low diluent concentration, EPS microspheres cannot be effectively expanded, while the barrier structure becomes incomplete when diluent content is high. Results from mechanical tests showed that the existence of the honeycomb-like barrier structure can considerably improve the foam mechanical performance, making the composite foam stiffer and more durable compared with the neat one. At last, fire-retardation tests demonstrated that the honeycomb-like barrier structure can effectively stop the fire path into the foam, suppress toxic smoke generation, and maintain foam structure integrity, enabling the composite foam to have substantially improved fire resistance in comparison with the neat foam.

# CHAPTER 4

# MODELING OF EXPANDABLE POLYSTYRENE EXPANSION*

## 4.1 Introduction

In Chapter 2, a microwave expansion process is designed and developed to address the emerging issues in the production of EPS-filled syntactic foams [115]. In this process, the unexpanded EPS microspheres are distributed and then directly foamed in the uncured thermosetting matrix using microwave heating. This process design is demonstrated with the capability of effectively expanding highly loaded EPS microspheres. The microwave expansion process was later extended to produce composite polystyrene foams with a unique honeycomb-like structure as shown in Chapter 3 [124]. The mechanical strength and fire resistance of the composite foams were found to be considerably improved compared with those made of neat polystyrene. In order to optimize the microwave expansion process, a further understanding on the fundamental aspect of this process is highly desired. It requests to establish a model that can simulate the core part of the process, the expansion of EPS microsphere, since kinetic parameters related to bubble nucleation and growth cannot be measured easily by experimental methods.

A number of modeling efforts have been made to simulate foaming processes involved with physical blowing agents in polymer melts. Existing methods include but are not limited to single bubble model [58-60], cell model [71, 73, 74], influence volume analysis [70, 77, 79, 80], level set method [125, 126] and biphase continuum approach [127]. However, these models cannot be directly applied to EPS expansion process because they almost exclusively focus on the foaming processes triggered by the

sudden decrease of system pressures. The expansion of EPS, on the other hand, is started by heating the system to the expansion temperature. Moreover, the methods mentioned above usually only simulate the formation of cell microstructure but do not take the geometry of foamed plastics into consideration. However, the geometry of EPS microsphere must be considered. This is because the shape and size of foamed EPS directly impact the morphology and property of the resulting foam. Another similar process to EPS expansion is the bubble growth of vapor in boiling water. This happens when water is heated to boiling temperature and small air bubbles that are dissolved or adhered to impurities quickly grow and collapse. The existing efforts to model this water boiling process usually do not consider the diffusion of vapor into the expanding bubbles since it plays a minor role [128, 129]. However, the gas diffusion cannot be neglected in the modeling of EPS microsphere, for it is directly related with the nucleation and expansion of bubbles.

Chapter 4 presents a general formulation for assistance in the further understanding on the basics of the expansion process of EPS microsphere. A semi-analytical solution was first obtained to provide a relatively simple tool to understand and optimize the expansion process. Dimensionless groups and characteristic parameters were defined. They were then employed to analyze the modeling results. In order to obtain an accurate prediction of EPS expansion, a numerical solution to the model that couples the nucleation and expansion of multiple bubbles in a finite matrix was subsequently developed. The kinetics and temperature dependence of EPS expansion from the numerical solution were studied and compared with those from the semi-analytical solution. At last, a parameter sensitivity study was performed to examine the effect of each parameter over the expansion process.

## 4.2 Experimental

### *4.2.1 Materials*

Cup grade unexpanded EPS microspheres DYLITE® F271T, obtained from Nova Chemicals Corporation (Moon Township, PA), were used in this study. The unexpanded EPS contains approximately 5.6% (w/w) of pentane with an average diameter of 388.6±17.8μm.

### 4.2.2 Characterization

Rheological properties of the polystyrene in EPS were characterized on a controlled-stress rotational rheometer with 21mm diameter parallel steel plates (model: Thermo Mars II, Thermo Fisher Scientific, Inc., Waltham, MA). The polystyrene was obtained directly from the EPS microspheres used in this study after a vacuum de-gassing process to remove the pentane inside.

Radial expansion of EPS microsphere as a function of time was recorded in real-time by a hot stage (Model T95-HS, Linkam Scientific Instruments Ltd, UK) mounted onto an Olympus BX51 optical microscope installed with an Olympus UC30 digital camera (Olympus Corporation of the Americas, Center Valley, PA).

## 4.3 Model Development

### *4.3.1 General Formulation*

Before the expansion, EPS microspheres are stored at room or lower temperatures to keep the pentane/polystyrene solution in a stable state. When the microspheres are

heated to expansion temperature, the solution becomes supersaturated because of the decrease of pentane solubility. In order to minimize the free energy of the system, bubble nucleation begins. The continuous expansion of bubbles is driven by the difference between bubble pressure and ambient pressure. During the expansion of old bubbles, new bubbles will be nucleated simultaneously. The termination of expansion of individual bubbles is reached when the bubble pressure, ambient pressure and matrix surface stress are balanced.

A scheme that illustrates the growth of bubble in the matrix during EPS expansion process is shown in Figure 4.1. The bubble radius is defined as $R(t,t')$ which represents the radius at time $t$ of the bubble nucleated at time $t'$. The bubble pressure at time $t$ of the bubble nucleated at time $t'$ is expressed as $P_b(t,t')$. The average pentane concentration in EPS matrix is defined as $\bar{c}(t')$. Before expansion, $\bar{c}(t')$ is equal to $c_0$ which is the initial pentane concentration. The EPS matrix has a surface tension of $\sigma$ and a viscosity of $\eta$. When $t=0$, the bubble has an initial radius of $R_0$ and initial bubble pressure of $P_{b0}$.

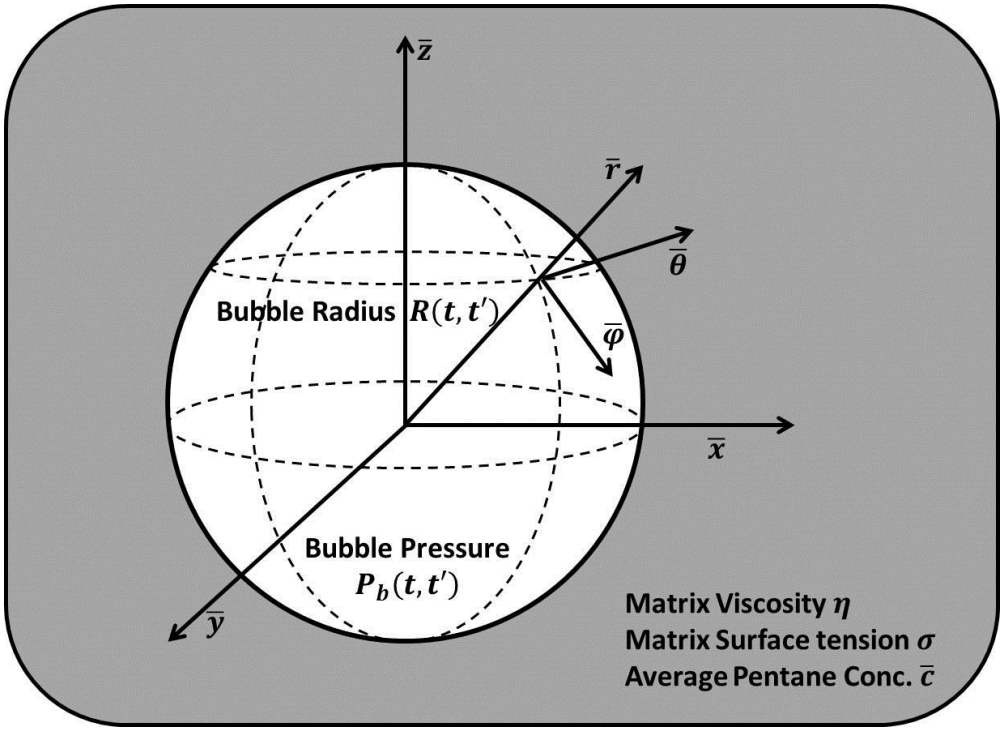


Figure 4.1 Scheme of bubble growth in EPS matrix.

The bubble is assumed to remain a spherical shape during the expansion. Then a spherical coordinate system can be established in each bubble with the coordinate origin fixed at the center of sphere. The continuity equation of the bubble with the boundary condition $v_r\big|_{r=R} = \frac{\partial R}{\partial t}$, can be written as

$$v_r = \frac{R^2}{r^2}\frac{\partial R}{\partial t}. \qquad (4.1)$$

Since the viscosity of polystyrene matrix is very high during EPS expansion, the effects of gravity and inertia can be neglected [130]. Therefore, the equation of motion in the radial direction is written as

$$0 = -\frac{\partial P}{\partial r} + \frac{\partial \tau_{rr}}{\partial r} + \frac{2(\tau_{rr} - \tau_{\theta\theta})}{r}. \qquad (4.2)$$

By integrating both sides and substituting the Young-Laplace equation for a spherical bubble, Equation (4.2) can be expressed as

$$0 = -\frac{2\sigma}{R} + P_b - P_a + 2\int_R^\infty \frac{(\tau_{rr} - \tau_{\theta\theta})}{r} dr. \qquad (4.3)$$

Here $P_a$ is the ambient pressure. Equation (4.3) is the governing equation that couples the momentum and mass conservations in the bubble expansion.

At the bubble surface, the diffusion of pentane molecules into the bubble can be expressed as

$$\frac{dn_g}{dt} = 4\pi D R^2 \left.\frac{\partial c}{\partial r}\right|_{r=R} \qquad (4.4)$$

where $D$ is the diffusion coefficient of pentane in polystyrene, $c$ is the pentane concentration, and the mole number of pentane molecules in the bubble is calculated by the ideal gas law $n_g = \frac{P_b V_b}{\Re T} = \frac{4\pi R^3 P_b}{3\Re T}$.

Therefore, Equation (4.4) can be re-organized as

$$R\frac{dP_b}{dt} + 3P_b\frac{dR}{dt} = 3D\Re T \left.\frac{\partial c}{\partial r}\right|_{r=R}. \qquad (4.5)$$

Equation (4.5) is the governing equation that considers the mass balance in the pentane transfer.

In this model, thermal effects are considered to be of negligible importance since the condition of EPS expansion is isothermal [131]. Moreover, because it usually takes only several seconds to fully expand the EPS microspheres, the loss of pentane to the surroundings is not taken into consideration.

*4.3.2 Semi-analytical Solution*

To obtain a semi-analytical solution to the model developed above, the bubble is assumed to expand in an infinite EPS matrix of which viscosity $\eta$ is constant and the pentane diffusion through the bubble surface is not considered.

Based on these simplifications, Equation (4.3) can be re-written as

$$P_b - P_a - \frac{2\sigma}{R} - \frac{4\eta}{R}\frac{\partial R}{\partial t} = 0. \qquad (4.6)$$

Here several dimensionless groups including dimensionless bubble radius $R^*$, dimensionless bubble pressure $P_b^*$ and dimensionless expansion time $t^*$ are defined, namely,

$$R^* = \frac{R\left(P_{b0} - P_a\right)}{2\sigma}, \qquad (4.7)$$

$$P_b^* = \frac{P_b - P_a}{P_{b0} - P_a}, \qquad (4.8)$$

$$t^* = \frac{t\left(P_{b0} - P_a\right)}{4\eta}. \qquad (4.9)$$

With these dimensionless groups, Equation (4.6) can be re-written as

$$\frac{dR^*}{dt^*} = P_b^* R^* - 1. \qquad (4.10)$$

The characteristic bubble expansion time $t_c$ and characteristic bubble radius $R_c$ are found to be

$$t_c = \frac{4\eta}{P_{b0} - P_a}, \qquad (4.11)$$

$$R_c = \frac{2\sigma}{P_{b0} - P_a}. \qquad (4.12)$$

According to the ideal gas law, the bubble pressure can be correlated with bubble radius as

$$P_b = \frac{P_{b0} R_0^3}{R^3}. \qquad (4.13)$$

The bubble radius and bubble pressure can be solved by substituting Equation (4.13) back to Equation (4.6). The constants used are given in Table 4.1 [132, 133].

To model the expansion process of the EPS microsphere, a bubble nucleation mechanism should be introduced. However, as pentane diffusion is not considered, existing diffusion-based nucleation theories cannot be adopted. Since experiments have shown that nucleation often undergoes an exponential decay, the nucleation rate is assumed to follow an exponential law [134]:

$$J(t') = N_1 \exp\left(-\frac{t'}{N_2}\right) \qquad (4.14)$$

where $J(t')$ is the bubble nucleation rate as a function of bubble nucleation time $t'$, $N_1$ is a pre-exponential constant ($7.5\times10^{14}\ s^{-1}\cdot m^{-3}$), and $N_2$ is a nucleation time constant ($0.45\ s$). Therefore, the EPS radius $\hat{R}(t')$ can be calculated by the following expression:

$$\hat{R}(t') = \sqrt[3]{\hat{R}_0^3 + V_0 \int_0^{t'} J(t') R^3(t,t') dt'} \qquad (4.15)$$

where $\hat{R}_0$ is the initial radius of EPS microsphere and $V_0$ is the initial volume of EPS microsphere.

Table 4.1 Summary of constants and characteristic parameters in semi-analytical solution.

| **Expansion Temperature** | **Matrix Viscosity** $\eta$ **(**$\times10^5 Pa\cdot s$**)** | **Matrix Surface Tension** $\sigma$ **(**$N\cdot m^{-1}$**)** | **Saturated Pentane Pressure** $P_{b0}$ **(**$\times10^5 Pa$**)** | **Characteristic Bubble Expansion Time** $t_c$ **(**$s$**)** | **Characteristic Bubble Radius** $R_c$ **(**$\times10^{-8} m$**)** |
|---|---|---|---|---|---|
| 130°C | 3.02 | 0.034 | 11.04 | 1.20 | 6.53 |
| 140°C | 1.33 | 0.033 | 13.31 | 0.43 | 5.21 |
| 150°C | 0.61 | 0.032 | 15.92 | 0.16 | 4.20 |

*4.3.3 Numerical Solution*

In the work mentioned above, the model is simplified so as to obtain a semi-analytical solution based on a single bubble growth in an infinite matrix. It has been found that the semi-analytical solution can only qualitatively predict the radial expansion of EPS. Detailed results will be shown in the Results and Discussion section. In order to more accurately predict the expansion of EPS, a numerical solution is then developed

based on the nucleation and expansion of multiple bubbles in a finite matrix at various temperatures and the diffusion of pentane.

A classical heterogeneous nucleation theory is applied to describe the bubble nucleation process of EPS expansion [92]. The nucleation rate is modeled as

$$J(t') = f_0 \bar{c} \sqrt{\frac{2\sigma N_A^3}{\pi M_w}} \exp\left(-\frac{\Delta E F}{k_B T}\right) \quad (4.16)$$

where $f_0$ is the Zeldovich correction factor, $N_A$ is Avogardro's number, $M_W$ is the molecular weight of pentane, $F$ is a correction factor of free energy barrier $\Delta E$, and $k_B$ is Boltzmann's constant.

The free energy barrier $\Delta E$ is expressed as

$$\Delta E = \frac{16\pi\sigma^3}{3(P_{b0} - P_a)^2} \quad (4.17)$$

where $\sigma$ can be expressed by the following semi-empirical equation [135]:

$$\sigma = \left[4.07 \times 10^{-2} - 7.2 \times 10^{-5}(T - 293)\right] \cdot N \cdot m^{-1}. \quad (4.18)$$

The temperature dependence of pentane saturated pressure is calculated using the Generalized Wagner model [133],

$$\ln P_{b0} = \ln P_{b0}^c + \frac{T^c}{T}\left(c_1\tau + c_{1.5}\tau^{1.5} + c_2\tau^2 + c_3\tau^3 + c_4\tau^4\right) \quad (4.19)$$

where $P_{b0}^c$ is the critical saturated pressure of pentane and $T^c$ is the critical temperature, and $\tau$ is a reduced temperature that can be expressed as

$$\tau = 1 - \frac{T}{T^c}. \qquad (4.20)$$

Since the pentane only occupies approximately 5.6% weight fraction in EPS, it is reasonable to assume that the rheological behavior of the polystyrene can represent that of the pentane/polystyrene solution. As shown in Figure 4.2 (A), the viscosity of polystyrene as a function of shear rate can be well fitted by a power-law model [121],

$$\underline{\underline{\tau}} = \eta_0 \left| \sqrt{\frac{1}{2}\underline{\underline{\dot{\gamma}}} : \underline{\underline{\dot{\gamma}}}} \right|^{n-1} \underline{\underline{\dot{\gamma}}} \qquad (4.21)$$

where $n$ is the power-law index and $\eta_0$ is the pre-exponent coefficient. With Equation (4.1), the second invariant in the power-law model can be written as $\frac{1}{2}\underline{\underline{\dot{\gamma}}} : \underline{\underline{\dot{\gamma}}} = 12\left(\frac{R^2}{r^3}\frac{\partial R}{\partial t}\right)^2$.

Then, by substituting Equation (4.21) into Equation (4.3), the following equation can be obtained:

$$P_b - P_a - \frac{2\sigma}{R} - \frac{4\eta_0}{n}\left(2\sqrt{3}\right)^{n-1}\left(R^2\frac{\partial R}{\partial t}\right)^n \frac{1}{R^{3n}} = 0. \qquad (4.22)$$

As shown in Figure 4.2 (B), the temperature dependence of the pre-exponent coefficient $\eta_0$ can be approximated using the Andrade-Eyring model [130]:

$$\eta_0 = K \exp\left(\frac{E_\eta}{\Re T}\right) \qquad (4.23)$$

where $K$ is a pre-exponent constant, $E_\eta$ is the activation energy, and $\Re$ is the universal gas constant. The power-law index $n$ at different temperatures is found to be

approximately 0.852 (Figure 4.2 (C)). Therefore, the temperature dependence of the rheological behavior of polystyrene is obtained. Predicted polystyrene viscosity as a function of shear rate at 140°C is shown in Figure 4.2 (D).

If it is assumed that pentane follows Henry's Law [78], and the gas concentration profile at the surface of a bubble can be expressed as

$$\frac{\partial c}{\partial r}\Big|_{r=R} = \frac{1}{\beta R}\left(\bar{c} - k_H P_b\right) \qquad (4.24)$$

where $k_H$ is Henry's solubility constant and $\beta$ is the diffusion radius correlation constant.

The average pentane concentration $\bar{c}$ can be calculated by

$$\frac{d\bar{c}}{dt} = -\frac{4\pi D}{\beta}\int_0^{t'} J(t')R(\bar{c} - P_b k_H)dt'. \qquad (4.25)$$

The temperature dependence of diffusion coefficient $D$ is found to follow an Arrhenius Equation [136]:

$$D = D_0 \exp\left(-\frac{E_D}{\Re T}\right) \qquad (4.26)$$

where $D_0$ is the pre-exponent diffusion coefficient and $E_D$ is the activation energy of diffusion.

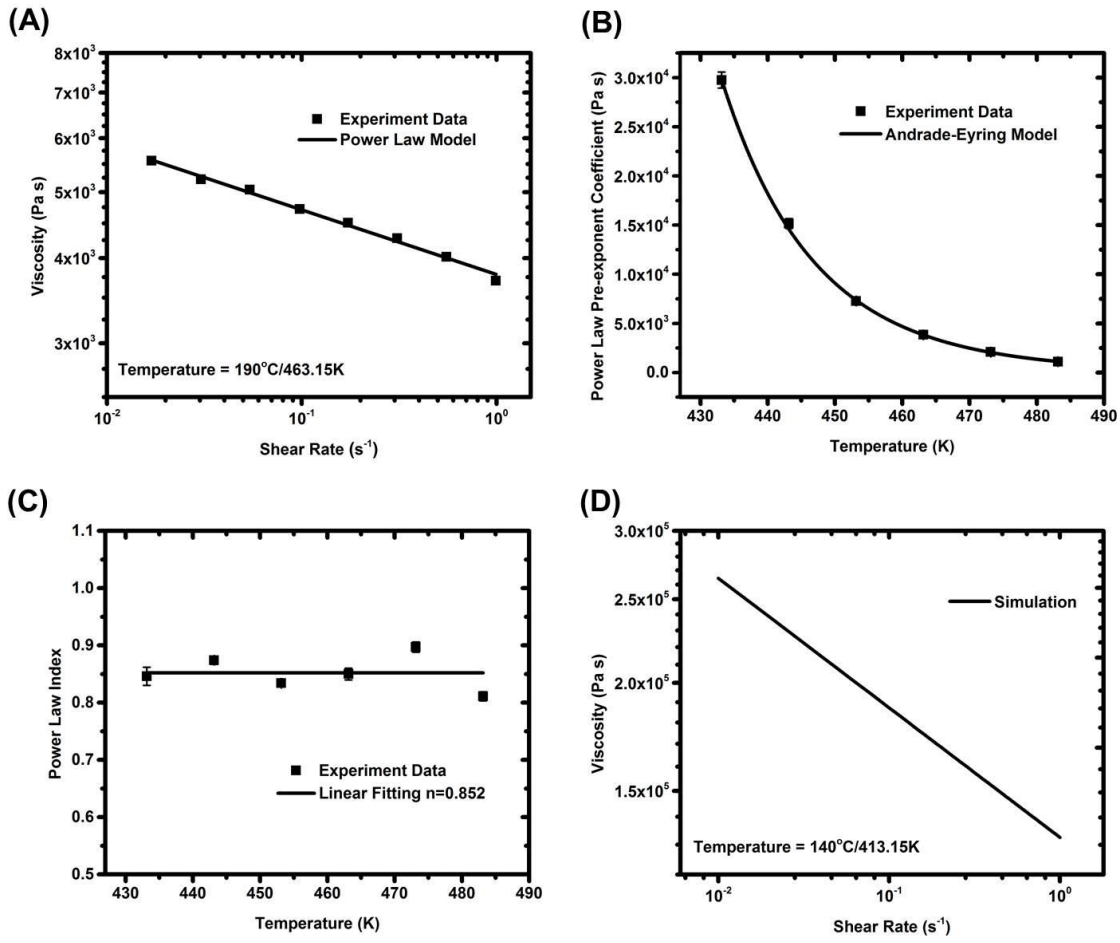


Figure 4.2 A) Power-law model fit to polystyrene viscosity as a function of shear rate at 190°C, B) Andrade-Eyring model fit to power-law model pre-exponent coefficient as a function of temperature, C) linear fit to power-law model index as a function of temperature, and D) predicted polystyrene viscosity as a function of shear rate at 140°C.

Table 4.2 Summary of constants in numerical solution.

| | Symbol | Value | Units |
|---|---|---|---|
| Ambient Pressure | $P_a$ | $1.01\times10^{5}$ | $Pa$ |
| Critical Pentane Gas Saturated Pressure | $P_{b0}^{c}$ | $3.37\times10^{6}$ | $Pa$ |
| Critical Temperature | $T^{c}$ | 469.7 | $K$ |
| Generalized Wagner Equation Constants | $c_1$ | -7.349492 | - |
| | $c_{1.5}$ | 2.382017 | - |
| | $c_2$ | -2.176618 | - |
| | $c_3$ | 0.891296 | - |
| | $c_4$ | -3.841503 | - |
| Correction Factor of Zeldovich Factor | $f_0$ | $3.15\times10^{-22}$ | - |
| Correction Factor of Free Energy Barrier | $F$ | $6.74\times10^{-5}$ | - |
| Power-law Model Index | $n$ | 0.852 | - |
| Andrade-Eyring Model Pre-exponent Constant | $K$ | $5.11\times10^{-10}$ | $Pa\cdot s^{-1}$ |
| Andrade-Eyring Model Activation Energy | $E_\eta$ | $1.14\times10^{5}$ | $J\cdot mol^{-1}$ |
| Diffusion Coefficient Pre-exponent Constant | $D_0$ | $2.42\times10^{11}$ | $m^2\cdot s^{-1}$ |
| Diffusion Activation Energy | $E_D$ | $1.59\times10^{5}$ | $J\cdot mol^{-1}$ |
| Initial Gas Concentration | $c_0$ | $7.04\times10^{2}$ | $mol\cdot m^{-3}$ |
| Diffusion Radius Correlation Constant | $\beta$ | 1.842 | - |
| Henry's Solubility Constant | $k_H$ | $7.8\times10^{-9}$ | $Pa\cdot mol^{-1}\cdot m^3$ |

Resistance to EPS microsphere expansion is generated when the process takes place in pre-cured epoxy resin. It is assumed that the resistant stress applied on the individual bubble equals to that on the whole microsphere. If a spherical coordinate system $(\hat{r},\hat{\theta},\hat{\varphi})$ is established to the entire EPS microsphere with the coordinate origin at the sphere center, the stress tensor of epoxy resin can be expressed as

$$\underline{\underline{\hat{\tau}}} = \eta_E \underline{\underline{\dot{\hat{\gamma}}}} \qquad (4.27)$$

where $\eta_E$ is the viscosity of epoxy resin and it is set to be constant for simplicity. Details can be found in the results and discussion section.

With the mass conservation of epoxy resin, the principal stress at the surface of EPS microsphere in the radial direction can be expressed as

$$\hat{\tau}_{rr}\big|_{\hat{r}=\hat{R}} = -\frac{4\eta_E}{\hat{R}}\frac{\partial \hat{R}}{\partial t} \qquad (4.28)$$

The influence of epoxy resin on the expansion kinetics of EPS can then be incorporated into the model by adding Equation (4.28) into Equation (4.3).

The accurate model is numerically solved by coupling the governing equations developed above. The constants in the model are summarized in Table 4.2 [78, 132, 133, 136].

## 4.4 RESUTLS AND DISCUSSION

### *4.4.1 Semi-analytical Solution*

The results of bubble radius growth as a function of time are presented in Figure 4.3 (A). Generally, the radius of bubble increases very fast after the start of expansion until an equilibrium state is reached when the bubble pressure is equal to the sum of ambient pressure and surface stress. Similar trends are also found in the change of bubble pressure presented in Fig.3 (B). The bubble pressure drops very fast to the equilibrium state during the expansion of bubbles.

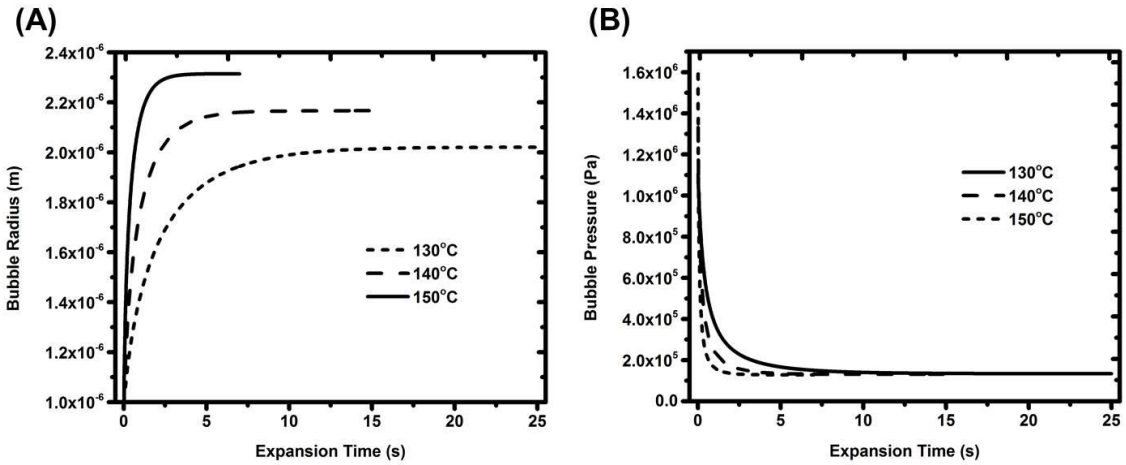


Figure 4.3 A) Bubble radius and B) bubble pressure as a function of expansion bubble time in the semi-analytical solution.

The characteristic bubble expansion time is an important characteristic parameter that correlates with properties of both matrix and bubble. It can be used to characterize the time scale of the expansion of bubbles. As found in Table 4.1, the characteristic expansion time decreases with the increase of expansion temperature. This is because a higher expansion temperature results in a lower matrix viscosity and larger saturated pressure of pentane. Therefore, it can be further deduced that the rates of bubble radius growth and bubble pressure drop at higher temperature will be larger. This deduction is affirmed by the results shown in Figure 4.3. Another important characteristic parameter is the characteristic bubble radius which can characterize the size of the equilibrated bubble radius. It correlates with the bubble surface energy and pressure difference. The former applies resistance to the expanding bubbles while the latter is the driving force for the expansion. As presented in Table 4.3 and Figure 4.3 (A), with the increase of characteristic bubble radius, the ultimate bubble radius increases.

With the obtained bubble radius and pressure, the dimensionless bubble radius and pressure can be calculated using Equation (4.7) and (4.8), respectively. It is found

that, in a large range of temperatures, the dimensionless bubble radius and the dimensionless bubble pressure are functions of dimensionless expansion time, following exponential relations:

$$R^* = -A_{A1}\exp\left(-\frac{t^*}{A_{A2}}\right) + A_{A3} \quad (4.29)$$

$$P_b^* = B_{A1}\exp\left(-\frac{t^*}{B_{A2}}\right) + B_{A3} \quad (4.30)$$

where $A_{Ai}$ and $B_{Ai}(i = 1,2,3)$ are constants that are dependent of expansion temperature. Their values are summarized in Table 4.3. It can be obtained that, while the values of $A_{Ai}$ change at different expansion temperatures, $B_{Ai}$ remain the same, indicating that $R^*$ is more sensitive to the variation of temperature.

Table 4.3 Summary of constants in the exponential fitting of dimensionless bubble radius and dimensionless bubble pressure as functions of dimensionless expansion time in semi-analytical solution.

| **Expansion Temperature** | $A_{A1}$ | $A_{A2}$ | $A_{A3}$ |
|---|---|---|---|
| 130°C | 14.03±0.025 | 1.95±0.006 | 30.77±0.006 |
| 140°C | 19.93±0.048 | 2.44±0.009 | 41.48±0.008 |
| 150°C | 27.78±0.110 | 2.92±0.018 | 54.91±0.017 |
| **Expansion Temperature** | $B_{A1}$ | $B_{A2}$ | $B_{A3}$ |
| 130°C<br>140°C<br>150°C | 0.81±0.006 | 0.78±0.008 | 0.031±0.0005 |

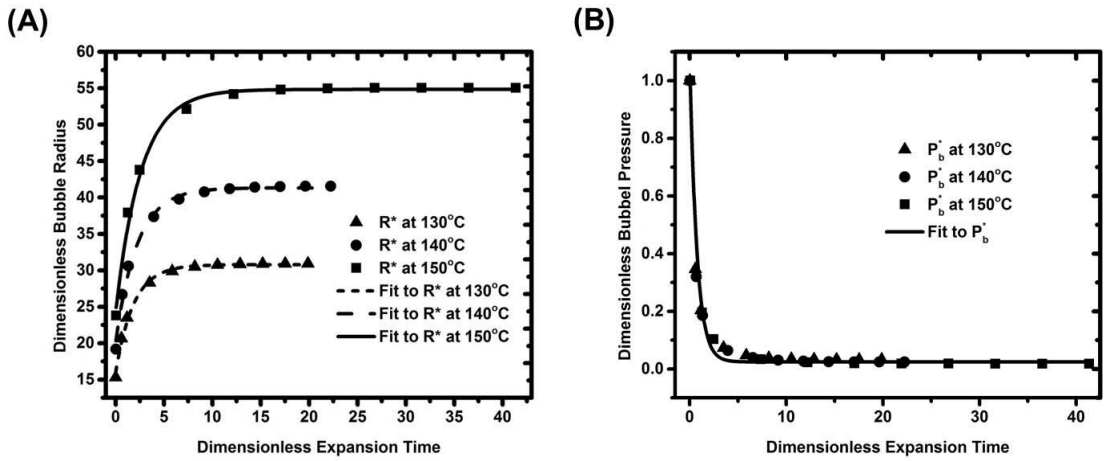


Figure 4.4 A) Dimensionless bubble radius and B) dimensionless bubble pressure as a function of dimensionless expansion time in the semi-analytical solution.

The fitting results are presented in Figure 4.4. It can be observed that the growing rate of dimensionless bubble radius increases with the increase of characteristic expansion time and reaches a larger ultimate value, corresponding to a smaller characteristic bubble expansion time and a larger characteristic bubble radius. The temperature, however, has little influence over the dimensionless bubble pressure. As the simple exponential relation of dimensionless bubble radius and pressure can be applied in a large range of expansion temperatures, the expansion kinetics of bubbles can thus be easily estimated, assisting in the design of process.

The radial expansion of the whole EPS microsphere can be calculated with an exponential bubble nucleation expression. The comparison between experimental and modeling results is shown in Figure 4.5. It can be seen that the semi-analytical solution is able to predict, at least at a qualitative level, the radius growth of the expanding EPS microsphere obtained from a real-time observation at different expansion temperatures.

Moreover, a faster expansion is obtained when the characteristic expansion time is smaller.

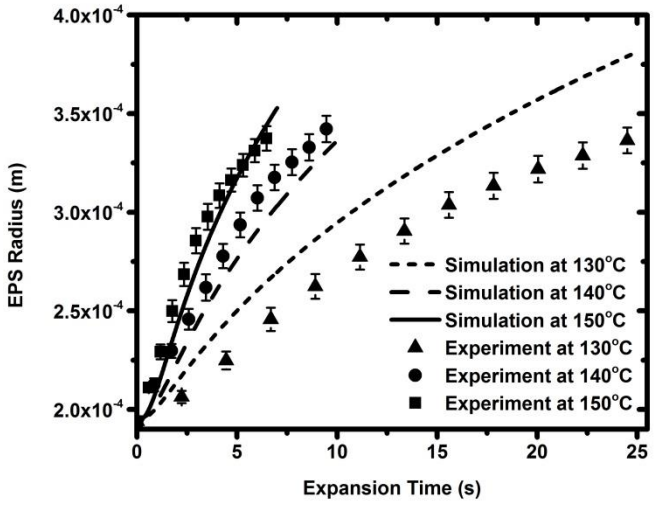


Figure 4.5 Comparison between experimental radial growth of EPS and the predicted one from the semi-analytical solution at different temperatures.

This simple semi-analytical solution can be easily employed to analyze the expansion kinetics of bubbles and EPS microspheres, providing references to the design and optimization of expansion process. However, such solution can only lead to a qualitative prediction to actual expansion process because several non-realistic simplifications are involved in the solution development. First, the bubble expansion is assumed to take place in an infinite matrix. However, the matrix is usually finite in actual cases. Second, the pentane transfer is assumed to be neglected between bubble and matrix. This is not true because, during the bubble expansion, the pentane dissolved in polystyrene diffuses into the bubble due to the existence of a concentration gradient. For the same reason, the existing bubble nucleation theory cannot be correlated with the

semi-analytical solution. Third, the viscosity of EPS matrix is assumed to be constant, but it is widely acknowledged that the polystyrene viscosity is shear-rate dependent. Therefore, in order to have a quantitative prediction of the actual expansion process of EPS microsphere, the model without these simplifications need to be solved.

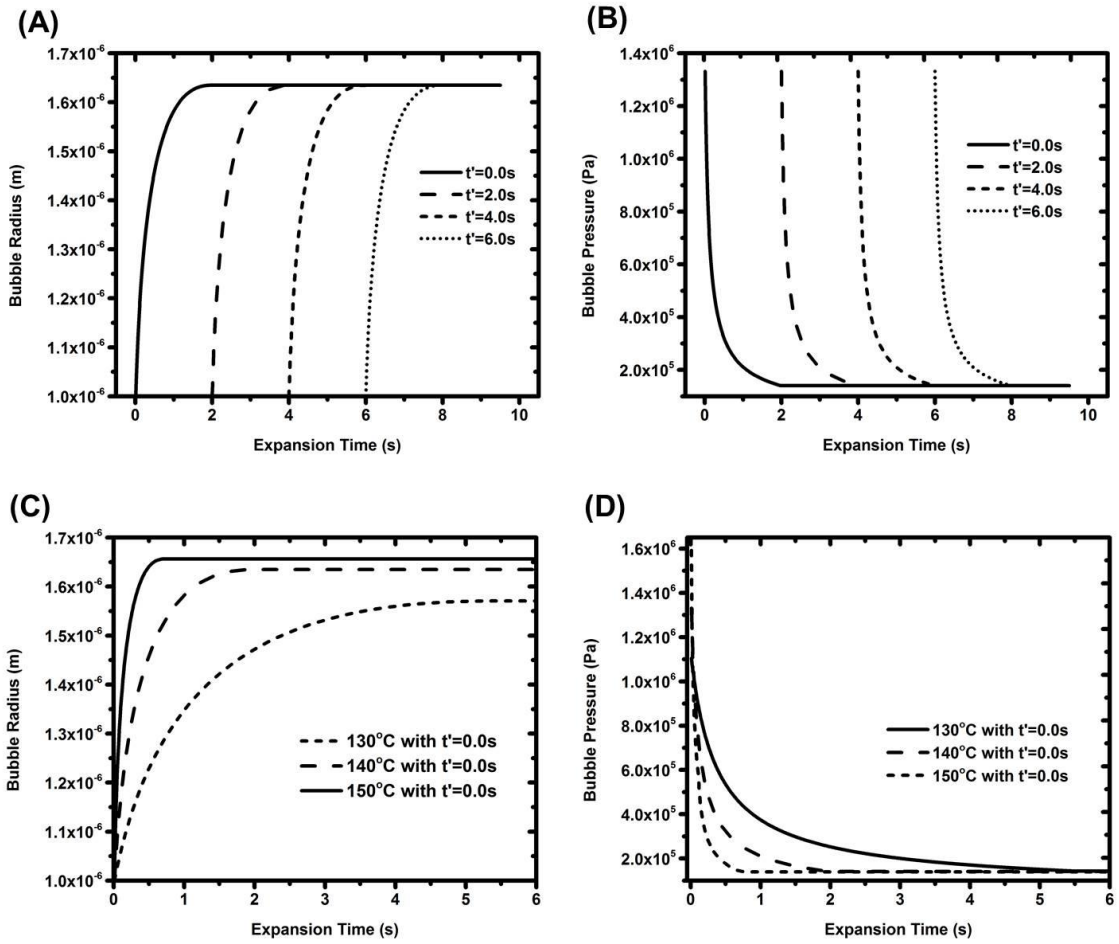


Figure 4.6 A) Bubble radius as a function of expansion time and nucleation time at 140°C, B) bubble pressure as a function of expansion time and nucleation rate at 140°C, C) bubble (nucleated at 0.0s) radius as a function of expansion time at various temperatures, and D) bubble (nucleated at 0.0s) pressure as a function of expansion time at various temperatures in the numerical solution.

*4.4.2 Numerical Solution*

To have a quantitative prediction of EPS expansion, a numerical solution that couples the nucleation and expansion of multiple bubbles in a finite matrix at various expansion temperatures is developed under the general formulation. The diffusion of pentane and rate-dependence of EPS matrix viscosity are taken into consideration.

The expansion kinetics of bubble is presented in Figure 4.6. As shown in Figure 4.6 (A) and Figure 4.6 (B), the bubble radius grows very fast at the initial several seconds after the nucleation. Meanwhile, the bubble pressure drops quickly. The rates of radius increase and pressure decrease gradually slow down to zero when the bubble expansion reaches an equilibrium state. Bubbles nucleated at different times follow a very similar expansion pattern. The radius growth of bubbles that are nucleated at 0.0s as a function of expansion temperature is shown in Figure 4.6 (C). A higher growth rate of bubble radius is reached when a higher expansion temperature is used, corresponding to a smaller characteristic bubble expansion time. It can be also noticed that, with the increase of expansion temperature, the equilibrated bubble radius also increases in accordance with the reversely changing trend of characteristic bubble radius. Figure 4.6 (D) represents the dropping rate of bubble pressure as a function of expansion temperature. As one can find in Equation (4.19), the initial bubble pressure which equates to saturated pentane pressure increases with the increase of expansion temperature. The pressure dropping rate of the bubbles nucleated at 0.0s is also found to increase as the temperature rises. The equilibrated bubble pressures at different expansion temperatures are very similar. This is because, compared with surface tension, the ambient pressure plays a more influential role to determine the balanced bubble pressure.

Table 4.4 Summary of constants in the exponential fitting of dimensionless bubble radius and dimensionless bubble pressure as functions of dimensionless expansion time in numerical solution.

| **Expansion Temperature** | $A_{N1}$ | $A_{N2}$ | $A_{N3}$ |
|---|---|---|---|
| 130°C | 8.77±0.047 | 0.90±0.001 | 24.06±0.009 |
| 140°C | 12.43±0.075 | 0.88±0.002 | 31.38±0.013 |
| 150°C | 16.83±0.031 | 0.84±0.004 | 39.44±0.005 |
| **Expansion Temperature** | $B_{N1}$ | $B_{N2}$ | $B_{N3}$ |
| 130°C<br>140°C<br>150°C | 1.01±0.022 | 0.51±0.029 | 0.037±0.0067 |

Similar to the semi-analytical solution, the dimensionless bubble radius and the dimensionless bubble pressure are also found to be as functions of dimensionless expansion time, following exponential relations

$$R^* = -A_{N1}\exp\left(-\frac{t^*}{A_{N2}}\right) + A_{N3} \qquad (4.31)$$

$$P_b^* = B_{N1}\exp\left(-\frac{t^*}{B_{N2}}\right) + B_{N3} \qquad (4.32)$$

where $A_{Ni}$ and $B_{Ni}(i=1,2,3)$ are constants that are dependent of expansion temperature. Their values are summarized in Table 4.4. As $B_{Ni}$ remains the same in a large range of temperatures, it can be deduced that $P_b^*$ is less sensitive to the variation of temperature. Moreover, $A_{Ni}$ are smaller than $A_{Ai}$ at the same temperature of expansion, corresponding to a slower growth rate of dimensionless bubble radius and a smaller equilibrated dimensionless radius. The comparison between $B_{Ni}$ and $B_{Ai}$ leads

to a similar result. This is because, in contrast with semi-analytical solution, the numerical solution models the expansion of bubble in a finite matrix with a consideration of the pentane diffusion process.

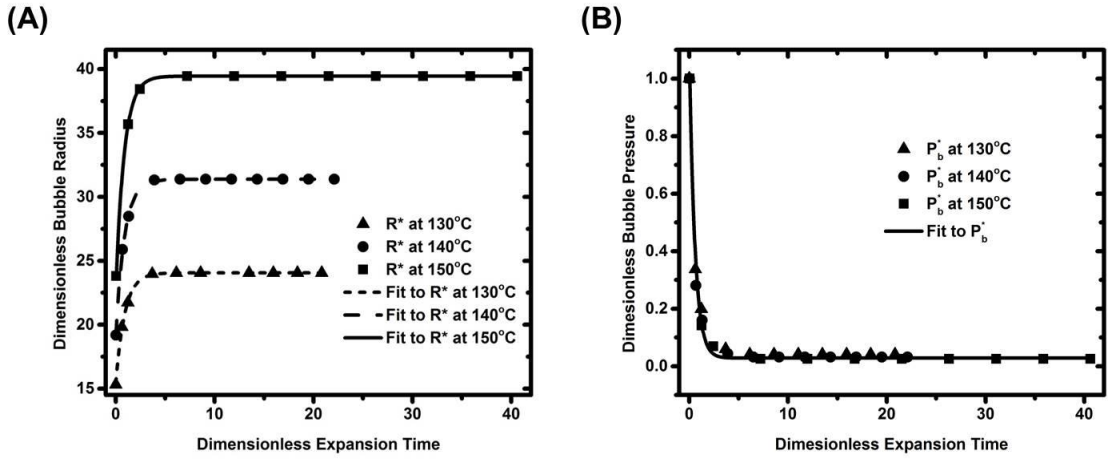


Figure 4.7 A) Dimensionless bubble radius and B) dimensionless bubble pressure as a function of dimensionless expansion time in the numerical solution.

The results of the dimensionless analysis on the numerical solution are also summarized in Figure 4.7. In Figure 4.7 (A), it can be observed that a higher expansion temperature, corresponding to a shorter characteristic bubble expansion time and a smaller characteristic bubble radius, leads to a larger growth rate and equilibrated size of dimensionless bubble radius. As indicated in the Table 4.4 and shown in Figure 4.7 (B), the variation of expansion temperature has limited influence over the dimensionless bubble pressure which can be fitted by an exponential function with dimensionless expansion time as independent variable in a large range of temperatures.

Figure 4.8 compares the experimental result of the radial expansion of EPS with the predicted one at various temperatures. In contrast with the semi-analytical solution, the numerical solution can quantitatively predict the experimental results obtained from the real-time observation at each of the selected temperatures. It can also be observed that, with the increase of expansion temperature, the growth rate of EPS radius increases, corresponding to a smaller characteristic bubble expansion time.

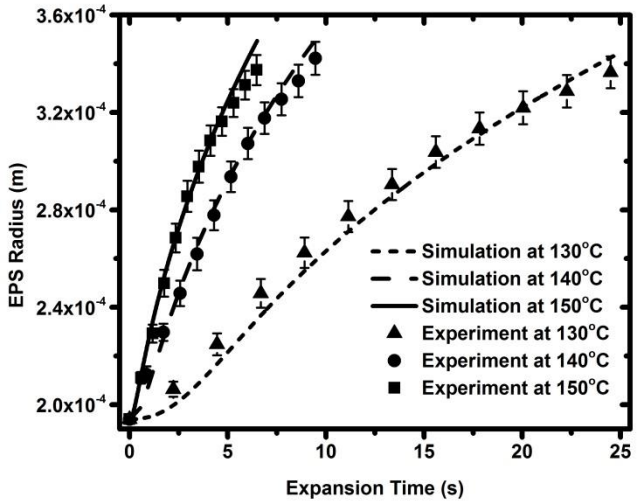


Figure 4.8 Comparison between experimental radial growth of EPS and the predicted one from the numerical solution at different temperatures.

*4.4.3 Parameter Sensitivity Study*

In the numerical solution, many parameters simultaneously influence the modeling results. It is worth performing a sensitivity study on them, including diffusion coefficient, Henry's solubility constant, power-law pre-exponent constant, and initial pentane concentration. This is because such study can evaluate the effect of each parameter,

assisting in the design and optimization of expansion system. In the parameter sensitivity study, while a set of conditions with the variation of a single parameter is in the run, the others remain unchanged.

The results of sensitivity study on influence of diffusion coefficient over the expansion kinetics of EPS microsphere at 140°C are summarized in Figure 4.9. As presented in Figure 4.9 (A), a higher growth rate of EPS radius is found to be with a lower diffusion coefficient. This is because the bubble radius can reach a larger equilibrium value by decreasing the diffusion coefficient, showing in Figure 4.9 (B). In Figure 4.9 (C), it is found that the dropping rate of bubble pressure is lowered at smaller diffusion coefficient since the diffusion of pentane from the EPS matrix into the bubble slows down. For a similar reason, the variation of average pentane concentration in pentane/polystyrene matrix also slows down, presenting in Figure 4.9 (D).

The influence of the variation of Henry's solubility constant is very similar to that of the diffusion coefficient. In Figure 4.10 (A), by increasing the Henry's solubility constant, it is observed that the radius of EPS microsphere can grow faster since the ultimate radius of bubble is increased as shown in Figure 4.10 (B). A lower Henry's solubility constant is also able to slow down the diffusion of pentane from EPS matrix to the bubbles, presenting in Figure 4.10 (C). However, it seems that the change of Henry's solubility constant has relatively limited influence over the average pentane concentration in pentane/polystyrene solution, presented in Figure 4.10 (D).

The results of sensitivity study on influence of the power-law pre-exponent constant over the expansion kinetics of EPS microsphere is shown in Figure 4.11. In Figure 4.11 (A), it can be found that the radius growth rate of EPS microsphere is increased as the power-law pre-exponent constant is lowered because there is less

resistance against the expansion of bubbles. This is confirmed by the results of bubble radius growth presented in Figure 4.11 (B). Moreover, as the bubble growth rate is increased at lower viscosity, the dropping rate of bubble pressure is also increased, showing in Figure 4.11 (C). In Figure 4.11 (D), the average pentane concentration in EPS matrix seems to be less affected by the variation of matrix viscosity.

The initial concentration of pentane in EPS microsphere is found to have a significant influence over the expansion kinetics of EPS microsphere. As shown in Figure 4.12 (A), since the bubble nucleation rate is increased when the initial pentane concentration is increased, it is found that the EPS radius grows faster at a higher initial concentration of pentane. However, because the initial pentane concentration does not influence the parameters that control the diffusion of gas, it has very limited influence over the increase of bubble radius and the decrease of bubble pressure, as presented in Figure 4.12 (B) and (C), respectively. Similarly, in Figure 4.12 (D), it can be found that the initial pentane concentration does not have much influence over average pentane concentration in the matrix of EPS microsphere.

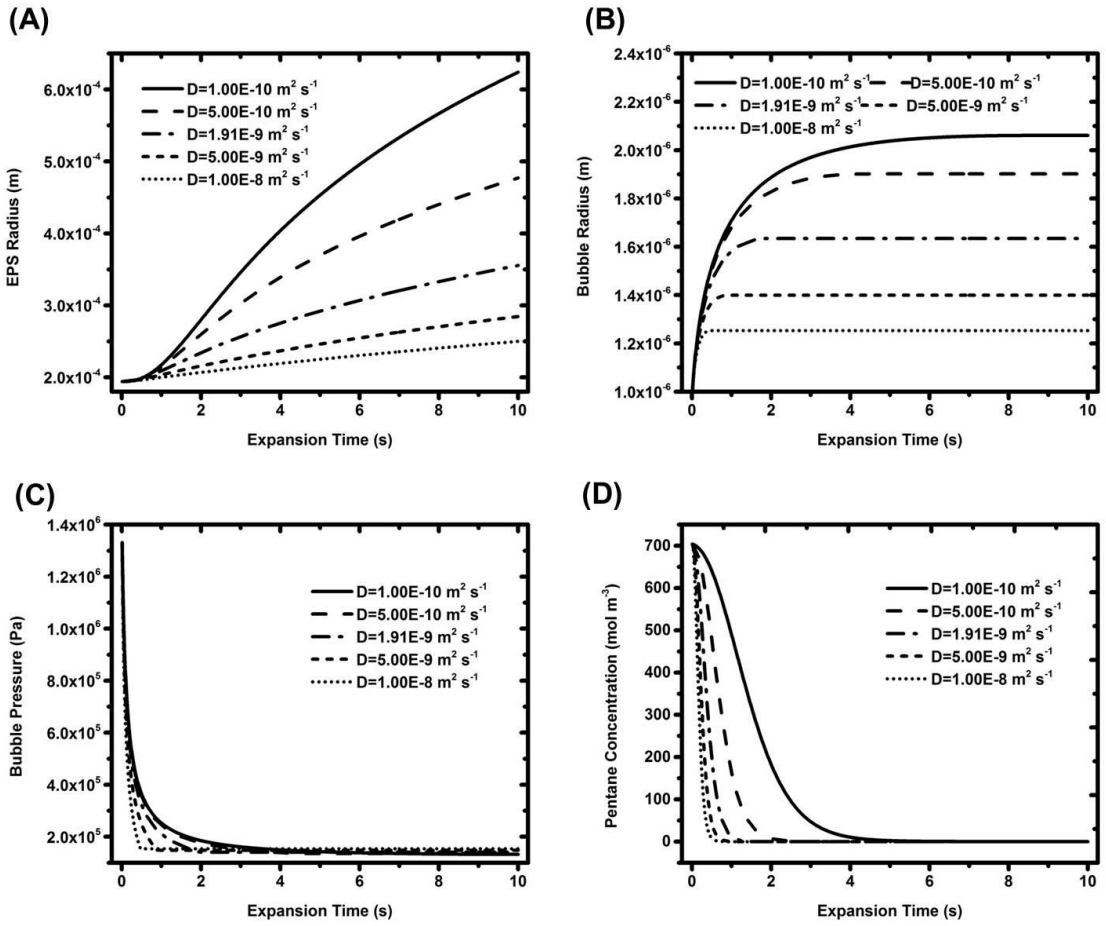


Figure 4.9 Sensitivity study on influence of diffusion coefficient over A) EPS radius, B) bubble radius, C) bubble pressure, and D) average pentane concentration in pentane/polystyrene solution in the numerical model (expansion temperature = 140°C).

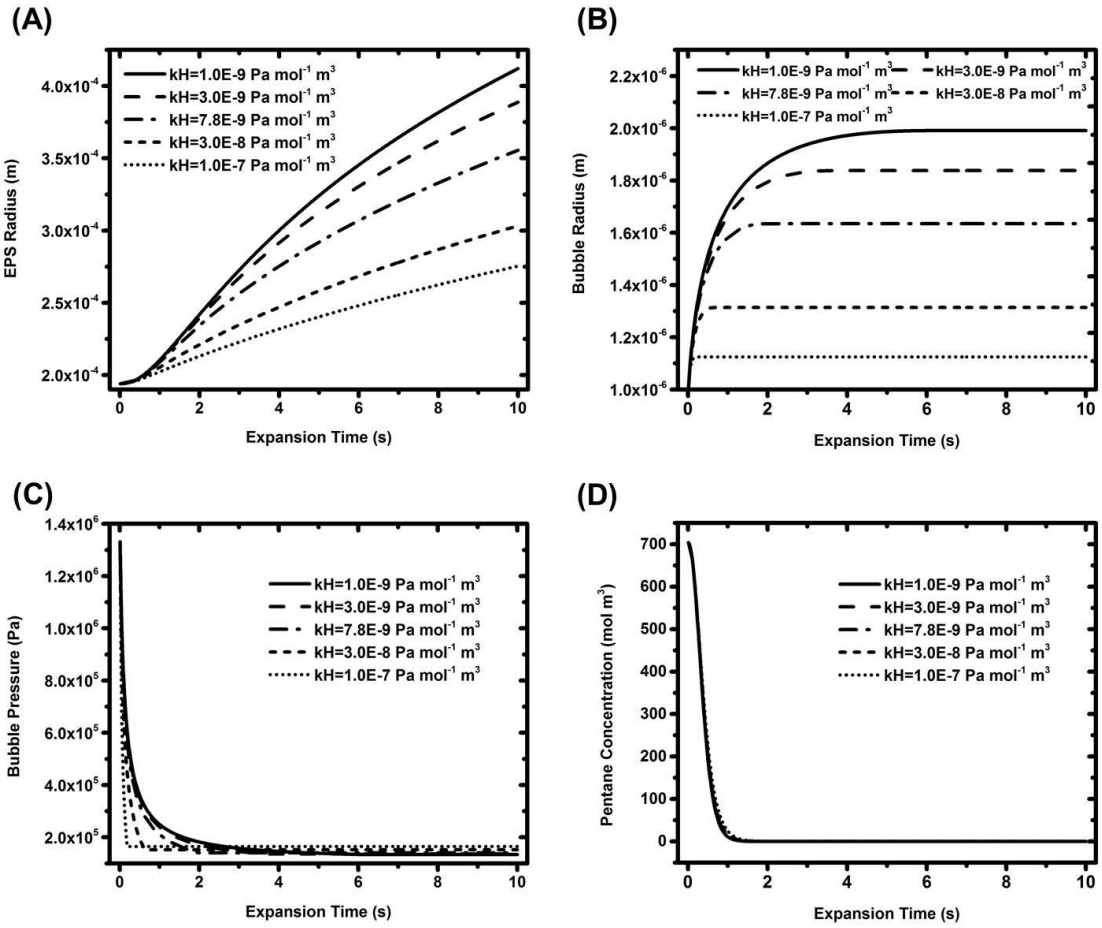


Figure 4.10 Sensitivity study on influence of Henry's solubility constant over A) EPS radius, B) bubble radius, C) bubble pressure, and D) average pentane concentration in pentane/polystyrene solution in the numerical model (expansion temperature = 140°C).

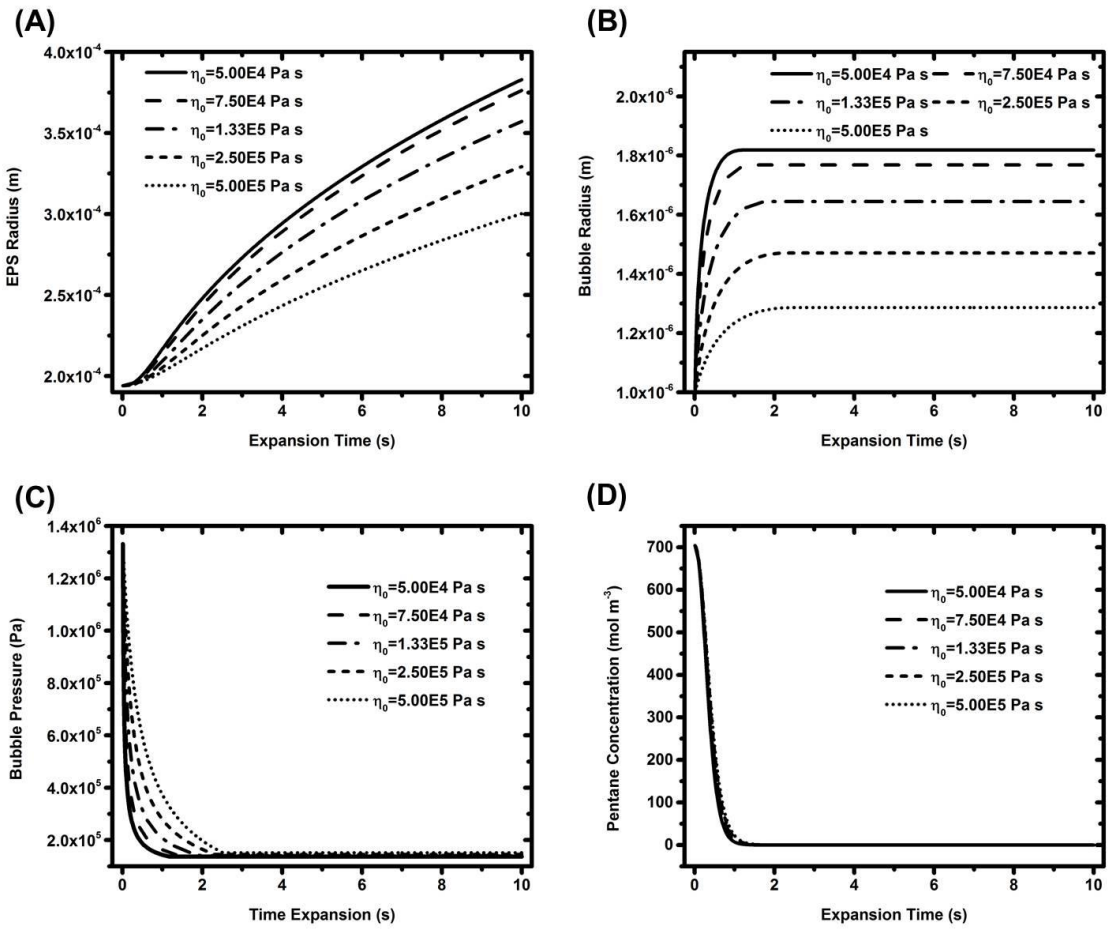


Figure 4.11 Sensitivity study on influence of power-law pre-exponent constant over A) EPS radius, B) bubble radius, C) bubble pressure, and D) average pentane concentration in pentane/polystyrene solution in the numerical model (expansion temperature = 140°C).

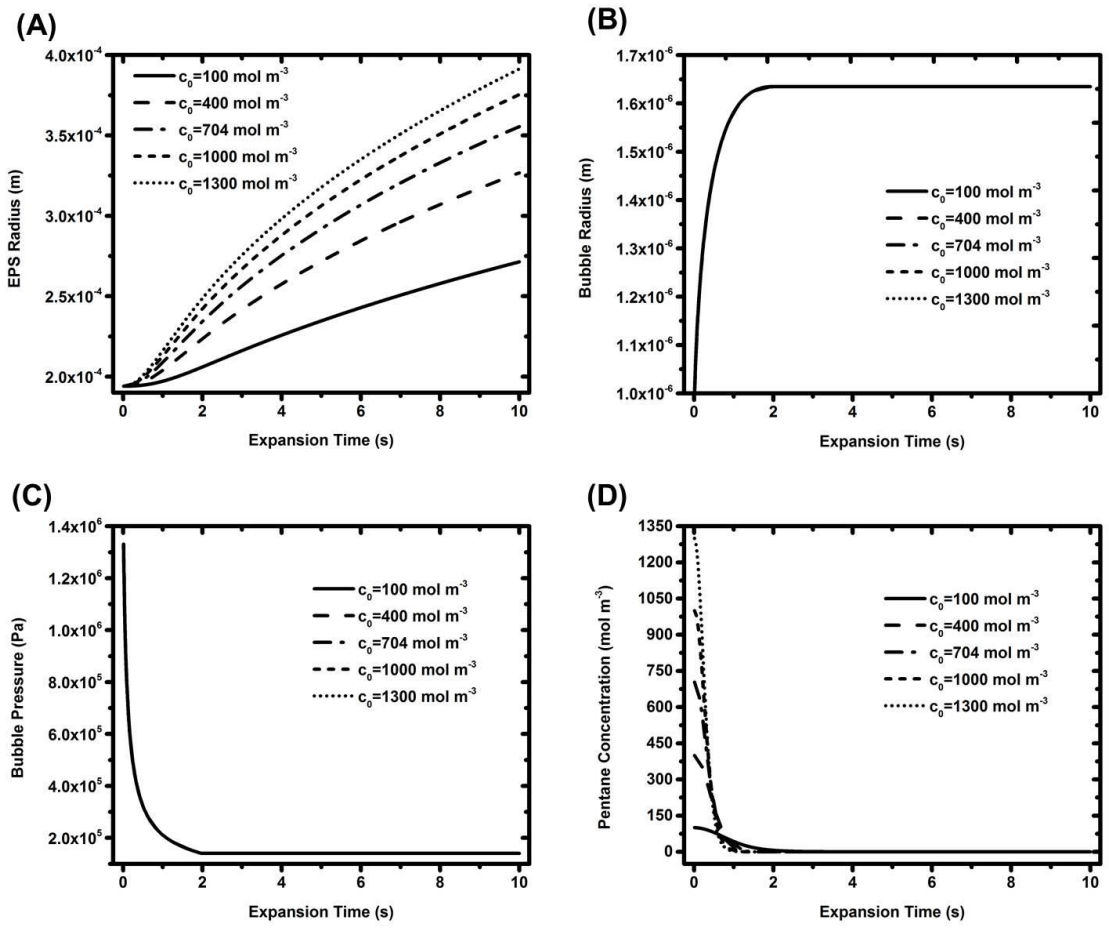


Figure 4.12 Sensitivity study on influence of initial pentane concentration over A) EPS radius, B) bubble radius, C) bubble pressure, and D) average pentane concentration in pentane/polystyrene solution in the numerical model (expansion temperature = 140°C).

*4.4.4 EPS Expansion in Epoxy Liquid*

In order to investigate the influence of existence of pre-cured epoxy resin over the EPS microsphere foaming in the previously developed microwave expansion process, the numerical solution can incorporate the resistance applied to EPS microsphere due to its radius enlargement in pre-cured epoxy liquid. The viscosity of pre-cured epoxy is assumed to be Newtonian for two reasons. First is because the pre-cured epoxy resin stays with unchanged viscosity during most of the process time. Second is to reduce the complexity of analysis. The results are summarized in Fig. 4.13. The influence of epoxy resin viscosity over the EPS microsphere expansion rate is shown. It can be noticed that only when the viscosity of epoxy liquid reaches a certain high value can it retard the growth of EPS radius, indicating that the retarding effect takes place in the late stage of the microwave expansion process. Generally, the higher the viscosity is, the slower the expansion is.

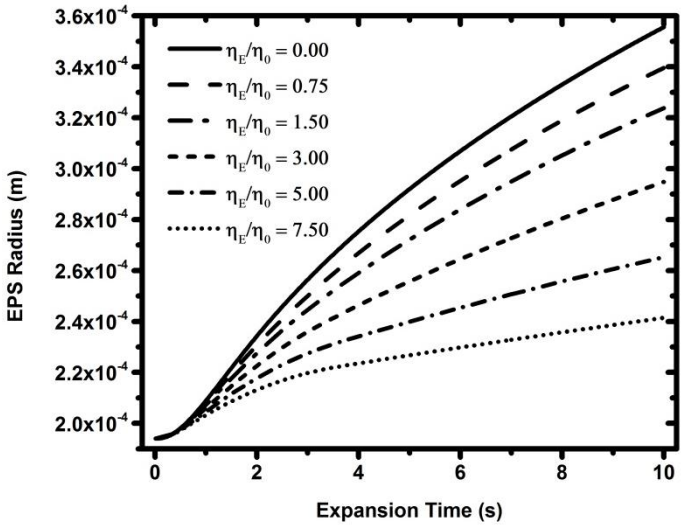


Figure 4.13 Influence of the uncured epoxy matrix over the growth of EPS radius during expansion (expansion temperature = 140$^{o}$C).

## 4.5 Conclusions

In Chapter 4, a general formulation for modeling the expansion process of EPS microsphere is presented. A semi-analytical solution was first obtained based on the simplified case of a single bubble expansion in an infinite matrix. This solution provides a relatively simple tool to understand and optimize the expansion process. The dimensionless bubble radius and dimensionless bubble pressure are obtained to be exponential functions of dimensionless expansion time. The characteristic bubble expansion time is able to characterize the time scale of the expansion process. The equilibrated bubble radius is in reverse proportion to the characteristic bubble radius. The semi-analytical solution can qualitatively predict the experimental results of radial expansion of EPS microsphere obtained in a real-time observation. However, this solution suffers from some unrealistic simplifications, including infinite matrix, exclusion of pentane diffusion, and constant viscosity of polystyrene.

To have a more accurate prediction of EPS expansion, a numerical solution was then developed to the model that correlates with the nucleation and expansion of multiple bubbles in a finite matrix at various expansion temperatures. The diffusion process of pentane and rate-dependent viscosity of EPS matrix were considered. It was discovered that the numerical solution is able to quantitatively predict the expansion of EPS microsphere. The temperature also plays an important role to determine the expansion kinetics. By increasing the expansion temperature, the process can be considerately accelerated. At last, a parameter sensitivity study was performed to examine the effect of each parameter over the expansion process. It was obtained that the growth rate of EPS microsphere during expansion can be increased by lowering the diffusion coefficient, Henry's solubility constant and matrix viscosity or raising the initial concentration of pentane. Finally, it was also found that only when the viscosity of epoxy

liquid reaches a certain high value can it retard the growth of EPS radius, indicating that the retarding effect takes place in the late stage of the microwave expansion process.

# CHAPTER 5

# CONCLUSIONS, RECOMMENDATIONS AND FUTURE WORK

## 5.1 Conclusions

In this thesis, the major body of research work was covered from Chapter 2 to Chapter 4. The design and development of a microwave expansion process was first presented in Chapter 2 with an aim to address some emerging issues in the processing of EPS-filled syntactic foam. To have a broader impact of the research, in the work shown in Chapter 3, the microwave expansion process was then extended to produce composite polystyrene foams with improved fire retardation and mechanical performance. With an effort to emphasize the fundamental aspect of the research, a process model which was capable to model the expansion kinetics of EPS microsphere was developed and presented in Chapter 4. Specific results of each of the three chapters are recapitulated as follows.

In Chapter 2, the design and development of a novel microwave expansion process is presented to produce thermoset-matrix syntactic foam containing expandable thermoplastic microspheres. Expandable polystyrene microsphere and epoxy resin were chosen as the model material system for feasibility study and demonstration. The microwave power was fixed to be 100W to ensure a controlled process. A two-stage hardener addition method was employed to prevent the dissolution and inhomogeneous distribution of EPS microspheres. The specific microwave energy and the pre-cured epoxy viscosity at room temperature are found to be the two governing parameters in the process. The feasible process window was quantitatively estimated based on rheological measurements and thermal analyses. The experimental results

demonstrated that the microwave expansion process is able to effectively expand EPS microspheres in EPS/epoxy syntactic foam even with high EPS loading. Mechanical tests showed that the specific flexural strength and modulus of syntactic foam are comparable with those of neat epoxy. By comparison, the flexural moduli over density squared or cubed of the foam are much higher, especially at high EPS loadings, than those of neat epoxy. The foamed EPS microspheres can also effectively toughen the syntactic foam, preventing propagation of cracks. Finally, the microwave expansion process is also capable of molding syntactic foamed parts of relatively sophisticated geometry with smooth surfaces.

Chapter 3 presents the extension of the microwave expansion process to produce composite EPS foam with improved fire-retardant performance. This process converts an expandable suspension containing a fire-retardant compound, unexpanded EPS microspheres and a diluent, into a composite foam with a honeycomb-like barrier structure. The expandable suspension process is featured with incorporation of high loadings of environmentally friendly and low-cost inorganic fire-retardant agents without undermining the foamability of EPS microspheres. The optical observation confirmed the formation of the honeycomb-like structure that encapsulates each individual foam microsphere in the composite foam. The diluent content was found to highly influence the suspension viscosity and the foam morphology. With low diluent concentration, EPS microspheres cannot be effectively expanded, while the barrier structure becomes incomplete when diluent content is high. Results from mechanical tests showed that the existence of the honeycomb-like barrier structure can considerably improve the foam mechanical performance, making the composite foam stiffer and more durable compared with the neat one. At last, fire-retardation tests demonstrated that the honeycomb-like barrier structure can effectively stop the fire path into the foam,

suppress toxic smoke generation, and maintain foam structure integrity, enabling the composite foam to have substantially improved fire resistance in comparison with the neat foam.

In Chapter 4, the development of a general formulation is presented to model the expansion process of EPS microsphere and obtain important kinetic parameters during this process. A semi-analytical solution was first obtained based on the simplified case of a single bubble expansion in an infinite matrix. This solution provides a relatively simple tool to understand and optimize the expansion process. The dimensionless bubble radius and dimensionless bubble pressure are obtained to be exponential functions of dimensionless expansion time. The characteristic bubble expansion time is able to characterize the time scale of the expansion process. The equilibrated bubble radius is in reverse proportion to the characteristic bubble radius. The semi-analytical solution can qualitatively predict the experimental results of radial expansion of EPS microsphere obtained in a real-time observation. However, this solution suffers from some unrealistic simplifications, including infinite matrix, exclusion of pentane diffusion, and constant viscosity of polystyrene. To have a more accurate prediction of EPS expansion, a numerical solution was then developed to the model that correlates with the nucleation and expansion of multiple bubbles in a finite matrix at various expansion temperatures. The diffusion process of pentane and rate-dependent viscosity of EPS matrix were considered. It was discovered that the numerical solution is able to quantitatively predict the expansion of EPS microsphere. The temperature also plays an important role to determine the expansion kinetics. By increasing the expansion temperature, the process can be considerately accelerated. At last, a parameter sensitivity study was performed to examine the effect of each parameter over the expansion process. It was obtained that the growth rate of EPS microsphere during expansion can be increased by lowering the

diffusion coefficient, Henry's solubility constant and matrix viscosity or raising the initial concentration of pentane. Finally, it was also found that only when the viscosity of epoxy liquid reaches a certain high value can it retard the growth of EPS radius, indicating that the retarding effect takes place in the late stage of the microwave expansion process.

## 5.2 Recommendations

From the results of the research work presented in this thesis, the following recommendations are made.

First, it is expected that some thermosetting materials other than epoxy and phenolic resin can be equally used in the microwave expansion process to produce syntactic foams with different properties. For example, when melamine resin is used as the matrix material, the resulting EPS-filled syntactic foams can have enhanced rigidity and fire resistance. Moreover, flexible syntactic foams which may find applications in packaging can be produced if elastomers, such as polysiloxane and polyurethane, serve as the matrix.

Second, properties of the composite polystyrene foams other than mechanical strength and fire retardation can also be altered when the composition of barrier layer is changed, resulting in foams with different functions. For instance, it is well known that termite invasion is one of the major threats to thermal insulating structures in buildings which are primarily made of polystyrene foam. An effective anti-termite capability can be incorporated into the design of composite polystyrene foams once the barrier layer contains proper pesticides. Also, when the honeycomb structure is made of conductive polymer or composites, conductive polystyrene foam can be obtained which may find many usages in electronic devices.

Third, it is found that the pre-cured epoxy liquid in the two stage hardener addition method can retain a certain viscosity for a relatively long time if the second part of the hardener is not added. This provides us with a simple way to produce viscous liquids whose viscosities can be easily altered by changing the ratio between base and hardener of epoxy. Such liquids may be applied in damping devices.

Finally, the process model developed in this work can be used to model the expansion process of other types of expandable microspheres. Moreover, since the nucleation of bubbles are not considered in the system foamed by chemical blowing agent, the analytical solution to the process model can be directly used, providing a simple way to simulate the expansion kinetics.

### 5.3 Future Work

Some future work that may be followed after the research presented in this thesis is recommended below.

First, a further study on the feasible process window of microwave expansion process should be conducted with a consideration of the variation of microwave power. While the microwave power is fixed at 100W to guarantee a controllable process in the work presented in Chapter 2, a higher microwave power might be used in industrial-scale production, especially when the molded parts are large. Issues, such as upper and lower boundaries of process window, variation of power compensation factor, and influence of effective depth of microwave, should be drawn attention to during the study.

Second, a study on the preparation of syntactic foams with large sizes using microwave expansion process should be carried out. While the results shown in Chapter

2 indicate that the developed process has a satisfactory molding capability to parts with small and medium sizes, its capability to mold large parts, such as meter-scale ones, should be further examined. Some issues should be considered when such study is conducted, such as the effective penetration depth and uniformity of the microwave heating, the competition between effective foaming time of EPS and the gelation time of epoxy, and the flowability change of the EPS-epoxy foaming feed as the heating process proceeds.

Third, the process-structure-performance relation in the research of composite polystyrene foam needs further investigation. In the work shown in Chapter 3, only one set of processing condition and suspension formulation was studied. In order to optimize the performance of the composite polystyrene foams, a further exploration into the process-structure-performance relation is highly desired. The aspects of the study should cover but are not limited to influence of processing conditions and suspension formulation over the average thickness of the barrier layers, controlling parameters of the connectivity of the expanded EPS microspheres, formulation optimization of fire retardation compound, and quantitative characterization of the completeness of the honeycomb-like structure formation.

Fourth, a feasible study on using pressurized steam as an alternative heating method to expand composite polystyrene foams is highly suggested. As presented in Chapter 3, the composite polystyrene foams were produced by expanding an expandable aqueous suspension system using microwave heating method. Since this system contains a considerable amount of water as diluent, it is possible to use pressurized steam to expand the unexpanded EPS microspheres instead of microwave. The change of heating method has several advantages. The cost can be further lowered because steam heating is a cheap heating method and little modifications need to be

made to the existing EPS foam production lines. Moreover, using steam is more environmentally friendly with almost no pollution that will be produced.

Finally, the process model which is presented in Chapter 4 can be further improved. The rheological model used in the numerical solution is a simple power-law model which is not able to accurately simulate the rheological behaviors of polystyrene in extensional deformation. An upper convected Maxwell rheological model can be used to replace the power-law model to have a more accurate prediction of viscosity change under deformation. Moreover, some of the parameters in heterogeneous nucleation process are obtained by fitting the simulation curves to the experimental data. In order to calculate these parameters based on the physics available, some properties of unexpanded EPS microspheres, such as the amount and type of nucleating agent, should be obtained from the material supplier.

# REFERENCES


1. Klempner, D. and V. Sendijarevic, *Polymeric Foams and Foam Technology, 2nd Edition*. 2004, Cincinnati, OH: Hanser Gardener Publication.
2. Karthikeyan, C.S., S. Sankaran, and Kishore, *Influence of chopped strand fibres on the flexural behaviour of a syntactic foam core system.* Polymer International, 2000. **49**(2): p. 158-162.
3. Guzman, M.E., et al., *Processing and properties of syntactic foams reinforced with carbon nanotubes.* Journal of Applied Polymer Science, 2012. **124**(3): p. 2383-2394.
4. Shutov, F.A., *SYNTACTIC POLYMER FOAMS.* Advances in Polymer Science, 1986. **73-4**: p. 63-123.
5. Wouterson, E.M., et al., *Effect of fiber reinforcement on the tensile, fracture and thermal properties of syntactic foam.* Polymer, 2007. **48**(11): p. 3183-3191.
6. Benderly, D., et al., *Effect of composition on the fracture toughness and flexural strength of syntactic foams.* Polymer Composites, 2004. **25**(2): p. 229-236.
7. Devi, K.A., et al., *Syntactic foam composites of epoxy-allyl phenol-bismaleimide ternary blend - Processing and properties.* Journal of Applied Polymer Science, 2007. **105**(6): p. 3715-3722.
8. Shutov, F., *Syntactic Polymer Foams*, in *Polymeric Foams and Foam Technology*, D. Klempner and V. Sendijarevic, Editors. 2004, Hanser Gardener Publication: Cincinnati, OH.

9. John, B., et al., *Foam sandwich composites with cyanate ester based syntactic foam as core and carbon-cyanate ester as skin: Processing and properties.* Journal of Applied Polymer Science, 2008. **110**(3): p. 1366-1374.

10. Karthikeyan, C.S., S. Sankaran, and Kishore, *Flexural behaviour of fibre-reinforced syntactic foams.* Macromolecular Materials and Engineering, 2005. **290**(1): p. 60-65.

11. Wouterson, E.M., et al., *Fracture and impact toughness of syntactic foam.* Journal of Cellular Plastics, 2004. **40**(2): p. 145-154.

12. Kumar, S.J.A. and K.S. Ahmed, *Compression behavior and energy absorption capacity of stiffened syntactic foam core sandwich composites.* Journal of Reinforced Plastics and Composites, 2013. **32**(18): p. 1370-1379.

13. Kumar, K.S.S., C.P.R. Nair, and K.N. Ninan, *Mechanical properties of polybenzoxazine syntactic foams.* Journal of Applied Polymer Science, 2008. **108**(2): p. 1021-1028.

14. Lawrence, E. and R. Pyrz, *Viscoelastic properties of polyethylene syntactic foam with polymer microballoons.* Polymers & Polymer Composites, 2001. **9**(4): p. 227-237.

15. Mae, H., M. Omiya, and K. Kishimoto, *Effects of strain rate and density on tensile behavior of polypropylene syntactic foam with polymer microballoons.* Materials Science and Engineering a-Structural Materials Properties Microstructure and Processing, 2008. **477**(1-2): p. 168-178.

16. Saha, M.C. and S. Nilufar, *Nanoclay-Reinforced Syntactic Foams: Flexure and Thermal Behavior.* Polymer Composites, 2010. **31**(8): p. 1332-1342.

17. Zegeye, E.F. and E. Woldesenbet, *Processing and mechanical characterization of carbon nanotube reinforced syntactic foams.* Journal of Reinforced Plastics and Composites, 2012. **31**(15): p. 1045-1052.

18. May, C.A., *Epoxy Resin: Chemistry and Technology, 2nd Edition*. 1988, New York: Marcel Dekker.

19. Ellis, B., *Chemistry and Technology of Epoxy Resins*. 1993, Glasgow, UK: Blackie Academic & Professional.

20. Pascault, J.-P. and R.J.J. Williams, *Epoxy Polymers*. 2010, Weinheim: Wiley-VCH.

21. Louis and Pilato, *Phenolic Resins: A Century of Progress*. 2010, Berlin Heidelberg: Springer-Verlag.

22. Knop, A., *Phenolic resins : chemistry, applications, and performance : future directions*. 1985, New York: Springer-Verlag.

23. Hull, T.R. and B.K. Kandola, *Fire retardancy of polymers: new strategies and mechanisms*. 2009, Cambridge: Royal Society of Chemistry.

24. John, B., C.P.R. Nair, and K.N. Ninan, *Low-density phenolic syntactic foams: Processing and properties.* Cellular Polymers, 2007. **26**(4): p. 229-244.

25. Gupta, N. and R. Nagorny, *Tensile properties of glass microballoon-epoxy resin syntactic foams.* Journal of Applied Polymer Science, 2006. **102**(2): p. 1254-1261.

26. Kim, H.S. and C. Mitchell, *Impact performance of laminates made of syntactic foam and glass fiber reinforced epoxy as protective materials.* Journal of Applied Polymer Science, 2003. **89**(9): p. 2306-2310.

27. Samsudin, S.S., et al., *Development and characterization of epoxy syntactic foam filled with epoxy hollow spheres.* Express Polymer Letters, 2011. **5**(7): p. 653-660.

28. Huang, Y.J., et al., *Enhancing Specific Strength and Stiffness of Phenolic Microsphere Syntactic Foams Through Carbon Fiber Reinforcement.* Polymer Composites, 2010. **31**(2): p. 256-262.

29. Shutov, F.A.e., G. Henrici-Olivé, and S. Olivé, *Integral/Structural Polymer Foams: Technology, Properties, and Applications*. 1986, New York: Springer-Verlag.

30. Lee, S.-T., C.B. Park, and N.S. Ramesh, *Polymeric Foams: Science and Technology*. 2007, Boca Raton: CRC/Taylor & Francis.

31. Huntsman, *General Introduction to Expandable Polystyrene*, in *Technical Bulletin: General Introduction*2006, Huntsman Corporation: Lawrenceville, GA.

32. Brooks, J.D. and L.G. Rey, *Polystyrene-Urethane Composite Foam for Crash Padding Applications.* Journal of Cellular Plastics, 1973. **9**: p. 232-235.

33. Aglan, H., et al., *Strength and toughness improvement of cement binders using expandable thermoplastic microspheres.* Construction and Building Materials, 2009. **23**(8): p. 2856-2861.

34. Kim, N.H. and H.S. Kim, *Toughening method and mechanisms for thermosets.* Journal of Applied Polymer Science, 2005. **98**(4): p. 1663-1667.

35. Kim, H.S. and N.H. Kim, *Toughening of thermosets by the creation of residual compressive stresses.* Journal of Applied Polymer Science, 2006. **100**(5): p. 4045-4051.

36. Bharadwaj-Somaskandan, S., et al., *Macro- and microfillers as reinforcing agents for polyurethane elastomers.* Journal of Elastomers and Plastics, 2003. **35**(4): p. 325-334.

37. Peng, J., et al., *Comparisons of microcellular polylactic acid parts injection molded with supercritical nitrogen and expandable thermoplastic microspheres: Surface roughness, tensile properties, and morphology.* Journal of Cellular Plastics, 2012. **48**(5): p. 433-444.

38. Hildado, C.J., *Flammability Handbook For Plastics*. 1998, Lancaster, PA: Technomic Publishing Company, Inc.

39. BARBOZA, D., *Workers Detained as Toll Hits 53 in Shanghai Fire*, in *The New York Times*2010.

40. Hahn, K., et al., *FLAME-PROTECTED POLYMER FOAMS*, 2012: US.

41. Beulich, I., et al., *Brominated butadiene/vinyl aromatic copolymers, blends of such copolymers with a vinyl aromatic polymer, and polymeric foams formed from such blends*, 2005: US.

42. Kim, Y.H., et al., *Flame Retardant Expandable Polystyrene-based Polymerized Beads, and Preparation Method Thereof*, 2010: US.

43. Allmendinger, M., K. Hahn, and J. Ruch, *Halogen-free flame-retarded polymer foams*, 2006.

44. GLÜCK, G., *METHOD FOR PRODUCING EXPANDABLE STYRENE POLYMERS CONTAINING EXFOLIATED GRAPHITE PARTICLES*, 2002.

45. Eberstaller, R. and G. Hintermeier, *FLAMEPROOF EXPANDABLE POLYMERIZATES*, 2012.

46. Moon, Y.-J., *Method for manufacturing flame-retardant expanded polystyrene blocks and molded products*, 2008.

47. Scherzer, D., et al., *Expandable styrene polymers containing halogen-free flame retardants*, 2004.

48. Nehls, B., et al., *COATING COMPOSITION FOR FOAM PARTICLES*, 2012.

49. Aslin, D.C., *Fire retardant composition*, 2003.

50. Bras, M.L., et al., *Fire Retardancy of Polymers: New Applications of Mineral Fillers.* . 2005, Cambridge, UK: Royal Society of Chemistry.

51. Mui, K.W., et al., *Formaldehyde exposure risk in air-conditioned offices of Hong Kong.* Building Services Engineering Research & Technology, 2009. **30**(4): p. 279-286.

52. Wu, P.C., et al., *Risk assessment of formaldehyde in typical office buildings in Taiwan.* Indoor Air, 2003. **13**(4): p. 359-363.

53. Golden, R., *Identifying an indoor air exposure limit for formaldehyde considering both irritation and cancer hazards.* Critical Reviews in Toxicology, 2011. **41**(8): p. 672-721.

54. Kim, K.H., S.A. Jahan, and J.T. Lee, *Exposure to Formaldehyde and Its Potential Human Health Hazards.* Journal of Environmental Science and Health Part C-Environmental Carcinogenesis & Ecotoxicology Reviews, 2011. **29**(4): p. 277-299.

55. Bras, M.L., et al., *Fire Retardancy of Polymers: New Applications of Mineral Fillers*. 2005, Cambridge, UK: The Royal Society of Chemistry.

56. Saiz-Arroyo, C., et al., *Moulded polypropylene foams produced using chemical or physical blowing agents: structure-properties relationship.* Journal of Materials Science, 2012. **47**(15): p. 5680-5692.

57. Xi, Z.H., et al., *Microcellular Injection Molding of In Situ Modified Poly(ethylene terephthalate) With Supercritical Nitrogen.* Polymer Engineering and Science, 2014. **54**(12): p. 2739-2745.

58. Epstein, P.S. and M.S. Plesset, *ON THE STABILITY OF GAS BUBBLES IN LIQUID-GAS SOLUTIONS.* Journal of Chemical Physics, 1950. **18**(11): p. 1505-1509.

59. Scriven, L.E., *ON THE DYNAMICS OF PHASE GROWTH.* Chemical Engineering Science, 1959. **10**(1-2): p. 1-&.

60. Barlow, E.J. and W.E. Langlois, *DIFFUSION OF GAS FROM A LIQUID INTO AN EXPANDING BUBBLE.* Ibm Journal of Research and Development, 1962. **6**(3): p. 329-337.

61. Rayleigh, *On the pressure developed in a liquid during the collapse of a spherical cavity.* Philosophical Magazine, 1917. **34**(199-04): p. 94-98.

62. Hobbs, S.Y., *BUBBLE-GROWTH IN THERMOPLASTIC STRUCTURAL FOAMS.* Polymer Engineering and Science, 1976. **16**(4): p. 270-275.

63. Rosner, D.E. and M. Epstein, *EFFECTS OF INTERFACE KINETICS, CAPILLARITY AND SOLUTE DIFFUSION ON BUBBLE GROWTH-RATES IN HIGHLY SUPERSATURATED LIQUIDS.* Chemical Engineering Science, 1972. **27**(1): p. 69-&.

64. Zana, E. and L.G. Leal, *DISSOLUTION OF A STATIONARY GAS BUBBLE IN A QUIESCENT, VISCOELASTIC LIQUID.* Industrial & Engineering Chemistry Fundamentals, 1975. **14**(3): p. 175-182.

65. Street, J.R., *The Rheology of Phase Growth in Elastic Liquid.* Journal of Rheology, 1968. **12**(1): p. 103-131.

66. Venerus, D.C., N. Yala, and B. Bernstein, *Analysis of diffusion-induced bubble growth in viscoelastic liquids.* Journal of Non-Newtonian Fluid Mechanics, 1998. **75**(1): p. 55-75.

67. Han, C.D. and H.J. Yoo, *STUDIES ON STRUCTURAL FOAM PROCESSING .4. BUBBLE-GROWTH DURING MOLD FILLING.* Polymer Engineering and Science, 1981. **21**(9): p. 518-533.

68. Yoo, H.J. and C.D. Han, *OSCILLATORY BEHAVIOR OF A GAS BUBBLE GROWING (OR COLLAPSING) IN VISCOELASTIC LIQUIDS.* Aiche Journal, 1982. **28**(6): p. 1002-1009.

69. Fogler, H.S. and J.D. Goddard, *COLLAPSE OF SPHERICAL CAVITIES IN VISCOELASTIC FLUIDS.* Physics of Fluids, 1970. **13**(5): p. 1135-&.

70. Joshi, K., et al., *Prediction of Cellular Structure in Free Expansion of Viscoelastic Media.* Journal of Applied Polymer Science, 1988. **67**(8): p. 1353-1368.

71. Amon, M. and C.D. Denson, *A STUDY OF THE DYNAMICS OF FOAM GROWTH - ANALYSIS OF THE GROWTH OF CLOSELY SPACED SPHERICAL BUBBLES.* Polymer Engineering and Science, 1984. **24**(13): p. 1026-1034.

72. Arefmanesh, A. and S.G. Advani, *DIFFUSION-INDUCED GROWTH OF A GAS BUBBLE IN A VISCOELASTIC FLUID.* Rheologica Acta, 1991. **30**(3): p. 274-283.

73. Arefmanesh, A., S.G. Advani, and E.E. Michaelides, *AN ACCURATE NUMERICAL-SOLUTION FOR MASS DIFFUSION-INDUCED BUBBLE-GROWTH IN VISCOUS-LIQUIDS CONTAINING LIMITED DISSOLVED-GAS.* International Journal of Heat and Mass Transfer, 1992. **35**(7): p. 1711-1722.

74. Arefmanesh, A. and S.C. Advani, *Nonisothermal Bubble Growth in Polymer Foams.* Polymer Engineering and Science, 1995. **35**(3): p. 252-260.

75. Ramesh, N.S., D.H. Rasmussen, and G.A. Campbell, *NUMERICAL AND EXPERIMENTAL STUDIES OF BUBBLE-GROWTH DURING THE MICROCELLULAR FOAMING PROCESS.* Polymer Engineering and Science, 1991. **31**(23): p. 1657-1664.

76. Shafi, M.A., K. Joshi, and R.W. Flumerfelt, *Bubble size distributions in freely expanded polymer foams.* Chemical Engineering Science, 1997. **52**(4): p. 635-644.

77. Otsuki, Y. and T. Kanai, *Numerical simulation of bubble growth in viscoelastic fluid with diffusion of dissolved foaming agent.* Polymer Engineering and Science, 2005. **45**(9): p. 1277-1287.

78. Mao, D.M., J.R. Edwards, and A. Harvey, *Prediction of foam growth and its nucleation in free and limited expansion.* Chemical Engineering Science, 2006. **61**(6): p. 1836-1845.

79. Leung, S.N., et al., *Computer simulation of bubble-growth phenomena in foaming.* Industrial & Engineering Chemistry Research, 2006. **45**(23): p. 7823-7831.

80. Leung, S.N., C.B. Park, and H. Li, *Numerical simulation of polymeric foaming processes using modified nucleation theory.* Plastics Rubber and Composites, 2006. **35**(3): p. 93-100.

81. Shimoda, M., et al., *Polymeric foaming simulation for extrusion processes.* Journal of Cellular Plastics, 2001. **37**(6): p. 517-536.

82. Taki, K., *Experimental and numerical studies on the effects of pressure release rate on number density of bubbles and bubble growth in a polymeric foaming process.* Chemical Engineering Science, 2008. **63**(14): p. 3643-3653.

83. Xu, D.L., et al., *Fundamental study of CBA-blown bubble growth and collapse under atmospheric pressure.* Journal of Cellular Plastics, 2005. **41**(6): p. 519-538.

84. Leung, S.N., et al., *Mechanism of extensional stress-induced cell formation in polymeric foaming processes with the presence of nucleating agents.* Journal of Supercritical Fluids, 2012. **63**: p. 187-198.

85. Xu, X.M., G.Q. Zhao, and H.P. Li, *Numerical Simulation of Bubble Growth in a Limited Amount of Liquid.* Journal of Applied Polymer Science, 2010. **116**(3): p. 1264-1271.

86. Leung, S.N., et al., *Change in the critical nucleation radius and its impact on cell stability during polymeric foaming processes.* Chemical Engineering Science, 2009. **64**(23): p. 4899-4907.

87. Leung, S.N., H.B. Li, and C.B. Park, *Impact of approximating the initial bubble pressure on cell nucleation in polymeric foaming processes.* Journal of Applied Polymer Science, 2007. **104**(2): p. 902-908.

88. Leung, S.N., et al., *Strategies To Estimate the Pressure Drop Threshold of Nucleation for Polystyrene Foam with Carbon Dioxide.* Industrial & Engineering Chemistry Research, 2009. **48**(4): p. 1921-1927.

89. Leung, S.N., et al., *Ideal surface geometries of nucleating agents to enhance cell nucleation in polymeric foaming processes.* Journal of Applied Polymer Science, 2008. **108**(6): p. 3997-4003.

90. Wang, C., et al., *Numerical Investigation of Nucleating-Agent-Enhanced Heterogeneous Nucleation.* Industrial & Engineering Chemistry Research, 2010. **49**(24): p. 12783-12792.

91. Wong, A., et al., *Role of processing temperature in polystyrene and polycarbonate foaming with carbon dioxide.* Industrial & Engineering Chemistry Research, 2007. **46**(22): p. 7107-7116.

92. Liao, R.G., W. Yu, and C.X. Zhou, *Rheological control in foaming polymeric materials: I. Amorphous polymers.* Polymer, 2010. **51**(2): p. 568-580.

93. Fujino, M., et al., *Mathematical models and numerical simulations of a thermally expandable microballoon for plastic foaming.* Chemical Engineering Science, 2013. **104**: p. 220-227.

94. Alazard, P., M. Palumbo, and A. Gourdenne, *Curing under continuous microwaves (2 450 MHz) of thermosetting epoxy prepolymers: Final statement.* Macromolecular Symposia, 2003. **199**: p. 59-72.

95. Tartrattanakul, V. and D. Jaroendee, *Comparison between microwave and thermal curing of glass fiber-epoxy composites: Effect of microwave-heating cycle on mechanical properties.* Journal of Applied Polymer Science, 2006. **102**(2): p. 1059-1070.

96. Boey, F.Y.C. and B.H. Yap, *Microwave curing of an epoxy-amine system: effect of curing agent on the glass-transition temperature.* Polymer Testing, 2001. **20**(8): p. 837-845.

97. Rao, S. and R. Rao, *Cure studies on bifunctional epoxy matrices using a domestic microwave oven.* Polymer Testing, 2008. **27**(5): p. 645-652.

98. Chaowasakoo, T. and N. Sombatsompop, *Mechanical and morphological properties of fly ash/epoxy composites using conventional thermal and microwave curing methods.* Composites Science and Technology, 2007. **67**(11-12): p. 2282-2291.

99. Bai, S.L., et al., *A COMPARATIVE-STUDY OF THE MECHANICAL-BEHAVIOR OF AN EPOXY-RESIN CURED BY MICROWAVES WITH ONE CURED THERMALLY.* European Polymer Journal, 1995. **31**(9): p. 875-884.

100. Boey, F.Y.C., B.H. Yap, and L. Chia, *Microwave curing of epoxy-amine system - effect of curing agent on the rate enhancement.* Polymer Testing, 1999. **18**(2): p. 93-109.

101. Park, S.J., H.Y. Lee, and J.R. Lee, *Curing and thermal properties of a microwave radiation-curable epoxy/latent catalyst system.* Journal of Industrial and Engineering Chemistry, 2005. **11**(5): p. 726-731.

102. Uyanik, N., et al., *Epoxy nanocomposites curing by microwaves.* Polymer Engineering and Science, 2006. **46**(8): p. 1104-1110.

103. Yarlagadda, K. and S.H. Hsu, *Experimental studies on comparison of microwave curing and thermal curing of epoxy resins used for alternative mould materials.* Journal of Materials Processing Technology, 2004. **155**: p. 1532-1538.

104. Zhou, S.J. and M.C. Hawley, *A study of effect of conducting additives on microwave heating and curing rates of epoxy*, in *2001: A Materials and*

*Processes Odyssey, Books 1 and 2*, L. Repecka and F.F. Saremi, Editors. 2001, Soc Advancement Material & Process Engineering: Covina. p. 2243-2251.

105. Wei, J.H., et al., *COMPARISON OF MICROWAVE AND THERMAL CURE OF EPOXY-RESINS.* Polymer Engineering and Science, 1993. **33**(17): p. 1132-1140.

106. Fu, B. and M.C. Hawley, *Comparative study of continuous-power and pulsed-power microwave curing of epoxy resins.* Polymer Engineering and Science, 2000. **40**(10): p. 2133-2143.

107. Tomalino, M. and G. Bianchini, *Heat-expandable microspheres for car protection production.* Progress in Organic Coatings, 1997. **32**(1-4): p. 17-24.

108. Hoz, A.d.l. and A. Loupy, *Microwaves in Organic Synthesis, 3rd Edition*. 2013, Weinheim, Germany: Wiley-VCH.

109. Pugliaa, D., et al., *Thermal degradation and fire resistance of epoxy–amine–phenolic blends.* Polymer Degradation and Stability, 2001. **73**: p. 521–527.

110. Kraynik, A.M., *Foam structure: From soap froth to solid foams.* Mrs Bulletin, 2003. **28**(4): p. 275-278.

111. Wilson, A.J., *Foams: physics, chemistry, and structure*. 1989, New York: Springer-Verlag.

112. Stevenson, P., *Foam Engineering: fundamentals and applications*. 2012, West Sussex, UK: John Wiley & Sons.

113. Wilkie, C.A. and A.B. Morgan, *Fire Retardancy of Polymeric Materials, Second Edition*. 2012, Boca Raton, FL: CRC Press.

114. Horrocks, A.R. and D. Price, *Advances in fire retardant materials*. 2008, Cambridge: Woodhead Pub.

115. Hong, Y., X. Fang, and D. Yao, *Microwave Processing of Syntactic Foam from an Expandable Thermoset/Thermoplastic Mixture.* Polymer Engineering & Science, 2014.

116. ASTM, *Standard Test Methods for Flexible Cellular Materials Made From Olefin Polymers*, 2014.

117. ASTM, *Standard Test Methods for Breaking Load and Flexural Properties of Block-Type Thermal Insulation*, 2012.

118. White, J.L. and D.D. Choi, *Polyolefins: processing, structure development and properties* 2005, Cincinnati: Hanser Gardner Publications.

119. Ruhl, E. and J. Thenner, *Foam based on phenolic resin and furan resin, containing aluminum hydroxide as part of filler system, curing agent*, 1985: U.S.

120. Kandola, B.K., L. Krishnan, and J.R. Ebdon, *Blends of unsaturated polyester and phenolic resins for application as fire-resistant matrices in fibre-reinforced composites: Effects of added flame retardants.* Polymer Degradation and Stability, 2014. **106**: p. 129-137.

121. Larson, R.G., *The Structure and Rheology of Complex Fluids*. 1998, Oxford, U.K.: Oxford University Press.

122. Moosa, A.S.I. and N.J. Mills, *Analysis of bend tests on polystyrene bead foams.* Polymer Testing, 1998. **17**(5): p. 357-378.

123. Miessler, G.L., P.J. Fischer, and D.A. Tarr, *Inorganic Chemistry (5th Edition)* 2013, New Jersey: Prentice Hall.

124. Hong, Y., X. Fang, and D. Yao, *Processing of Composite Polystyrene Foam with a Honeycomb Structure.* Polymer Engineering and Science, 2015.

125. Rao, R.R., et al., *A level set method to study foam processing: a validation study.* International Journal for Numerical Methods in Fluids, 2012. **68**(11): p. 1362-1392.

126. Seo, D. and J.R. Youn, *Numerical analysis on reaction injection molding of polyurethane foam by using a finite volume method.* Polymer, 2005. **46**(17): p. 6482-6493.

127. Markert, B., *A Biphasic Continuum Approach for Viscoelastic High-Porosity Foams: Comprehensive Theory, Numerics, and Application.* Archives of Computational Methods in Engineering, 2008. **15**(4): p. 371-446.

128. Chang, D.L. and C.F.F. Lee, *Development of a simplified bubble growth model for flash boiling sprays in direct injection spark ignition engines.* Proceedings of the Combustion Institute, 2005. **30**: p. 2737-2744.

129. Mukherjee, A. and S.G. Kandlikar, *Numerical simulation of growth of a vapor bubble during flow boiling of water in a microchannel.* Microfluidics and Nanofluidics, 2005. **1**(2): p. 137-145.

130. Macosko, C.W., *Rheology: Principles, Measurements, and Applications*. 1994, New York: Wiley-VCH, Inc.

131. Joshi, K., et al., *Prediction of cellular structure in free expansion of viscoelastic media.* Journal of Applied Polymer Science, 1998. **67**(8): p. 1353-1368.

132. Tuladhar, T.R. and M.R. Mackley, *Experimental observations and modelling relating to foaming and bubble growth from pentane loaded polystyrene melts.* Chemical Engineering Science, 2004. **59**(24): p. 5997-6014.

133. Ewing, M.B. and J.C.S. Ochoa, *Vapour pressures of n-pentane determined by comparative ebulliometry.* Journal of Chemical Thermodynamics, 2006. **38**(3): p. 289-295.

134. LAURI, A., *THEORETICAL AND COMPUTATIONAL APPROACHES ON HETEROGENEOUS NUCLEATION*, in *Department of Physical Sciences*2006, University of Helsinki.

135. Park, C.B. and N.P. Suh, *Filamentary extrusion of microcellular polymers using a rapid decompressive element.* Polymer Engineering and Science, 1996. **36**(1): p. 34-48.

136. Fike, L.R., *Transport Properties of Polystyrene above and below Glass Transition Temperature*, in *Chemical Engineering*1983, Texas Tech University: Lubbock, Texas.